TECHNISCHE UNIVERSITÄT MÜNCHEN
Lehrstuhl für Bauchemie

Interactions of Polycarboxylate based Superplasticizers with Montmorillonite Clay in Portland Cement and with Calcium Aluminate Cement

Geok Bee Serina Ng

Vollständiger Abdruck der von der Fakultät für Chemie der Technischen Universität München zur Erlangung des akademischen Grades eines

Doktors der Naturwissenschaften (Dr. rer. nat.)

genehmigten Dissertation.

Vorsitzender: Univ.-Prof. Dr. Volker A. Sieber

Prüfer der Dissertation: 1. Univ.-Prof. Dr. Johann P. Plank
2. Univ.-Prof. Dr. Peter Müller-Buschbaum

Die Dissertation wurde am 05.12.2012 bei der Technischen Universität München eingereicht und durch die Fakultät für Chemie am 20.12.2012 angenommen.

Acknowledgement

I would like to express my heartfelt gratitude to Professor Plank and the Chair for Construction Chemicals, TUM for giving me the opportunity to conduct my doctoral work here in Munich, Germany. I would also like to thank Jürgen Manchot Stiftung for financing this Ph.D. work.

I greatly appreciate Dr. Coutelle from Rockwood for the RXM 6020 clay sample, Kerneos® for the calcium aluminate cement and my colleagues; Nadia Zouaoui, Alex Lange and Michael Glanzer-Heinrich for their support with the polycarboxylate polymers used in this project.

I like to take this opportunity to express my deepest thanks to the following people who have helped and supported me during these 3.5 years of my Ph.D.:

The two key figures in our lab, Richard Beiderbeck and Dagmar Lettrich for their technical assistance; Markus Gretz, Helena Keller, Friedrich von Hoessle, Hang Bian and Christof Schröfl who have guided and taught me, especially at the beginning of my studies; Dr. Oksana Storcheva, Thomas Pavlitschek, Yu Jin, Tobias Kornprobst, Matthias Lesti, Nan Zou, Johanna de Reese for helping to make my stay such a pleasant and great experience.

Special thanks to Elina Dubina and Ahmad Habbaba for being there through all the good and bad times at the Chair. I would always remember all the laughter and tears we shared during our studies.

I would also like to give appreciation to Mirko Gruber for his unswerving encouragement and positive outlook, especially during the darkest periods of my studies. Also much gratitude to his parents, Ute and Ludwig Gruber for constantly giving me support through this period of time.

Lastly, I would like to thank my family for always being there for me even when I am ~ 13,000 km away from home. Thank you for the constant advises and encouragement. The regular visits from everyone and the special homemade chili pastes from my mum ensured that I am well nourished and doing well here in Germany. Without all of you, this would have not been possible.

Life is simple ... don’t complicate it.

Summary

The purpose of this thesis was to investigate the fundamental mechanisms in the interaction of methacrylate poly(ethylene) glycol type comb polycarboxylate based superplasticizers with two different cementitious systems: (1) in Ordinary Portland cement where clay was present as a contaminant, and (2) in calcium aluminate cement. Whereby, in the second investigation, for the first time, experimental evidence was obtained for PCE intercalation into CAC hydrates under actual application conditions.

In the first study on the effect of clay contaminant on the workability of PCEs in concrete, two main areas were investigated as follow:

- Effect of the graft chain density of the polycarboxylate copolymers on their undesired consumption by clay contaminants
- Effect of the side chain lengths of these copolymers on their consumption by clay contaminants

To which potential remedies for both effects were derived in our investigation.

The main findings were that the mode of interaction between clay and PCEs possessing long side chains (45 EOUs) is independent of their graft densities, and is mainly driven by intercalation of the PEO side chain between the alumosilicate layers of the clay. The mechanism underlying this effect is based on hydrogen bonding between the polarized oxygen atoms along the PEO side chain and water molecules anchored by the silanol groups on the alumosilicate surfaces. Therefore, polyethylene glycol which can intercalate in place of the PEO side chains of PCE was found to be an ideal remedy.

In the investigation on PCEs possessing varying side chain lengths, the main result was that at low dosages, the mode of interaction between clay and these PCEs is dominated by intercalation of the PEO side chains. However, the dependency on electrostatic attraction increases when the side

chains of the PCEs decrease in length. At higher dosages, the contribution from electrostatic attraction to the overall sorbed amounts of PCEs becomes more significant. Anionic polymers such as polymethacrylate (PMA) present as effective remedy for PCEs possessing high anionic charge density.

The investigations here were performed using 'mini slump' test, sorption and zeta potential studies, XRD analysis and theoretical calculations.

In the study on the interaction between PCEs and calcium aluminate cement, two main areas were investigated:

- Effect of the grafting density of PCEs on their chemisorption behaviour in CAC slurry
- Correlation to the dispersing power of PCE with their chemisorption behavior under actual application conditions
- Reliability of instrumental methods in detecting the formation of organo-mineral phases

The investigations were performed using 'mini slump' test, XRD, SAXS and elemental analyses, and TEM and SEM imaging.

The main finding here was that other than surface adsorption of PCEs onto the CAC particles, intercalation of the anionic PCEs between the cationic $[Ca_2Al(OH)_6]^+$ main layers also occurs. This process is governed by the electrostatic attraction of the cationic main layers and the anionic methacrylate backbone of the PCEs. Therefore, the intercalation phenomenon of PCEs into calcium aluminate hydrates is charge dependent, whereby more anionic PCEs are consumed in higher amount through intercalation than the less anionic PCEs. This results in a higher dosage of the more anionic PCEs required in achieving the same dispersing effectiveness as when less anionic PCEs are employed, which is contrary to that observed in OPC.

The second finding here was that small angle x-ray scattering (SAXS) analysis proposed to present a reliable method for studying such intercalates. Due to the minute amount and nanocrystallinity of the intercalates formed, especially under actual application conditions, a very sensitive and reliable method was required to surely characterize these formations. SAXS analysis proved to be a far more superior method than XRD analysis, due to its greater sensitivity to such intercalates. Whereas XRD analysis can only be utilized under carefully controlled conditions.

Zusammenfassung

Im Rahmen dieser Dissertation wurden die grundlegenden Mechanismen für die Wechselwirkung zwischen Fließmittel auf Polycarboxylatether-Basis und zwei Zementleimsystemen geklärt. Für die Untersuchungen wurden das Zementleimsystem (1) auf Basis von Portlandzement mit einem Anteil an Tonmineralien als Beispiel für Verunreinigungen, sowie als System (2) ein Calcium-Aluminat-Zementleim gewählt. Erstmalig ist es in dieser Arbeit gelungen, einen experimentellen Nachweis für die Interkalation von PCE-Molekülen in Hydratphasen des Calcium-Aluminat-Zements unter praxisgerechten Anwendungsbedingungen zu erbringen.

Das Zementsystem (1) wurde gewählt, da in der Praxis weitreichende Probleme mit Tonverunreinigungen eine große Rolle spielen. Die Mechanismen der Wechselwirkung zwischen PCE und Ton wurden in Abhängigkeit von folgenden Parametern untersucht:

- Einfluss der Seitenkettendichte der Polycarboxylatether-Moleküle auf die Tendenz zur Interkalation in Tonmineralien
- Einfluss der Seitenkettenlänge der PCEs auf die Einlagerung in die Tonmineralien.

Aufbauend auf den Ergebnissen und der Kenntnis des Wirkmechanismus wurden Opfersubstanzen ermittelt, welche die Interkalation von PCEs in Tonmineralien abschwächen oder ganz verhindern können.

Es wurde gefunden, dass bei niedriger PCE-Dosierung die Interkalation der Polymere vornehmlich über die Polyethylenoxidseitenketten erfolgt. Diese erfolgt durch Ausbildung von Wasserstoffbrückenbindungen zwischen den polarisierten Sauerstoffatomen in der PEO-Kette und den Silanolgruppen des Montmorillonits. der in den Zwischenschichten verankerten Wassermoleküle. Da PEO sehr gut interkaliert, konnte basierend auf diesem Wirkmechanismus der Einsatz von Polyethylenoxid (PEO) als ideale Opfersubstanz an Stelle von PCE nachgewiesen werden.

Die Versuche zur Variation der Seitenkettenlänge zeigten, dass die Einlagerung der PCE-Moleküle in Tonmineralien vorwiegend bei niedriger, praxisrelevanter PCE-Konzentration auftritt. Je kürzer die Seitenkette, umso mehr gewinnt der Einfluss der elektrostatischen Anziehung an Bedeutung, vor allem nach erfolgter Gleichgewichtseinstellung. Auf Grund dessen eignen sich vornehmlich Polymethacrylate als Opfersubstanzen. Eine optimale Dispergierwirkung für ein PCE-Produkt wird durch demnach Kombination des PCEs mit Polymethacrylsäure und Polyethylenoxid als Opfersubstanzen erreicht.

Für die Untersuchungen wurden "Mini Slump Tests", Sorptions- und Zeta-Potential-Messungen, XRD-Analytik und theoretische Betrachtungen herangezogen.

Im System (2) wurden folgende Parameter und Effekte untersucht:

- Einfluss der Seitenkettendichte auf das Interkalationsverhalten in Calcium-Aluminat-Zement (CAC)
- Wirksamkeit von PCE-Molekülen unter realen Anwendungsbedingungen in CAC
- Zuverlässigkeit der instrumentellen Methoden zur Detektion von PCE-Interkalationsverbindungen

Zusätzlich zur bereits bekannten Oberflächenadsorption von PCE-Molekülen auf den CAC-Partikeln wurde hier die Einlagerung der PCEs in die kationischen $[Ca_2Al(OH)_6]^+$-Schichten nachgewiesen worden. Dieser Prozess wird durch die elektrostatische Anziehung zwischen der kationischen Zwischenschicht und dem negativ geladenen Rückgrat des PCE-Moleküls bestimmt. Da die Interkalation von PCE somit ladungsabhängig ist, werden die stärker anionisch geladenen PCEs in höherem Maße verbraucht als weniger geladene Moleküle. Dies führt bei vergleichbarer Dispergierwirkung zu einer entsprechend höheren Dosierung für PCEs mit höherer negativer Ladung. Diese Erkenntnis steht im Gegensatz zu früher am System Portlandzement beobachteten Effekten.

Für die Untersuchungen wurden “Mini Slump Tests”, XRD-Analytik, SAXS, Elementaranalyse, TEM- und SEM- Bilder herangezogen. Erweiternd wurde die Zuverlässigkeit der verwendeten Methoden für die sichere Detektion von Interkalaten überprüft. Bedingt durch die sehr geringe Menge und Nanokristallinität der gebildeten Einlagerungsverbindungen, besonders unter praxisgerechten Anwendungsbedingungen, erwies sich SAXS als die weitaus exaktere Methode im Vergleich zur XRD-Analytik.

Chemical Notations

In this work, the chemical formulae of many cement compounds are expressed as a sum of oxides. In accordance to a special notation established by cement chemists, these clinker and hydrate phases are abbreviated as follows:

Clinker phases

Cement notation	Chemical formula	Mineral name
C_3A	$3\ CaO \cdot Al_2O_3$	Tricalcium aluminate
$C_{12}A_7$	$12\ CaO \cdot 7\ Al_2O_3$	Calcium aluminate, Mayenite
CA	$CaO \cdot Al_2O_3$	Monocalcium aluminate
CA_2	$CaO \cdot 2\ Al_2O_3$	Calcium dialuminate, Grossite
CA_6	$CaO \cdot 6\ Al_2O_3$	Calcium aluminate

Hydrate phases

Cement notation	Chemical formula	Mineral name
AF_m or $C_4A\,\overline{S}\,H_{12}$	$Ca_4Al_2(OH)_{12}SO_4 \cdot 6\ H_2O$	Calcium monosulfoaluminate hydrate, Monosulfate
AH_3	$Al_2O_3 \cdot 3\ H_2O$	Gibbsite
CAH_{10}	$CaO \cdot Al_2O_3 \cdot 10\ H_2O$	Calcium aluminate hydrate
C_2AH_8	$2\ CaO \cdot Al_2O_3 \cdot 8\ H_2O$	Calcium aluminate hydrate
C_3AH_6	$3\ CaO \cdot Al_2O_3 \cdot 6\ H_2O$	Calcium aluminate hydrate, Katoite
C_4AH_{13}	$4\ CaO \cdot Al_2O_3 \cdot 13\ H_2O$	Calcium aluminate hydrate
C_4AH_{19}	$4\ CaO \cdot Al_2O_3 \cdot 19\ H_2O$	Calcium aluminate hydrate
H	H_2O	Water

Abbreviations

APEG	α-allyl-ω-methoxy or hydroxy poly(ethylene glycol)
BET	Brunauer, Emmet and Teller (BET theory)
bwoc	By weight of cement
bwo clay	By weight of clay
CAC	Calcium aluminate cement
EDX	Energy dispersive X-ray analysis
EOU	Ethylene oxide unit
(E)SEM	(Environmental) Scanning electron microscope
GPC	Gel permeabillity chromatography
h	Hours
IPEG	Isoprenyl oxy poly(ethylene glycol)
LDH	Layered double hydroxide
MA	Methacrylic acid
min	Minutes
MMT	Montmorillonite
MPEG	Methoxy poly(ethylene glycol)
MPEG-MA	ω-methoxypoly(ethylene glycol) methacrylate ester
nm	Nanometer
OMP	Organo-mineral phases
OPC	Ordinary Portland Cement
PAAM	Polyamidoamine
PC	Polycondensate
PCE	Polycarboxylate
PDI	Polydispersity index
PEG	Poly(ethylene glycol)
PEO	Poly(ethylene oxide)
PMA	Poly(methacrylic acid)
s	Seconds
SAXS	Small angle x-ray scattering
SEC	Size Axclusion Chromatography
T	Temperature
t	Time
TEM	Transmission electron microscopy
TOC	Total Organic Carbon
VPEG	Vinyl ether
w/c	Water-to-cement ratio
w/clay	Water-to-clay ratio
wt. %	Weight percentage
XPEG	Crosslinked PCEs
XRD	X-ray diffraction
XRF	X-ray fluorescence
µ	Micro

List of Publication

This thesis includes the following publications:

SCI(E) journal papers:

(1) "Interaction Mechanisms between Na montmorillonite Clay and MPEG-based Polycarboxylate Superplasticizers"

S. Ng, J. Plank, Cement and Concrete Research 42 (2012) 847–854.

Manuscripts submitted to journals:

(2) " Effect of Graft Chain Length of Methacrylate Ester Based PCE Superplasticizers on their Interactions with Na-Montmorillonite Clay "

S. Ng, J. Plank, Submitted to Applied Clay Science.

(3) " Occurrence of Intercalation of PCE Superplasticizers in Calcium Aluminate Cement under Actual Application Conditions, as evidenced by SAXS Analysis "

S. Ng, J. Plank,. Submitted to Cement and Concrete Research.

Refereed Conference Proceedings:

(4) "Formation of Organo-mineral Phases Incorporating PCE Superplasticizers During Early Hydration of Calcium Aluminate Cement"

S. Ng, J. Plank, Proceedings of the 13th ICCC International Congress on the Chemistry of Cement, Abstract book p. 251, Madrid/Spain (2011); ISBN: CD 978-84-7292-400-0.

(5) "Study on the Interaction of Na-montmorillonite Clay with Polycarboxylates"

S. Ng, J. Plank, V. M. Malhotra (Ed.) 10th CANMET/ACI Conference on superplasticizers and other chemical admixtures in concrete, ACI, Prague, Czech Republic, SP–288 (2012) 407–420.

Table of contents

1 Introduction

Superplasticizers impart workability during the initial dispersion of cement particles in concrete. Among which, polycarboxylate copolymers represents a very interesting class of superplasticizers. PCE is a commonly used high-performance superplasticizer in the field of construction chemistry, and is commonly employed at much lower dosages for the same effectiveness as its counterparts such as the polycondensates [1]. Due to its high workability in a wide span of applications, ranging from ready mixed to ultra-high strength concretes [2, 3], much research has been placed on this class of PCE superplasticizers. In recent years, a significant rise in variation of cementitious systems such as increased use of CEM II and III cements prompted tremendous research to be focused on the performance, particularly the compatibility, of PCEs with these different systems. Among which, two specific systems of interest will be explored in this thesis; namely (1) clay contaminated ordinary Portland cement (OPC) and (2) high alumina calcium aluminate cement (CAC).

(1) Clay contaminated OPC

Sometimes, cement pastes with PCE superplasticizers failed to deliver as promised in recent years. This created devastating losses in terms of cost, manpower and materials as the workability of concrete was compromised. Thus, it became crucial to determine the factors causing this undesirable issue. It was found by other researchers that clay contamination can present a potential cause for this reduction in PCE performance [4, 5], whereby expanding clays such as montmorillonite are the most detrimental [6]. The source of clay can be backtracked to the addition of sand, gravel or even in the usage of limestone powder. These materials which are usually added to cement slurries for addition volume can be loaded with clay impurities. To cleanse them, they were often washed or processed. However, this procedure was omitted or shortened to minimize the cost of handling, thus amplifying the clay content.

Here, the influence of clay, more specifically of montmorillonite clay on the workability of cement pastes was investigated. To ascertain the interaction of PCEs with clay, TOC, XRD, GPC and zeta potential measurements and theoretical calculations were conducted. The clay/ PCE systems were

subjected to different mediums such as synthetic cement pore solution and alkaline solution adjusted to pH 12.8 to distinguish between intercalation and surface adsorbed PCEs. Additionally, PMA and PEG (representative of the main chain and side chain building blocks of PCEs) were also analyzed to pinpoint the specific site of interactions between PCEs and clay. This way, the effect of varying properties of PCEs on their mechanism of interaction with clay and potential remedies were sought to be clarified.

(2) CAC system

Calcium aluminate cement has grown in importance, especially in the applications of dry mixed mortar [7] and monolithic refractories [8]. F. Massazza (1981) was among the first to discuss the interaction between calcium aluminate hydrates present in OPC (C_3A) and polycondensates [9]. Thereafter, only few investigations have been performed on the interaction between CAC hydrates and PCE superplasticizers [10]. Therefore, in the second part of this thesis, the aim was to expand on this field of study, with a clear focus on PCEs.

During hydration at room temperature, layered calcium aluminate hydrates may form. In turn, the anionic PCE superplasticizers may intercalate into their interlayer regions, and render the PCEs unavailable for effective dispersion of the cement particles. Intercalation of superplasticizers under such conditions has only been reported using model systems where C_3A was hydrated for 2 days or 2 h at elevated temperatures [11]. However, these conditions do not truly represent the actual cement system where PCEs are commonly employed.

Here, the performance and underlying mechanism of PCE in CAC under actual application conditions is presented. A commercial white CAC (~ 70 % Al_2O_3) was selected for this purpose. The dispersing ability of several PCEs in CAC was ascertained by ‘mini slump’ test. Further analyses were performed using XRD, SAXS, TEM, SEM and elemental analysis.

2 Aims and limitations

This PhD thesis aims to determine the effective performance of PCE superplasticizers and the mechanism driving these behaviors in two different systems; (1) clay contaminated OPC, and (2) CAC.

For system (1) concerning OPC and clay, the goal was to decipher the specific interaction between PCEs and an expanding clay, sodium montmorillonite. This work attempted to understand the rheological behaviour of cement pastes containing cement, clay and PCEs. Next, a model system in synthetic cement pore solution containing only PCE and clay was utilized to determine the dependency of the grafting density and PEO side chain lengths of the PCEs on the mode and extent of influence from clay on PCEs. The mechanisms driving the interaction between such PCEs and clay were sought to be clarified in this thesis, from which potential remedies can be devised.

A potential limitation in our investigation was the utilization of a model system in synthetic cement pore solution which is only an idealized depiction of the actual working conditions. Therefore, factors such as the dynamic replenishing of Ca^{2+} ions in an actual cement suspension were not accounted for.

In system (2) involving CAC, this work aimed to bridge the gap in CAC research by addressing the occurrence of PCE intercalation there, first under idealized conditions and, followed by actual application conditions. The results obtained were correlated to the dispersing effectiveness of the PCEs in CAC pastes.

This was performed by: First, determination of the dispersing power of PCEs in CAC. And second, a detailed mechanistic breakdown on the chemical consumption of PCEs by CAC, to identify the extent and mode of chemisorption. In this way, the dispersing ability of the PCEs in CAC and their

interactions during hydration were explored. Also, a highlight on the limitations of conventional methods for the detection of such intercalated will be given.

The main limitation of this investigation rested in the experimental deficiency for effective determination of potential intercalation products. Due to the realistic application conditions applied here (low w/c ratio and PCE dosages), the products formed are difficult to detect by conventional methods. Additionally, the lack of general research on CAC also impacted the research progress. Extrapolation from studies with OPC was thus required.

3 Theory on Polycarboxylate based Superplasticizers

The invention of superplasticizers back as early as in 1936 [12] represents the most significant advance in concrete technology over the last 70 years. Nowadays, superplasticizers can be categorized into four chemically distinctly different classes: (1) polycondensates; (2) polycarboxylates; (3) 'small molecules' and (4) biopolymers. Among these four classes of superplasticizers, PCEs are the most researched upon, driven by a commercial demand from the industry. For 2011, the global volume of PCE applied in concrete was estimated at 2.4 mio. tons, based on liquid with 20 wt. % solid content [13]. Accordingly, China is the largest market for PCE products, holding up to 40 % of the total PCE consumption worldwide with an annual volume of 1.27 mio. tons (data from 2010) [14]. Additionally, substantial volumes of PCE powder are manufactured e.g. for dry-mix mortar products such as self-leveling underlayments or machinery grouts.

PCE comb copolymers were introduced as a new class of superplasticizers in 1981 [15]. They constitute the first type of PCE product which was introduced into the Japanese market by Nippon Shokubai under the name 'FC 600' [16]. In the whole class of superplasticizers, it is the second type of superplasticizers to be introduced into the market, after the polycondensates [17–20]. The structural characteristic of PCE is an anionic (medium to low charge density) polymer backbone, with protruding lateral graft chains at periodical intervals. These side chains instigate a steric hindrance effect between the cement particles suspended in water [21] and enable the PCE superplasticizers to exhibit superior dispersing force compared to polycondensates. Consequently, a great diversity of chemically different PCE products is on the market, including the MPEG-type PCEs [22], APEG-type PCEs [23], VPEG-type PCEs [24], IPEG-type PCEs [25], HPEG-type PCEs [26], XPEG-type PCEs [27] and PAAM-type PCEs [28] (**Figure 1**).

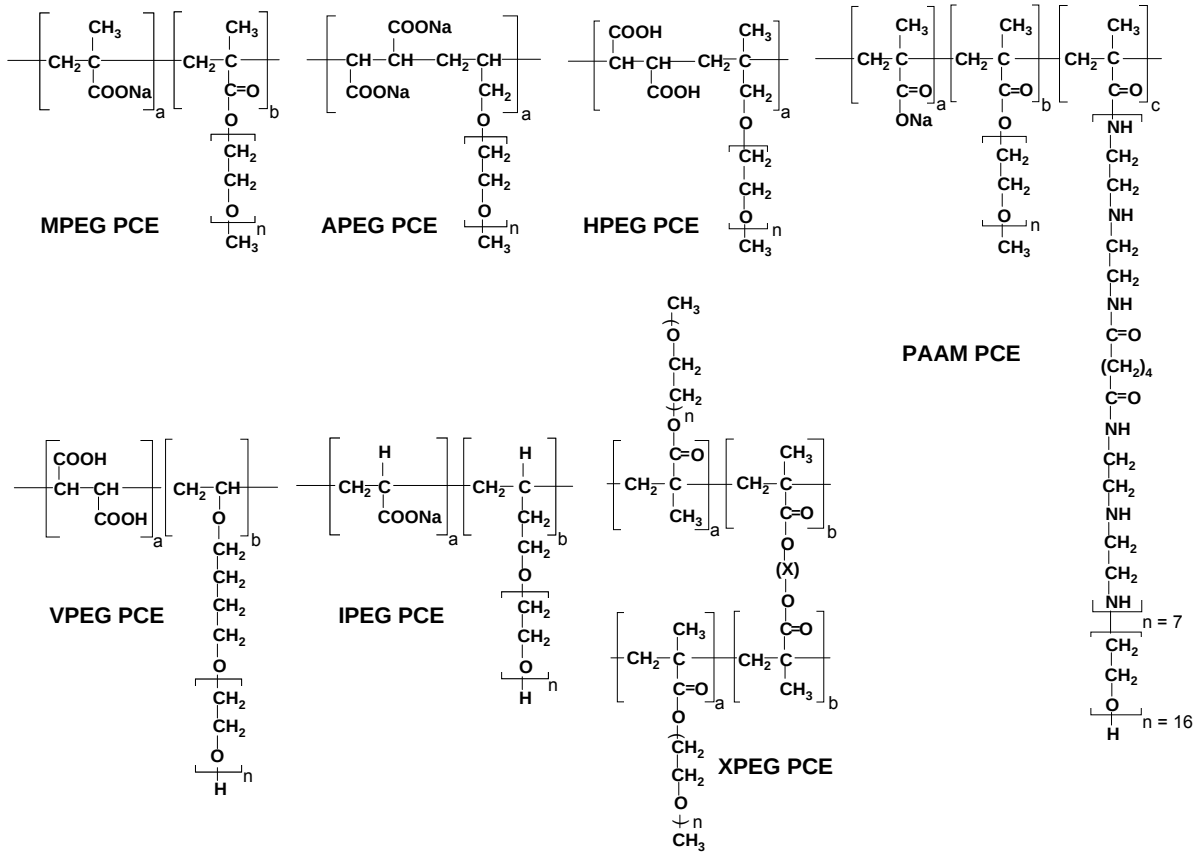

Figure 1. Chemical structures of PCE type superplasticizers currently applied by the concrete industry [29]

Among which, MPEG-type PCEs are the most commonly used PCEs available on market. They are made from MPEG-MA, either by (a) aqueous free radical copolymerisation [30] or by (b) esterification/ transesterification reaction [22].

(a) Aqueous free radical copolymerisation of ω-methoxy poly(ethylene glycol) methacrylate ester macromonomer with methacrylic acid presents the most common method to synthesize MPEG-PCEs [30]. This reaction is so popular due to three main factors: (1) the simplicity of operation, (2) the wide variation in achieving controllable composition by varying the molar ratios of the monomers and thus, performance of the polymer, and (3) the ease in adjusting trunk chain length by utilizing chain transfer agents such as methallyl sulfonic acid. Here, the relative reactivities of both monomers vary as a function of pH. Also, the macromonomer can exhibit a higher reactivity than the methacrylic acid, giving rise to gradient polymers (**Figure 2**) which possess higher side chain

density at the beginning of polymerisation, and decrease towards the end of the reaction. Normally, such gradient PCEs possess relatively high PDIs of ~2 to 3.

Recently, specific gradient polymers were synthesized by applying RAFT polymerisation techniques [31]. Such copolymers possess a higher electrostatic affinity for cement as a result of their large anionic blocks, making them particularly robust and favourable in systems where sulfate tolerance is needed as they are less susceptible to anionic displacement by SO_4^{2-} anions in the cement pore solution than comparable PCE molecules possessing random distribution of the lateral chains.

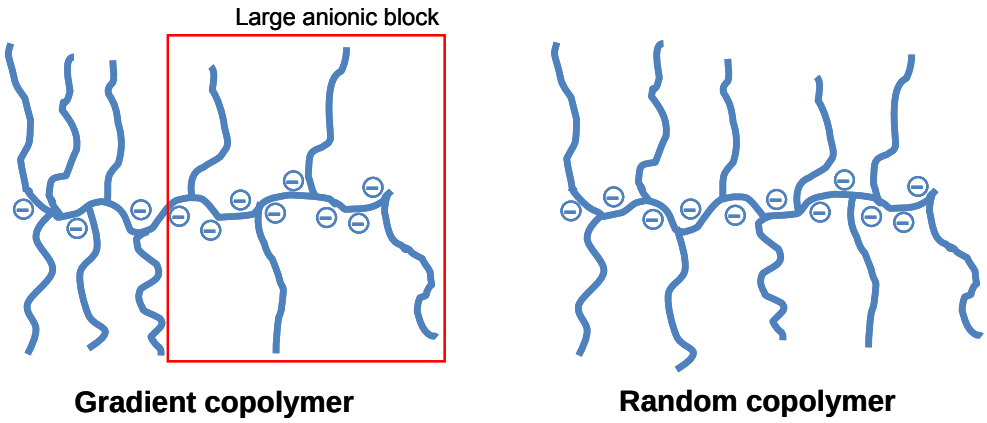

Figure 2. Illustration of MPEG–type PCEs (left) as gradient polymer produced, by free radical copolymerisation, and (right) as random copolymer produced by grafting/ esterification

(b) Esterification of poly(methacrylic acid) with methoxy poly(ethylene glycol) utilizes an acid catalyst (e.g. p-toluol sulfonic acid) and an azeotrop or vacuum to remove the water [32]. This method is less favourable in industry due to the high cost for the monomer PMA methyl ester and the requirement to hydrolyse the methyl ester after grafting. Additionally, a long reaction time and low conversion rate (~ 70 %) also add to the list of disadvantages for using this synthesis method. However, the method produces a highly uniform comb polymer with statistical distribution of the MPEG side chains along the PCE main chain (**Figure 2**).

As mentioned, the main chain length of a PCE is set by the polymerization, and the side chain length by the number of EO repeating units in the ester macromonomer. The difference in molar ra-

tio between MA and MPEG-MA can be regulated by the concentration of monomers added from the onset of the synthesis. Further modifications were introduced to enhance the performance of MPEG-type PCEs. In addition to the 2 monomers, other comonomers such as e.g. methacrylic acid methylester were also included in the radical polymerisation synthesis. Also, new chain transfer agents (e.g. mercaptanes) were utilised, to minimise PDIs of the polymers.

Application of these PCE admixtures which are effective at surprisingly low dosages (as low as 0.02 % by weight of cement) allows the production of a highly durable concrete, yet with excellent workability. The influencing factors for the workability of a superplasticizer include the nature of the superplasticizer, the dosages, the time of addition (immediate or delay), the w/c ratio, and the consumption and amount of cement used. Specifically, a large quantity of PCEs is synthesized for application in two main classes of concrete: ready mixed and precast. In ready mixed concrete, PCEs possessing low anionic charge and a high grafting density are utilised. Whereas for the production of precast concrete, PCEs possessing high anionic charge and a low grafting density are ideal. Owed to their unique tuneable chemical and molecular structure, PCEs also can accommodate many other different purposes such as formulate self-compacting concrete [33], providing long slump retention (2+ hours) [34], effectiveness at ultra-low w/c ratios (w/c < 0.25) [35], or even exert a ‘Saratto–kan’ effect [36]. These modern advancements allow building of structures such as long-span bridges and high rise buildings, which were impossible before superplasticizers were invented. However, there still exist disadvantages in utilizing PCEs which include irregular dosage control, wear of truck mixers and the tendency to overdose water on site [37].

4 Theory on Montmorillonite Clay and its Interaction with Polymers

Clay is present in abundance as a naturally occurring, fine-grained and argillaceous raw material with a long history in applications. It is a non-hydraulic binder and has more than 100 documented industrial applications [38]. Depending on their mineral structures and compositions, clays are utilized in a wide scope of fields, ranging from food industries, agricultural applications, engineering and construction applications, environmental remediation, geology, pharmaceutical and paper industries, etc. Due to its diversity in application, a wide scope of research has been performed, and is still ongoing in an effort to optimize the usage of this raw material. Such developments result in improvement of many technologies, including but not restricted to drug delivery [39], specialized adsorbents such as for oil spill [40], cosmetics [41] and water treatments [42], etc.

Macroscopically, clays are hydrous aluminum silicates that are usually defined as 'phyllosilicate minerals'. They impart plasticity to aqueous clay suspensions and harden upon drying or firing. The prime factor in the determination of clay properties is its structure. Most clays possess a mica-type structure, whilst clay flakes consist of stacked platelets where a single platelet is a unit layer (**Figure 3**) [43]**. Table 1** shows the general classification of clay minerals, and their properties.

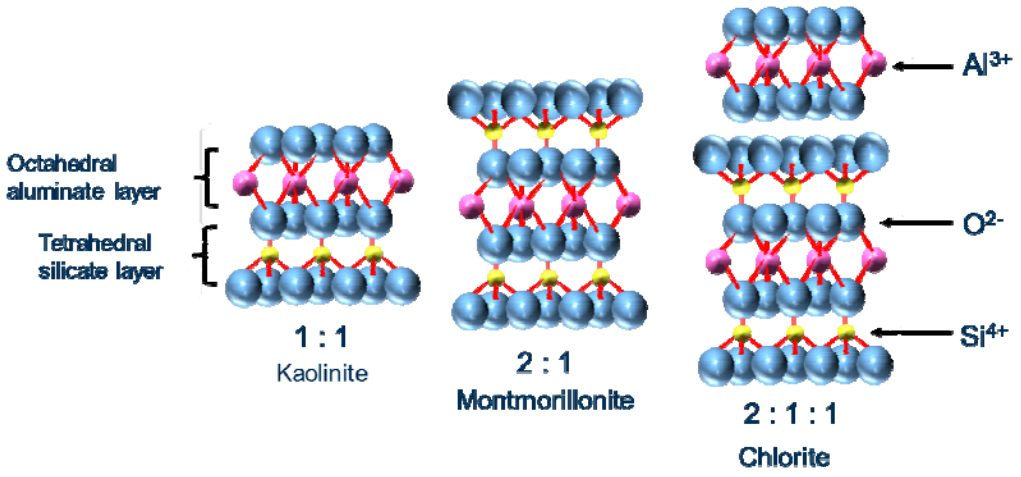

Figure 3. Graphical representation of the layered structure of different clay minerals

Table 1. Classification of clay minerals and their properties

Layer structure Silicate:aluminate	Clay minerals	Properties
1:1	Kaolinite	Strong H-bonding between layers Little substitutions Nonexpanding Large, well-ordered crystals Few cations adsorbed on basal surfaces
2:1	Smectite	Weak bonding between layers Layer surfaces possess Na monolayer Available for hydration and cation exchange Expandable lattice, thus increase colloidal activity
	Illite	Strong interlayer bonding No expanding lattice, no interlayer water K^+ acts as the main balancing cation Ion Exchange occurs at aggregate surface Substitution predominately Al for Si in tetrahedral sheet
2:1:1	Chlorite	Negatively charged surface layer Brucite layer: Substitution of Mg by Al Some interlayer hydration and lattice expansion
mixed-layered		Different clay minerals stack in the same lattice Disperse in water more easily Regular or irregular

4.1 Mineralogy of Montmorillonite Clay

Among the different types of clay, montmorillonite belongs to the class of expanding 2:1 smectite clay minerals. Montmorillonite clay in particular is unique in the fact that it exists in nature in turbostratic units that are hydrophilic and can be broken down into one nanometer thick platelets. Chemically, it consists of stacked octahedral aluminate layers sandwiched between two tetrahedral silicate layers (**Figure 3**). The resulting alumosilicate layers measure about 1 nm in thickness [44]. The general composition of montmorillonite can be expressed as $M_x(Mg,Al,Fe)_2(OH)_2[Si_4O_{10}]\cdot nH_2O$, with $M^+ = Na^+$, K^+, 0.5 Mg^{2+} or 0.5 Ca^{2+}. Due to the similar ionic size, Si^{4+} can be partially substituted by Al^{3+} to generate an overall innate negative charge of

the basal surfaces. This charge is balanced by intercalation of cations (M^+; hydrated or non-hydrated) in between the expandable alumosilicate layers [45].

All classes of clays take up water, but smectites sorb much larger volumes than other types of clay due to their expanding lattices. When montmorillonite clays come into contact with water, the water molecules penetrate between the layers and push them apart at a distance equivalent to one to four monomolecular layers of water [46]. This occurs mainly through two swelling mechanisms, crystalline and osmotic. Crystalline swelling, also known as surface hydration involves the adsorption of mono-molecular layers of water on the basal crystal surfaces (both external and inter-layer surfaces) [47]. Whereas, osmotic swelling occurs due to the concentration gradient of cations between the layers and in bulk solution. Owing to the intra-swelling effect, a distinctive increase in basal spacing of the clay to definite values of 12.5 – 20 Å occurs, depending on the type of clay and cation present.

When dispersed in electrolyte rich medium, cations can also adsorb onto the permanently negatively charged basal surfaces of the clay platelets. Other anchoring sites for cations are the crystal edges where terminal -OH groups from aluminates and silicates are present [48, 49]. These terminal –OH groups are pH dependent where at high pH, they are deprotonated and develop a negative charge. Consequently, cations such as Ca^{2+} occurring in cement pore solution can be taken up by the basal surfaces as well as by the crystal edges [50]. Physisorption of cations on these charged surfaces occurs with the general order of affinity as follows: $H^+ > Ba^{2+} > Sr^{2+} > Ca^{2+} > Cs^+ > Rb^+ > K^+ > Na^+ > Li^+$ [51]. In general, the total amount of cations adsorbed is called cation exchange capacity (CEC), and it varies considerably among the clay minerals. With montmorillonite and illite, the basal surface accounts for some 80 % of the CEC. On the other hand, in kaolinite, the crystal edges account for the most of the CEC [51].

In many applications, cations exercise a significant influence on the functionality and adsorption behavior of the clay. The hydration dynamics of these cations and the interaction of water with these metal ions underlie many of the important processes associated with clay minerals including their ability to swell in water. Potassium ions, in particular, restrict the interlayer expansion of clay minerals to only a monolayer of water. In fact, hydration of bentonites and vermiculites is virtually

impeded by KCl solutions at concentrations above 0.01 M [52]. The water molecules are displaced from between the layers when exchangeable cations such as K^+ are intercalated into the interlayer space. The 'fixation' of K^+ ions is well known to clay scientists and can be explained by the reduced hydration energy and an ideal geometric fit of the potassium ion to the surface oxygen hexagons of the main layer. In fact, K^+ is often used in oilwell drilling to stabilize shale exposed to water-based drilling fluids [52].

4.2 Interaction of Clay with Polymers

Polymer-clay nanocomposites are formed through the union of two very different materials with organic and mineral origins. In general, clay minerals offer three types of surfaces to the macromolecules: external basal plane, edge surfaces and the internal intergallery surfaces. The degree of sorbed polymer generally depends on the levels of polymer concentration, pH, ionic strength and temperature [53]. Due to the unique properties of montmorillonite, this clay can undergo a variety of interactions with polymers, giving rise to the creation of a diverse range of materials. Montmorillonite clay interacts through these surfaces mainly in three ways: electrostatic attraction, cation-dipole interaction, and intercalation (**Figure 4**). Here, we will discuss each mode of interaction in details.

Electrostatic attraction occurs as a result of the overall negative charge of montmorillonite clay. Due to this, montmorillonite clay has a high cation exchange capacity which promotes rapid consumption of cationic polymers such as amines or amides [54]. The affinity for cationic polymers is permanent due to the innate negative basal surfaces. On the other hand, adsorption of anionic polymers is pH dependent. Under acidic conditions, these polymers can adsorb onto the protonated crystal edges. Whereas at high pH, the clay is fully negatively charged, thus electrolytes are needed to facilitate the adsorption of anionic polymers.

Cation-dipole interaction is characteristic for the attachment of unpolar, polyfunctional organic polymers to the clay surface. The translational entropy gained in the system in replacing many wa-

ter molecules from the mineral surface by a single macromolecule chain, provides the driving force for polymer adsorption [55, 56].

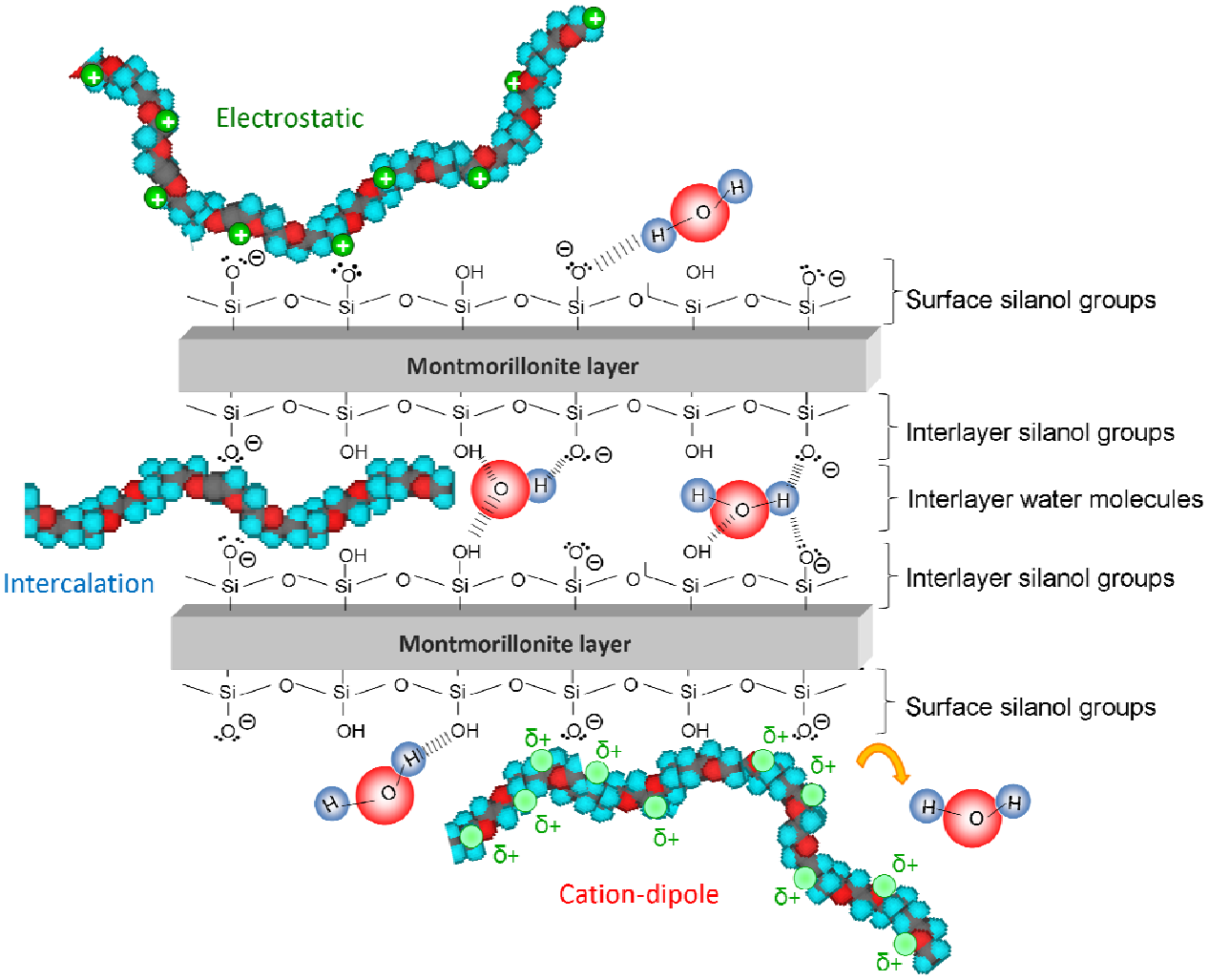

Figure 4. Three modes of interaction between montmorillonite clay and polymers

Intercalation is predominant for montmorillonite clay due to its expanding lattices and highly active surface area. Much research was focused on this class of clay and several reviews have recently been published on polymer-nanocomposites based on smectite clays [57, 58]. In general, intercalation of polymers into the clay lattices occurs by (1) ion exchange with organic cations [59], (2) silylation and esterification of interlayer silanol groups present on the clay layers [60] and (3) via dipo-

lar interactions of polar organic molecules with ions and/or to silanol groups by hydrogen bonds [61, 62]. Of interest, the polyethylene glycols show significant intercalation into montmorillonite clay by hydrophilic interaction with the water molecules and interlayer silanol groups, giving rise to a high consumption of these polymers by montmorillonite clay. As a tradition, glycol is used as an indicator for the presence of montmorillonite clay in samples. The intercalation ability of glycols is molecular weight dependent; the higher the molecular weight, the more uptake [63, 64].

4.3 Current State of Art

In the construction field, applicators have observed that the presence of certain clays may affect and can be detrimental to the initial workability of concrete [65–67]. The impact of this process is dependent on the type of admixtures used. For superplasticizers, polycondensates were shown to be less affected by the presence of clay than polycarboxylates [68, 69], where a strong detrimental impact was found when the latter was used. This indicates that when concrete is contaminated by a significant quantity of montmorillonite, competing demands by different components (cement and clay) for the polycarboxylate superplasticizer can occur, thus reducing its availability for dispersion.

Mechanistically, little evidence has been drawn to show the impact of montmorillonite clay on the performance of PCEs. Jaknovarian *et al.* have proposed that intercalation of PCEs via their side chain is the possible mode of interaction between clay and PCE in cementitious systems [65]. In 1990, a US patent described the employment of polyglycols as a sacrificial agent to counter the negative impact of clay [70].

5 Theory on CAC and Intercalation Chemistry

The first documentation of isolated calcium aluminate species dates back to 1848 when Ebelman reacted alumina with marble. However, the industrial development of CAC was mainly associated with the work of Jules Bied in the laboratories of the J & A Pavin de Larfarge company at Le Teil, France [71], where bauxite and lime were fired together in a cupola furnace. At this time, this cement was invented to compensate the deficiency of ordinary Portland cement, where a high resistance to chemical attack by sulphate was needed. Later, CAC was found to also have excellent resistance to a wide variety of conditions such as abrasion under low temperatures, high temperatures, weak acids and seawater, etc. More crucially, this cement showed tremendous early strength gain, thus concrete produced useful strength already after 6 h and by 24 h, a strength equal to that given by Portland cement in 28 days could be obtained [72]. Thereafter, a wide range of general and specialized applications were found for this class of cements due to their wide properties and specific advantages.

The main application of CAC is as a binder in monolithic refractories. When utilized with appropriate refractory aggregates, CAC may be used to generate refractory castables commonly employed in the steel and other 'heat-using' industries. In general, the CAC made from bauxite may be employed up to a temperature of 1350 °C. Whereas white CAC that is low in iron, but high in alumina contents can be used to make castables which can withstand temperatures of up to 2000 °C. These refractory castables are known to possess good resistance to thermal shock. On the other extreme, due to the high reaction rate and thus heat generation, CAC is also suitable for usage at low temperature (down to – 10 °C), e.g. for repairs in cold stores or winter construction in cold climates. Other applications of CAC include industrial flooring products (such as cast house floors), chemical resistant mortars and concretes, expansive grouts, floor screeds, sewer applications, protective coatings, tile adhesives, mortar and building chemistry products, etc. In such applications, CAC is often utilized in combination with Portland cements, sometimes with slaked lime or additional gypsum to produce rapid setting mixtures which can achieve relatively high strengths [73].

5.1 High Alumina Content CAC

In 1915, Rankin and Wright published the lime-alumina phase diagram (**Figure 5**) representing the five calcium aluminate compounds, C_3A, $C_{12}A_7$, CA, CA_2 and CA_6 (in order of reactivity). In CAC, the main clinker phases present are CA, CA_2 and $C_{12}A_7$. Whereas C_3A is the main aluminate phase in OPC.

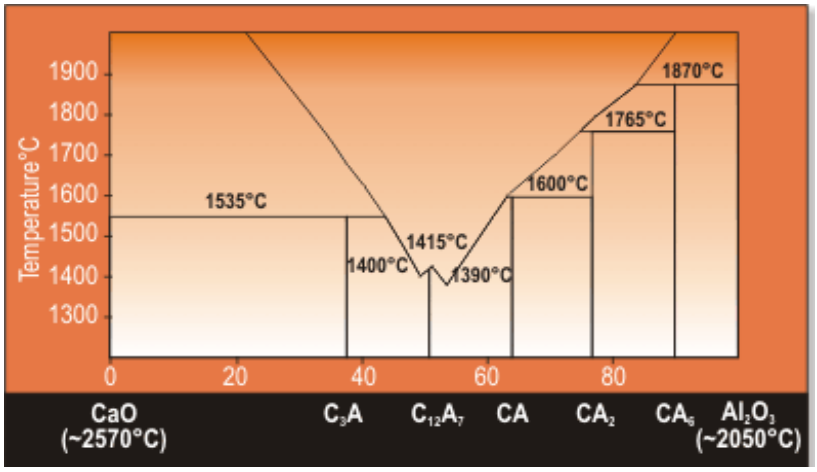

Figure 5. Lime-alumina phase diagram [74]

The classification of CAC types can be loosely grouped according to the Al_2O_3 content (**Table 2**). Depending on the iron content, the colour of cements produced from bauxite can vary from yellow-brown to black, but it is commonly greyish black (**Figure 6**). Here, of interest is the white CAC which possesses high alumina content (> 70 wt. %). It is usually made by sintering calcined alumina with quick lime (CaO) or high purity limestone, where there is a low percentage of iron present. Most commercially produced white CACs contain CA (main component) and $C_{12}A_7$ (mayenite). Additionally, those high in Al_2O_3 may also contain CA_2, CA_6 or α-Al_2O_3. In the sintering process by which these cements are made, the reaction conditions are very important, as the products of a given mix can vary from a mixture of CA and CA_2 to the full range of phases in the CaO-Al_2O_3 system. Most of the grains of the ground cement are polymineralic, with CA being the first phase to crystallize during production.

Table 2. Typical composition of calcium aluminate cements (mass %) [72]

Type of cement	Al_2O_3	CaO	Fe_2O_3/FeO	SiO_2	TiO_2	MgO	K_2O/Na_2O
40% Al_2O_3	40 ~ 45	42 ~ 48	< 10	< 5	~ 2	< 1.5	< 0.4
50% Al_2O_3	49 ~ 55	34 ~ 39	< 3.5	< 1.5	~ 2	~ 1	< 0.4
50% Al_2O_3	50 ~ 55	36 ~ 38	< 2	<1	~ 2	~ 1	< 0.4
70% Al_2O_3	69 ~ 72	27 ~ 29	< 0.3	< 0.2	< 0.1	< 0.3	< 0.5
80% Al_2O_3	79 ~ 82	17 ~ 20	< 0.25	< 0.2	< 0.1	< 0.2	< 0.7

Secar® 71 ~70 % Al_2O_3 | Secar® 51 ~50 % Al_2O_3 | Fondu® 36~42 % Al_2O_3

Figure 6. Commercial CAC samples possessing different Al_2O_3 contents

In the presence of water, the CA phases can undergo hydration to form three main hydrate phases; CAH_{10}, C_2AH_8 and C_3AH_6 at different rates. CAH_{10} crystals are hexagonal prisms and possess a unit cell and ionic constitution of $Ca_3[Al_6(OH)_{24}]$. Structurally, the anions form rings of six edge-sharing octahedra, and Al is octahedrally coordinated. Chemically, much of the water molecules in CAH_{10} are very loosely bound. On the other hand, C_2AH_8 belongs to the AF_m family and is made up of platy, hexagonal crystals with excellent (001) cleavage. Microscopically, it is a layered double hydroxide made up of cationic $[Ca_2Al(OH)_6]^+$ main layers which are stabilized by negatively charged anions, OH^- located in the interlayer spacing by electrostatic attraction (**Figure 7**).

Figure 7. Schematic illustration of the layered structure of C_2AH_8

These first two hydrate phases are metastable, and with time they undergo conversion to form the stable, cubic hydrogarnet, katoite. Katoite (C_3AH_6) is the only stable ternary phase in the CaO–Al_2O_3–H_2O system at room temperature. Despite its stability, it is generally not a typical constituent of the hydrates of OPC due to its reactions with other components such as sulphate present. In such cases, ettringite is formed. However, during the hydration of CAC, C_3AH_6 is usually the main final product. This hydrogarnet phase crystallizes in various cubic forms, of which icositetrahedra are the most common at ordinary temperatures.

The rate of formation of the hydrated phases is dependent on the moisture, the temperature, the duration of reaction, and the presence of nucleating agents, etc. A simplified scheme utilizing CA as an example is shown in ***Scheme 1***. CA_2 and $C_{12}A_7$ react similar to CA. The formation of the calcium aluminate hydrates is responsible for the stiffening and rapid hardening of CAC concrete. However, due to the conversion process of the hydrate phases, an average decrease of 53 % in volume without a dramatic alteration of the overall dimensions of a concrete element can occur, resulting in increased paste porosity and decreased compressive strength [75]. The utilization of CAC must therefore be based on long term strength performance, and not on the initially high but transient strengths. For a typical CAC concrete, a final compressive strength of ~ 40 MPa is expected, while higher strengths can be obtained with limestone as coarse aggregate.

Reaction at low temperature, < 10°C:

$$CA + 10\ H \longrightarrow CAH_{10}$$
$$2\ CAH_{10} \longrightarrow C_2AH_8 + AH_3 + 9\ H$$
$$3\ C_2AH_8 \longrightarrow 2\ C_3AH_6 + AH_3 + 9\ H$$

Reaction at intermediate temperature:

$$2\ CA + 19\ H \longrightarrow 2\ C_2AH_8 + AH_3$$
$$3\ C_2AH_8 \longrightarrow 2\ C_3AH_6 + AH_3 + 9\ H$$

Reaction at high temperature, > 50°C:

$$3\ CA + 12\ H \longrightarrow C_3AH_6 + 2\ AH_3$$

Scheme 1. Reaction scheme for the hydration of CA at different temperatures

5.2 Layered Double Hydroxides and their Relevance in CAC

LDHs represent a class of layered materials with chemical composition expressed by the general formula $[M^{2+}_{1-x}M^{3+}_{x}(OH)_2]^{x+}[A^{n-}_{x/n} \cdot yH_2O]^{x-}$ where M^{2+} and M^{3+} are divalent and trivalent metal cations, A^{n-} is an anion/ anionic polymer possessing a charge of n-, and x attains a value between 0.20 and 0.33. In hydrotalcite type LDHs, the general lattice arrangement of the hydroxide layers is based on that of brucite, $Mg(OH)_2$, where each Mg^{2+} cation is octahedrally surrounded by six hydroxide groups and the different octahedra share edges to form infinite sheets [76]. In the LDHs, the M^{2+}/M^{3+} isomorphous substitution in octahedral sites of the hydroxide sheets results in a net positive charge, which is neutralized by existing anions and water molecules in the interlayers. A commonly known mineral is hydrotalcite which possesses the chemical formula of $[Mg_6Al_2(OH)_{16}CO_3 \cdot 4\ H_2O]$. It is a hydroxycarbonate of magnesium and aluminium and can be considered as another prototype of this class of LDH materials [77]. Such hydrotalcite-like materials are characterized by a disordered cation distribution within the hydroxide layers and a variable layer charge density.

In general, LDHs are also known as anionic clays. Alike clays, LDHs are made up of flexible, charged, nano- to micro-layers possessing incorporated water and compensating ions in the interlamellar space. Thus, these materials can also act as ion exchangers, and may swell and delaminate in suitable solvents. The main difference between LDH and clay is that while clays are cationic exchangers, LDHs work as anionic exchangers as they are cationic charged. Additionally, LDHs do not swell and delaminate expansively in water as a result of the high ion correlation forces [78] and the cohesive hydrogen bond network between the sheets of hydroxyl groups and intercalated hydration water present [79]. Due to the diverse possibilities of producing a host inorganic structure for the preparation of hybrid materials with interesting physical and chemical properties, the applications of LDHs cover a wide range of areas including catalysis [80], absorbents of anionic species [81], electrochemistry [82] and pharmaceutical [83].

In cement technology, LDH chemistry also plays an important role. During the hydration of ordinary Portland cement, in the presence of C_3A, sulfates and carbonate contaminants from CO_2, such layered AF_m phases including the calcium monosulfoaluminate ($Ca_4Al_2(OH)_{12}SO_4 \cdot 6\ H_2O$) and calcium monocarboaluminates (e.g. $3\ CaO \cdot Al_2O_3 \cdot CaCO_3 \cdot 11\ H_2O$) can be formed. Likewise, during CAC hydration at room temperature, C_2AH_8 is formed as the first product through rehydration of the CA clinker phases (**Scheme 1**). As mentioned previously, C_2AH_8 possesses a layered structure. This hydrate phase is similar to the hydrated products of C_3A, C_4AH_{13} and C_4AH_{19}. When left to stand for a few hours, C_2AH_8 undergoes partial depletion to form $C_2AH_{7.5}$ or C_2AH_{8-x} [84].

From a macroscopic view, all these hydrate phases belong to the family of hydrocalumite. Unlike the typical Mg based brucite or hydrotalcite, the calcium ions present in the main layers of these CaAl–LDH host do not occupy sites in the center of the layers. Instead, half of the Ca^{2+} ions are shifted up along the c direction and the other half, down. The Ca^{2+} ions are seven-coordinated, stabilized by the usual six hydroxyl groups and also bonded to a further water molecule present in the interlayer towards which they are shifted. As a result, the water molecules form two sub layers on either side of the center of the interlayer along the c-axis (**Figure 7**). Due to the unusual coordination environment of the Ca^{2+} ions, an ordered distribution of the cations within the hydroxide layers is induced, thus giving rise to a unique constant molar Ca^{2+}/Al^{3+} ratio of 2. In this respect, a differ-

ent model exists for such LDHs and independent studies are needed to further probe their chemistry and specific effects on polymers present during cement hydration, and the resulting mechanical properties.

The unique layered structure of the hydrate phase C_2AH_8 makes specific chemisorption of anionic molecules from solution possible. Anionic superplasticizers have been shown to intercalate into C_4AH_{13} and C_4AH_{19} to form layered organo-mineral phases (OMPs) of the general composition $[Ca_2Al(OH)_6](A)_x \cdot (OH)_y \cdot nH_2O$ [85]. The formation of intercalates has been analytically proven in model systems such as hydrating C_3A [86–88]. Plank *et al.* have shown that hydrating C_3A under idealized conditions with PCEs leads to the formation of organo-mineral phases of Ca–Al–PCE–LDH type [89, 90]. This sequestration of PCE into the AF_m crystallites depletes the dispersant from the pore solution and can reduce its effectiveness.

6 Materials

A complete set of the materials applied is presented in this chapter. A general overview on their usage and the motivations of these choices are reported here. Additional details and related results can be found in the publications which are part of this thesis.

6.1 PCE Polymers

A class of methacrylate based polycarboxylate superplasticizers with varying side chain lengths and MA:MPEG-MA molar ratios were used in this investigation. Their general formula is shown in **Figure 8**. The polycarboxylates employed here are widely known as 1st generation PCEs and they share a common anionic poly(methacrylate) trunk chain and hydrophilic PEO as their pendant groups. PCEs are weakly acidic due to the COOH groups, rendering them ionized (charged) in alkaline environments. Additionally, they are effective complexants for di- and tri-valent metal ions.

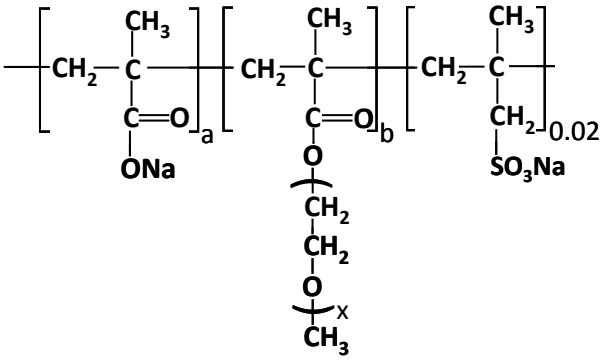

Figure 8. Chemical formula of MPEG- based PCE

Variation in the length of the polymer backbone, in the grafting density, or in the length of the side chains yields a great variation in the physicochemical and functional properties [91–93], giving rise to different workability in cement and concrete [94, 95]. Here, the superplasticizers tested in this work differentiate between a:b = 6; 3 and 1.5, and x = 45; 17 and 8.5. They are denoted by *x*PC*y*,

where *x* refers to the number of EOUs in the side chain, and *y* corresponds to the molar ratio of MAA:MPEG-MA. The PCE copolymers employed in this thesis contained an average of 4 to 29 methacrylate functionalities respectively. The specific anionic charge amounts increase as follow: 45PC1.5 < 45PC3 < 45PC6 < 17PC6 < 8.5PC6. The molecular characteristics and anionic charge amounts of the polymers are reported in Paper 1 and 3 for the experiments with OPC and clay systems, whereas those for calcium aluminate system are presented in Paper 4 and 5.

Poly(methacrylic acid) (PMA) was synthesized by aqueous free radical polymerization of MA [96], while the series of PEGs (2000, 750 and 350) were used as per obtained (Clariant, Frankfurt am Main/Germany).

6.2 Powder Materials

A sodium montmorillonite clay possessing a Si/Al ratio of ~ 3 and a specific surface area (measured by BET) of 467,000 cm^2/g was employed. Na montmorillonite clay was chosen as the clay due to its particularly strong influence on the workability of PCEs in the OPC system, as shown in previous work [6]. Detailed characterization of this clay can be found in Paper 1. As an OPC, a common CEM I 52.5 R HS/NA cement was utilized to generalize the impact of clay to common onsite systems (Paper 1–3). For the study on the workability of PCEs in CAC, a white CAC possessing 70 % Al_2O_3 content was employed to ensure a high purity, and to minimize the presence of other minerals such as gehlenite (Paper 4 and 5). A depiction of all 3 powder materials can be seen in **Figure 9**.

All studies were performed in cement pastes at different w/c ratios, or only in clay with synthetic pore solutions to minimize the influence from external factors. In all, 3 different core systems were employed: OPC + clay, clay alone and finally, only calcium aluminate cement. The w/c ratio employed varied from 0.52 to 15, and are presented in **Table 3**.

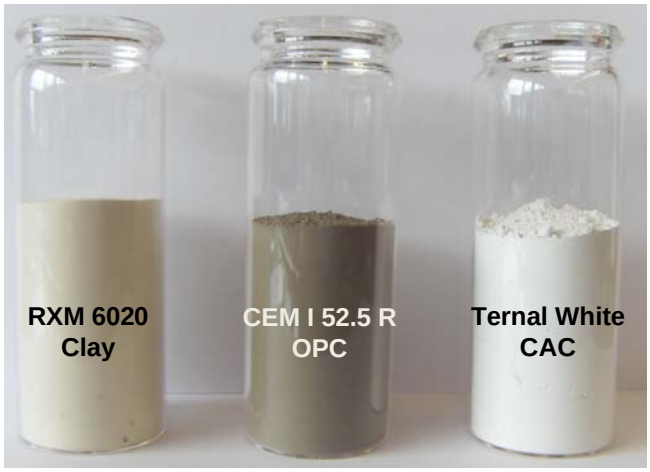

Figure 9. Powder materials employed in this study

Table 3. Water : cement (clay) ratio employed for the cementitious systems

Series	Experimental conditions	w/c ratio
1	Ordinary Portland Cement + clay	0.53
2	Clay in synthetic cement pore solution	53*
3	Clay in alkaline solution, at pH 12.8 w/ NaOH	53*
4	Calcium aluminate cement (actual application conditions)	0.52
5	Calcium aluminate cement (idealized conditions)	15

* w/clay ratio

6.3 Cement Pore Solution

For the model clay system presented in **Table 3** (System 2), the synthetic pore solution was conjured based on the actual composition of a cement pore solution [97]. The composition is presented in

Table 4.

Table 4. Composition of the synthetic cement pore solution (mmol/L)

Ions	SO_4^{2-}	Na^+	K^+	Ca^{2+}	OH^-	pH
Content	86	100	180	10	127	12.8

7 Methods

In this chapter, an overview of the main methods engaged in this thesis is presented. The scope and the working principles of the techniques used are described. Focus will be placed on small angle X-ray scattering analysis as it proofed especially useful in the analysis of the intercalation compounds. The sample preparation and further details regarding the measurements can be found in the publications.

7.1 Rheology Measurements

Rheological measurements on cement pastes yield direct information on the evolution of hydration reactions and on the relative performance of different superplasticizers and cement-superplasticizer combinations. Generally, it is accepted that the rheological behavior of cementitious materials such as concrete, mortar, cement pastes and grouts may be approximated using the Bingham model [98]. For this approximation, two independent parameters are needed to describe the rheological behavior: yield value and the plastic viscosity. In many cases such as the assumption based on steady state simple shear data [99–101], the plastic viscosity can be accounted for but the former variable has still to be measured. Traditional rheometry tests (Couette viscometer for cement paste) may be employed but these tests are often costly, time consuming and give too many information when only the yield value is required. On the contrary, in situ tests such as the stoppage test (or the "mini slump'' test) is much cheaper and simpler to conduct. This test is based on the theory that when shear stress drops to a value smaller than the yield value, the flow stops. The final spread of the paste is directly linked to the yield value, which can be calculated.

The rheological behavior of cement pastes and the dispersing power of the PCEs were thus determined by 'mini slump' test according to DIN EN 1015 (Paper 1–4). An illustration of the setup is presented in **Figure 10** and the correlated yield stress can be calculated by employing the equation from Roussel *et al*. [102]:

$$\tau_o = 1.747\,\rho\,V^2\,R^{-5} - \lambda\,(R^2 / V) \qquad \text{(Equation 1)}$$

Where τ_o = yield stress, ρ = density of the cement paste, V = volume of the cement paste, R = radius of cement and λ coefficient is a function of both the unknown tested fluid surface tension and contact angle. The application of this conversion can be seen in Paper 2.

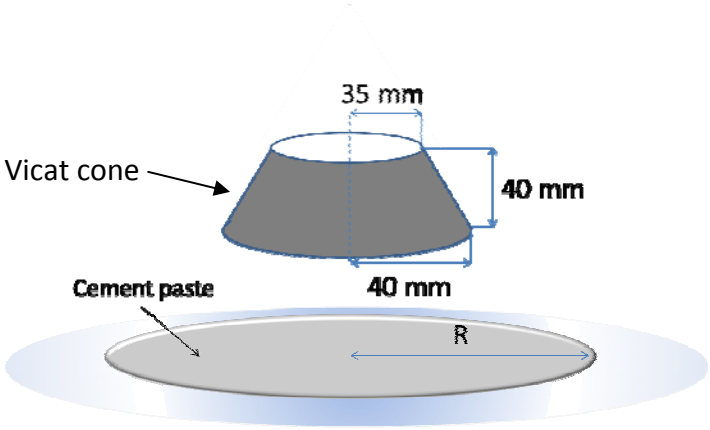

Figure 10. Setup of a "mini slump" test, R = radius of final spread

In general, the 'mini slump' test was used to give an indication of the rheological properties of the cement pastes in this thesis and the spread values were directly used for analyses. The main limitation of the 'mini slump' test is that it can only predict yield stress data for cement paste, but it does not give an idea for the strength development of the cement paste.

7.2 Sorption Studies

PCE sorption was determined by the depletion method utilizing the TOC and GPC analysis. For this purpose, the concentration of PCE polymer present in the mixing water prior to contact with cements or clay, and the non-adsorbed portion of the PCE remaining in solution after mixing with the cement or clay were measured (**Figure 11**). It was assumed that the removal of PCE from the cement pore solution solely was the result of interaction with cement or clay and that no precipitation had occurred. For the determination of isotherms, a range of PCE concentrations of up to 3 % bwoc

or 300 % bwo clay were utilized (Papers 1–3). For direct comparison to the results obtained in the "mini slump" tests, the fixed dosage used for these tests were employed.

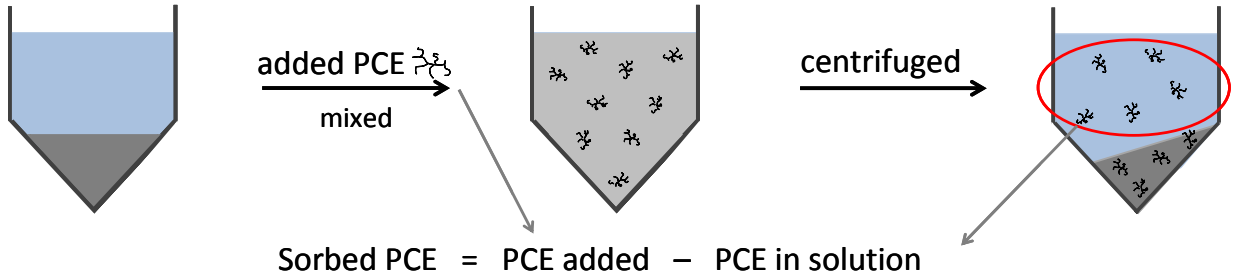

Figure 11. Principle of measuring PCE adsorption on cement and/or clay using the solution depletion method

Analysis of the carbon content of the solutions was mainly performed by combustion at 890 °C in a HIGH TOC II instrument (Elementar, Hanau/Germany; Papers 1, 2 and 3). However, this method has an acute limitation due to its disability to differentiate between surface adsorption and chemical absorption. Additionally, it only gives an overview of the total change in the organic content of the sample and cannot distinguish between different organic substances present. Therefore, in specific cases where quantified differentiation of PCEs from PEG was required, size exclusion chromatography (SEC or otherwise known as gel permeation chromatography, GPC) was utilised. SEC works based on size differences between polymers. Thus, it is an ideal method for the quantification of polymers when the difference in molecular weight is greater by an order of magnitude. Further details can be found in Paper 2.

7.3 X-ray Diffraction

X-ray diffraction is a very important experimental technique that has long been utilized to address challenges related to the crystal structure of solids, including lattice constants and geometry, identification of unknown materials, orientation of single crystals, preferred orientation of polycrystals, defects, stresses, etc [103]. In XRD, a collimated beam of X-rays possessing a wavelength typically

ranging from 0.7 to 2 Å, is incident on a specimen and is diffracted by the crystalline phases in the specimen according to Bragg's law, as displayed in **Figure 12**.

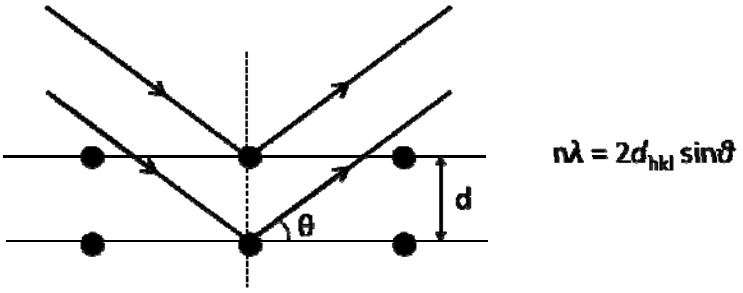

Figure 12. Schematic illustration of x-ray diffraction and Bragg's law, *d* refers to the spacing between the atomic planes in the crystalline phase and λ is the X-ray wavelength

This diffracted beam is characteristic of the fingerprint lattices of each individual sample, making identification of known crystalline compounds easy. In such a way, it also enables the calculation of change in *d*-spacing arising from the change in lattice constants under a strain. Peak broadening of reflections can also give further information on the finite size of crystallites or the inhomogeneous strain from samples. Typically, analysis of cement samples is first done with conventional XRD, followed by quantitative analysis using Rietveld refinement. XRD can detect the change in *d*-spacing characteristic for the formation of organo-mineral phases and for hydrated clay samples (**Figure 13,** Papers 4 and 5).

7.4 Small Angle X-ray Scattering (SAXS)

SAXS is a small angle technique for the study of structural features of samples which have inhomogeneities. It works based on elastic scattering of X-rays (λ = 0.1 ~ 0.2 nm) at low angles (typically 0.1 ~ 10 °2θ, close to the primary beam). The scattering of the radiation in the sample leads to interference effects, resulting in a scattering pattern (**Figure 14**), which can be analyzed to provide information on the inhomogeneities of electron density with characteristic dimensions between one and a few hundred nanometers [104].

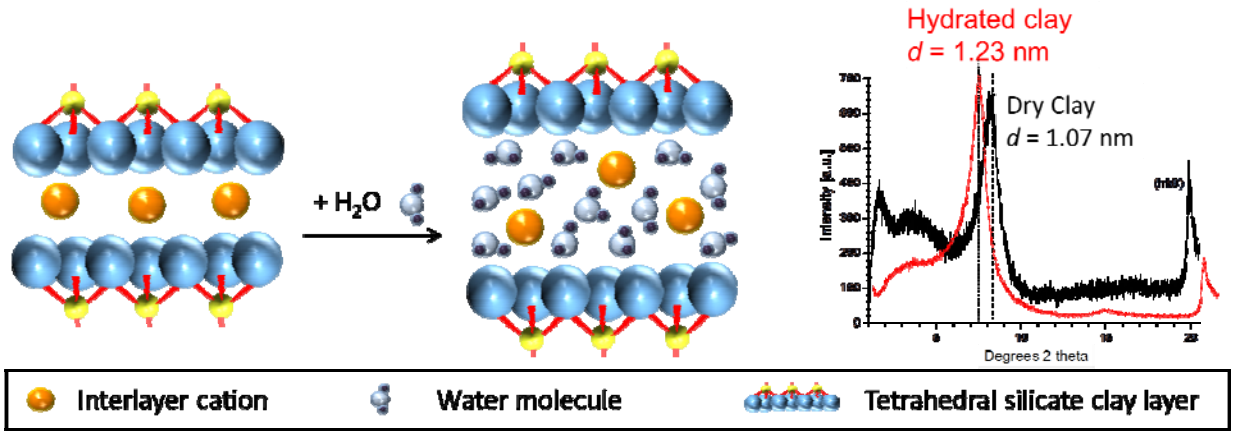

Figure 13. Schematic illustration of (left) the change in *d*-spacing of Na montmorillonite clay after hydration and (right) XRD spectrum of clay before and after hydration

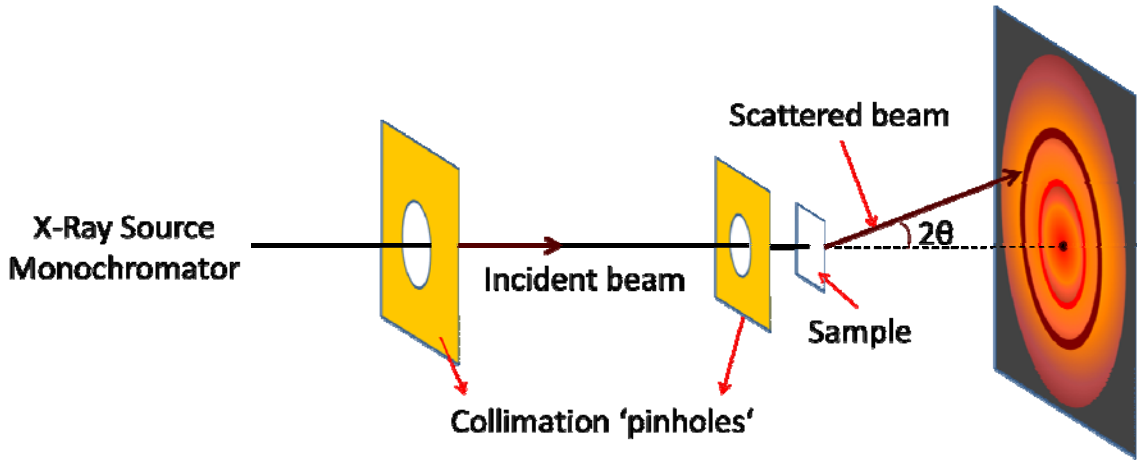

Figure 14. Illustration of a typical SAXS setup

Using a SAXS system, regular WAXS (wide angle X-ray scattering) analysis is often performed too. As its name implies, WAXS analysis scans across a wide range of angles, making the analytical results similar to that obtained from a XRD analysis. WAXS analysis focuses on the location, width and shift of the Bragg peaks which arise from crystalline lattice structures. In SAXS analysis, on the other hand, the size and shape of particles in solution or solid state can be derived from the scanned data. The angular range from SAXS analysis makes it also viable to still observe Bragg peaks as a result of characteristic distances arising from partially ordered materials. Thus, structural informa-

tion of substances possessing repeated distances between 5 and 25 nm in partially ordered systems of up to 150 nm can be obtained [105]. Therefore, in the analysis of organo-mineral phases, this method is an ideal alternative method to XRD analysis, especially in cases when the intercalates possess low nanocrystallinity (high degree of disorderness) and large intergallery spacings (Paper 5).

Interpretation of SAXS data can be a very difficult task. When interpreting the data, mathematical idealized models are often used to determine the nature of the sample being analyzed. In turn, these models are developed and are fine-tuned according to specific structural forms of the particles present. For example, a fit based on hollow cylinders cannot be used in the analysis for a system containing spherical particles. Therefore, it is important to perform complementary analysis such as SEM imaging to determine the morphology of the products before interpreting any SAXS data.

When analyzing SAXS data, the main information can be obtained from the 2D imaging of a scanned sample. For ease of interpretation, this 2D image is often mathematically translated into a spectrum with characteristic reflections corresponding to the distribution of electron densities shown in the 2D image. **Figure 15** shows the 2D representation and the corresponding SAXS profile (spectrum) of the colloidal particles from an OPC sample hydrated in the presence of 40 % bwoc of a PCE superplasticizer. Whereby the SAXS profile is obtained by mathematical integration of the entire SAXS image (left).

The (00*1*) and (00*2*) reflections displayed in the SAXS profile are characteristic for layered structures and they correspond to the electron rich rings present in the 2D image. The sharp signal at ~ 0.22 A^{-1} corresponds to an artifact generated during the SAXS scan. Therefore, it is important to countercheck all 'weird' reflections in the SAXS profile against the 2D image. The *d*-spacings of layered structures can be derived from the q values (x-axis) of the (00*1*) reflection using Equation 2.

d-spacing of the layered structure = $2\pi / q$ Å (Equation 2)

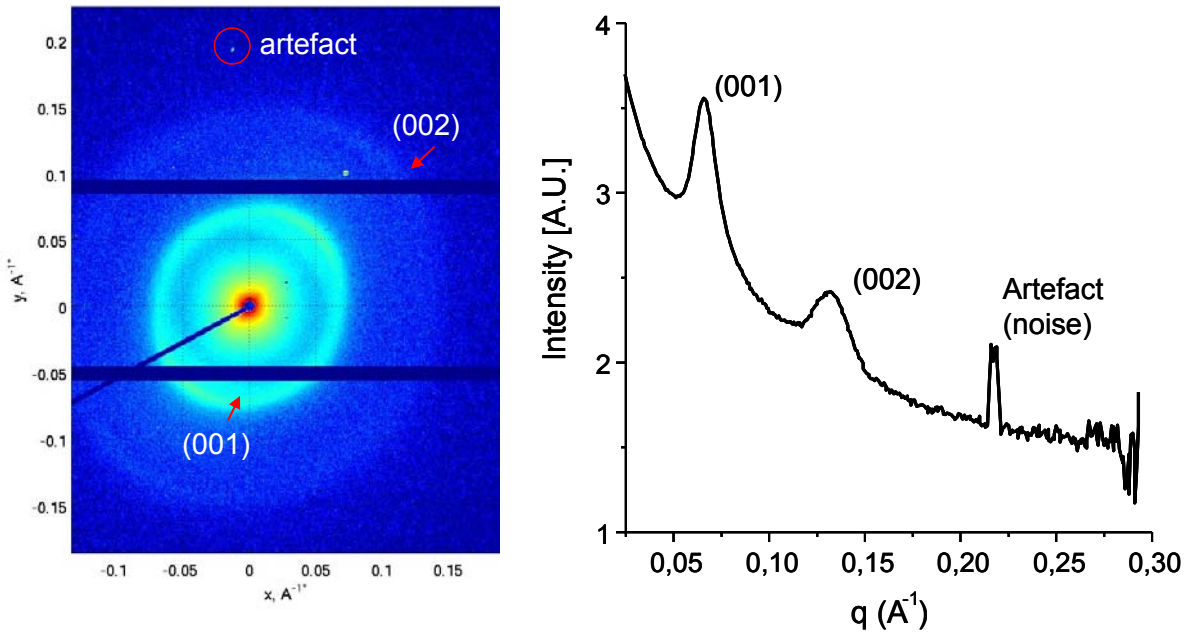

Figure 15. SAXS analysis showing (left) 2D representation and (right) spectrum for an OPC sample hydrated at room temperature with 40 % bwoc of PCE polymer 45PC6 (90 min, w/c = 15)

The highly diffused rings shown in the 2D image contribute to the broadness of the reflections and can be attributed to the low degree of orderness of the layered compounds present in the sample. Furthermore, the eclipsed nature of the ring present in the 2D image represents a preferential arrangement of the electron density in the sample, possibly arising from a preferred orientation of the copolymers in the intercalates. In general, an increase in the orientation and crystallinity of a product will result in higher distortion of the rings (more eclipsed) in a 2D image which will finally give rise to well defined rings and 'pinpoint dots' for an ordered and crystalline material (**Figure 16**).

For the experiments reported here, SAXS was performed on a Ganesha 300XL SAXS-WAXS system (SAXSLAB ApS, Copenhagen/Denmark) equipped with a GENIX 3D microfocus X-ray source and optic, a three-slit collimation system, a fully evacuated sample chamber and beam path, and a movable 2D Pilatus 300K detector.

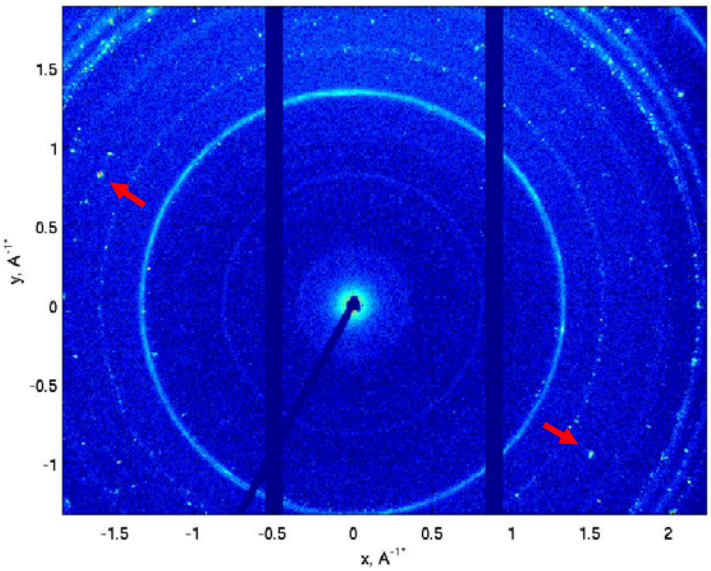

Figure 16. SAXS 2D representation of an OPC sample hydrated at room temperature for 90 min (w/c = 15)

7.5 Scanning and Transmission Electron Microscopy

SEM was performed on a XL30 ESEM FEG instrument (FEI Company/USA) for the visualization of surface topography of the samples. It works based on a beam of electrons which is scanned in a raster scan pattern and the magnification is controlled by the current supplied to the x,y scanning coils. In this work, the highest magnification achieved was 100,000 times. An added advantage of SEM is its ability to provide information on the chemical composition of samples near the surfaces through EDX. This enhances the working capacity of this instrument to look at both the morphological details, but also detailed information on the chemical composition and distribution. The TEM, on the other hand has a much higher magnification as it is focused on the penetration of electron beams through ultrathin specimens, giving an in-depth observation of the sample. Here, TEM images were captured with a JEOL JEM-2100 instrument (JEOL Company, Tokyo/Japan). Typical sample holders for SEM and TEM can be observed in **Figure 17**.

In such visualization methods, sample preparation plays a huge role in the capturing of desired images. Here, the samples were resuspended in isopropanol and sonicated for a minute to decrease the agglomeration of particles before subjecting to the sample holders. Thereafter, they were left to dry at room temperature. In this way, better dispersed samples were obtained, enabling ease of image capturing on both devices (Papers 4 and 5).

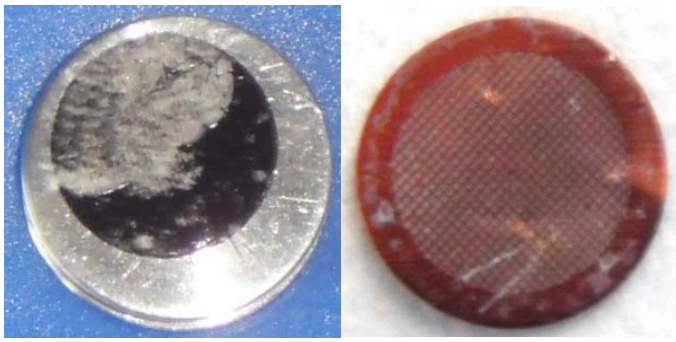

Figure 17. Sample holder for SEM (left) and copper grid (3mm) for TEM (right) holding CAC samples

7.6 Zeta Potential

Zeta potential is the potential difference between the dispersion medium and the stationary layer of fluid attached to the dispersed particle (**Figure 18**). Therefore, it is also considered as the electric potential in the interfacial electric double layer at a location of the slipping plane. In liquids, the surfaces often bind layers of molecules or ions or polyelectrolytes. This results in a deviation of the slipping plane from the solid-liquid interface.

Quantification of the zeta potential of the particles in suspension was performed by the electroacoustic method applying a model DT 1200 Electroacoustic Spectrometer from Dispersion Technology, Inc. (Bedford Hills, NY/USA). The principle is based on ultrasound propagation through the medium, resulting in an electroacoustic phenomenon called colloid vibration current, from which the zeta potential is then calculated. The advantage of this method lies in its ability to

perform measurements in intact samples, i.e. without dilution. Here, all the zeta potential tests were performed in concentrated suspension, in order to compare the results with the ‘mini slump’ test measurements (see Papers 1–3).

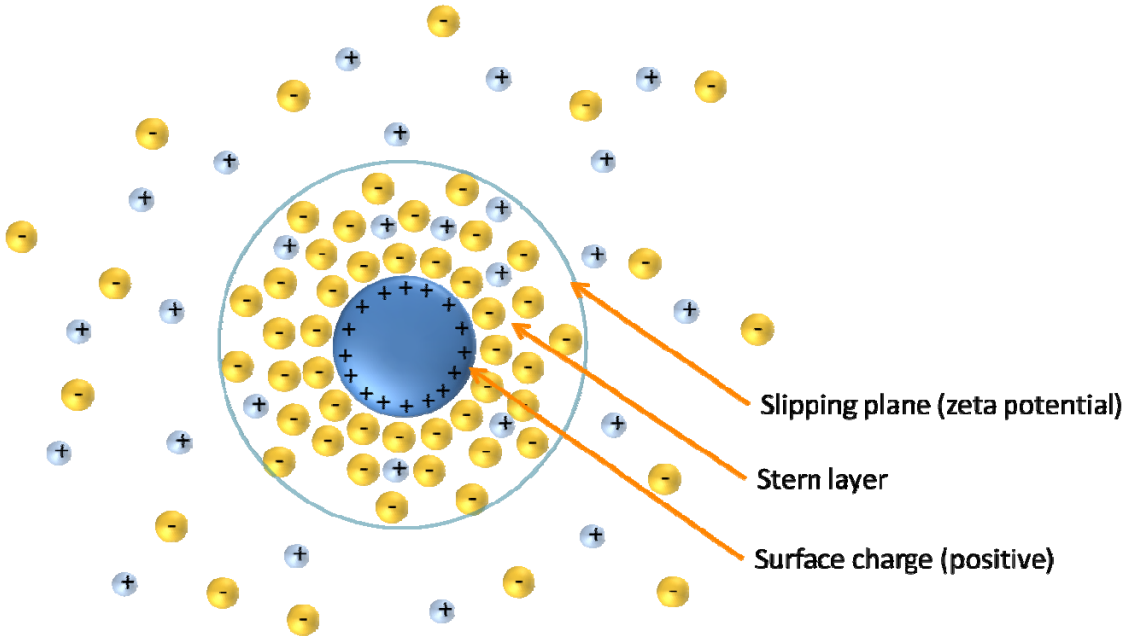

Figure 18. Schematic illustration of electric double layer and zeta potential

8 Main findings

The key results from the whole set of publications are summarized in this chapter accordingly.

8.1 Effect of Clay on PCEs possessing Varying Grafting Density (Papers 1 and 2)

In this investigation, two PCEs possessing a long side chain (45 EOUs), but with varying grafting densities (MA:MPEG-MA molar ratios of 6 and 1.5) were employed. The presence of sodium montmorillonite clay was confirmed to greatly impact the flowability of cement pastes, particularly when the PCEs were added (**Figure 19**). This was due to the extremely high affinity of clay for water and PCEs, thus achieving a significantly high sorbed amount (~ 100 times that for OPC).

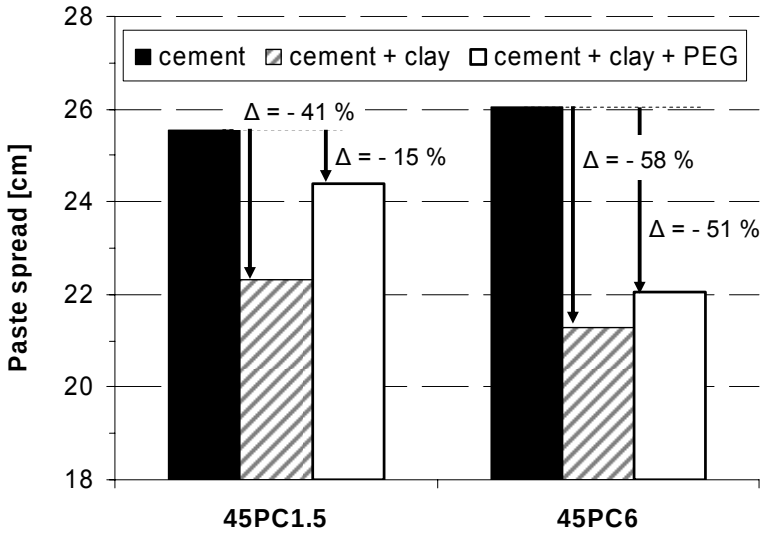

Figure 19. Paste spread of cement slurries with and without 1 wt. % of clay added, in the presence of 1.07 % bwoc of PCE polymer 45PC1.5 and 0.09 % bwoc of 45PC6, with or without PEG–2000 added in equivalence to the PCE dosages (w/clay = 0.53)

The main driving force behind this process was found to be chemisorption driven by the intercalation of the PEO side chain of PCE into the clay layered structure via hydrogen bonding with water

molecules anchored by the silanol groups between the alumosilicate layers. This is alike that for PEGs (**Figure 20**). On the other hand, surface adsorption of the PCE onto the clay surfaces by electrostatic attraction accounts only for a minor amount of PCEs consumed by clay.

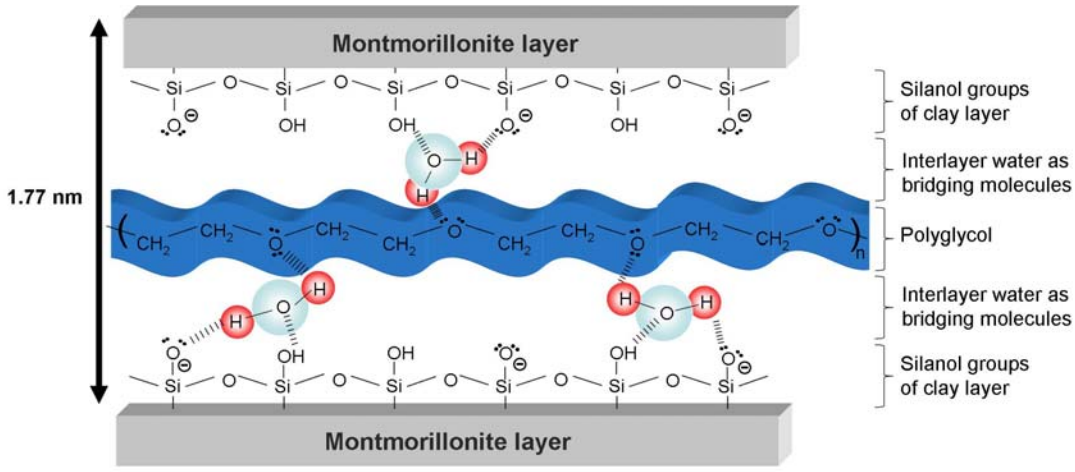

Figure 20. Conceptual illustration of polyglycol intercalation between the alumosilicate layers of montmorillonite

Due to the high affinity of the PCEs for clay via intercalation of their PEO side chains, PEG–2000 (same M_w as the PEO chain) was added as a sacrificial agent. The addition was found to be highly effective and greatly reduce the negative impact of clay, particularly when 45PC6 possessing high grafting density and long side chains was utilized (**Figure 19**).

8.2 Influence of Clay on PCEs with Varying Side Chain Lengths (Paper 3)

The impact of clay contaminant on cement paste when PCEs possessing varying side chain lengths but fixed grafting density (molar ratio MA:MPEG-MA = 6:1) were utilized is presented in paper 3.

Here, the length of the PEO side chain was varied from 8.5 to 45 EOUs. Alike previous results, clay contaminant has a high affinity for PCEs and this consumption of PCE by clay drastically decreased the dispersing performance of all PCEs in cement pastes. Effectiveness of PCEs with longer side

chains was more affected than from those with shorter side chains (**Figure 21**), suggesting that at the range of working dosages, failure of such PCEs might be correlated to their ease of intercalation.

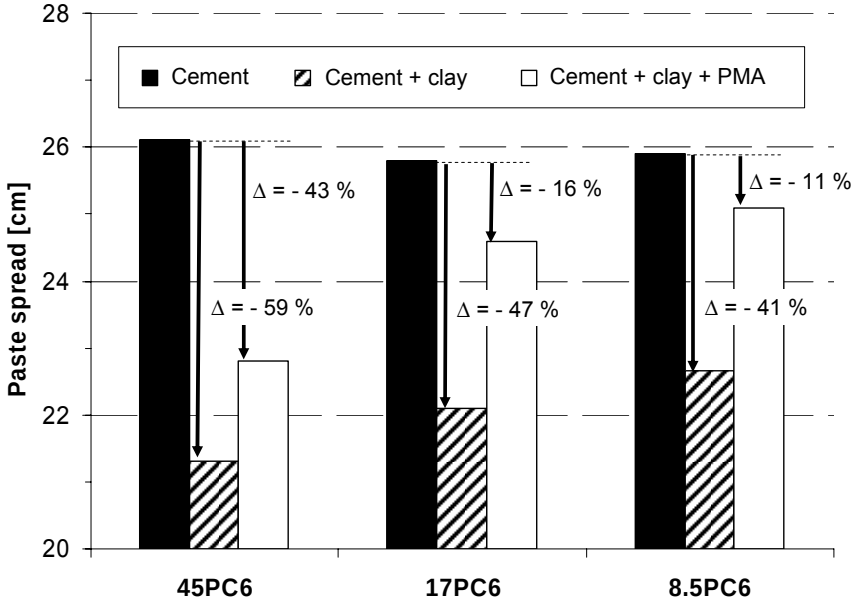

Figure 21. Paste spread of cement slurries with and without 1 wt. % of clay added, in the presence of 0.09 % bwoc of PCE polymer 45PC6, 0.07 % bwoc of 17PC6 and 0.07 % bwoc of 8.5PC6, with or without PMA added in equivalence to the PCE dosages (w/clay = 0.53)

At higher dosages, the PCE possessing longer side chains (45 EOUs) remained sorbed by clay mainly through intercalation via their poly(ethylene oxide) side chains into the interlayer space of the alumosilicate layers. However, for PCEs possessing shorter side chains (17 and 8.5 EOUs), the electrostatic attraction mediated by surface adsorbed Ca^{2+} cations contribute greatly. In the case of 17PC6, electrostatic attraction accounts for almost 50 % of the total sorbed amount of PCE (**Figure 22**). This demonstrated that for such PCEs, PEG which works solely against the consumption of PCE via intercalation is not an ideal sacrificial agent. Instead, a linear anionic polymer, poly(methacrylate) (PMA) proved to be an effective remedy for such PCEs which possess shorter side chains (**Figure 21**).

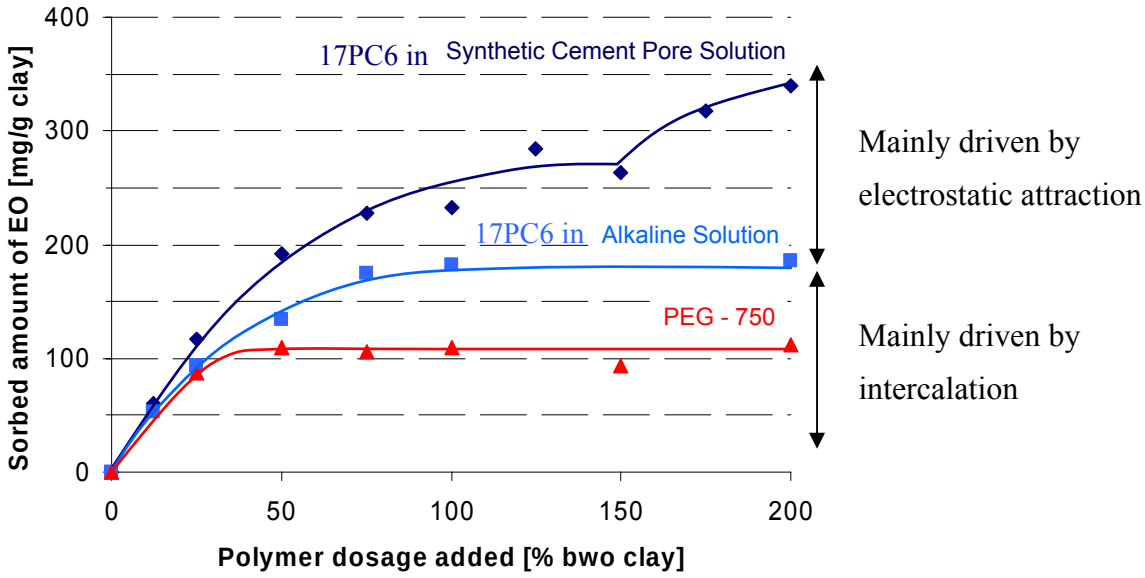

Figure 22. Amount of EO in 17PC6 and PEG–750 sorbed by clay in synthetic cement pore solution and alkaline solution, adjusted to pH 12.8

8.3 Organo-Mineral Phases Formed During Early Hydration of CAC (Papers 4 and 5)

The mechanism at play during early hydration of a high alumina cement in the presence of PCEs and the consequential effects on the workability of PCEs in cement paste were demonstrated in Papers 4 and 5.

Parametric studies showed that PCEs are extremely effective dispersants for CAC. These PCE copolymers disperse CAC at dosages an order of magnitude lower than those required for OPC. Also, PCEs display differing dispersing ability in a CAC system compared to an OPC system, whereby the more anionic copolymers disperse the cement more effectively (**Figure 23**). This difference can be attributed to the intercalation ability of the PCEs into the hydrate phases such as C_2AH_8 formed during early hydration of CAC. Under idealized condition (PCE dosages = 40 % bwoc, w/c = 15), preferential intercalation of the more anionic PCEs was shown in XRD analysis (**Figure 24**). This accounts for the difference in efficiencies of the PCEs during actual application: more anionic PCEs

are less effective in dispersing CAC than the less anionic ones. This result was confirmed by SAXS analysis where the intercalating ability of the PCEs was found to be independent of their M_w and only dependent on their PDIs.

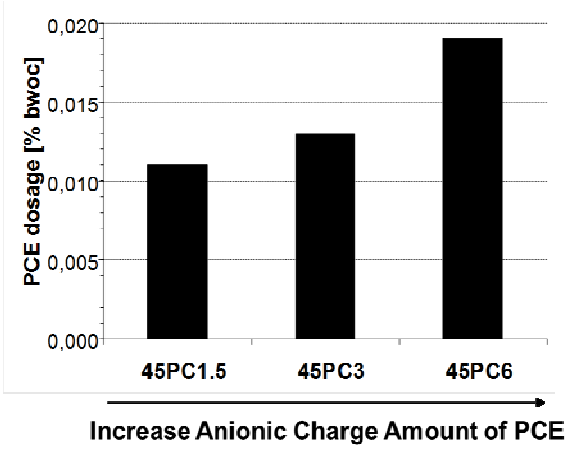

Figure 23. PCE dosages required to achieve a CAC paste spread of 26 ± 0.5 cm (w/c = 0.52)

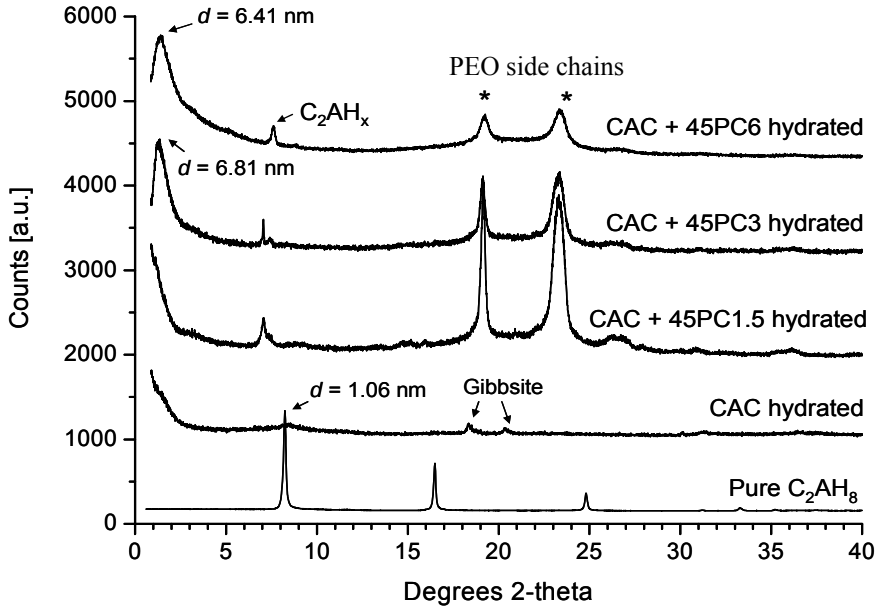

Figure 24. XRD patterns: C_2AH_8 (relative intensity = 1/16); hydrated CAC sample; CAC hydrated in the presence of PCE polymers 45PC1.5, 45PC3 and 45PC6 respectively

Similarly, under actual application conditions, formation of organo-mineral phases holding PCE was confirmed by SAXS analysis (**Figure 25**). The broad reflection observed in SAXS analysis can be attributed to the polydispersity of the PCEs and the short reaction time of mere 4 minutes for the mixing of the PCEs in the cement slurry. Further confirmation was obtained from SEM (with EDX) and TEM imaging (**Figure 26**) where layered nanofoils with high carbon contents were observed, confirming that intercalation of such PCEs indeed had occurred during the actual early hydration of CAC.

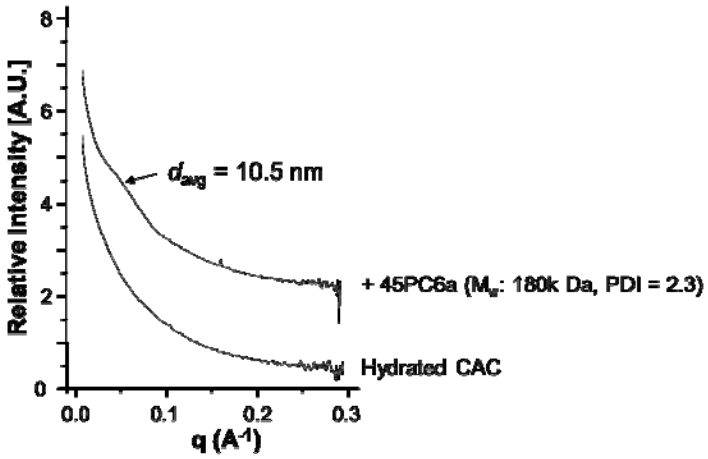

Figure 25. SAXS profiles of the CAC sample hydrated in the presence and absence of 0.05 % bwoc of 45PC6 (M_w = 180,000 Da) at a w/c ratio of 0.52, reacted for 4 min at room temperature

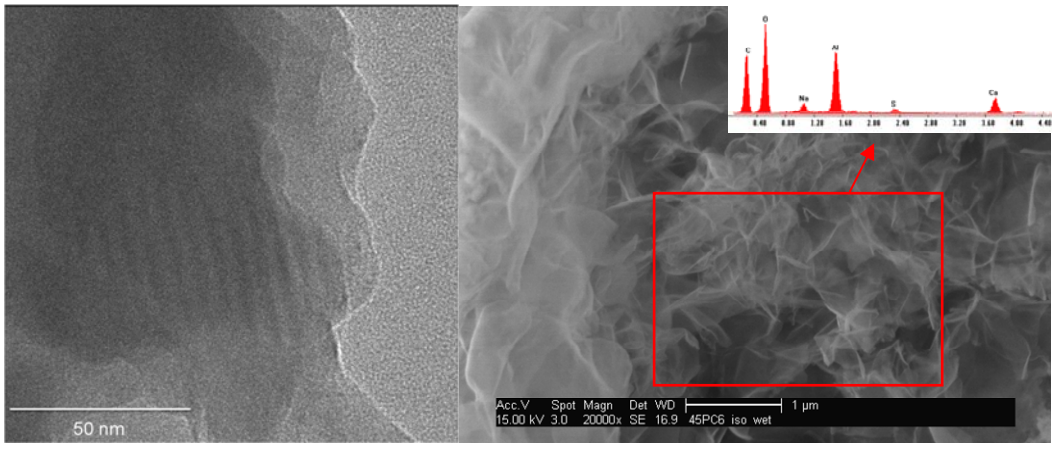

Figure 26. TEM (left) and SEM (right) images of CaAl-45PC6-LDH obtained from CAC hydration under real application conditions (0.019 % bwoc of 45PC6, w/c = 0.52)

The results confirmed that CAC is best dispersed by PCEs possessing lower anionic charge amounts as their consumption by intercalation is lower and thus the availability for dispersion in a CAC paste is higher.

Another conclusion from this investigation is the reliability of experimental instrumentation. A common detection method of layered structures (or lattices) is XRD analysis. However, during our investigations, detection of PCE–LDH intercalates via conventional XRD analysis was only possible under optimized conditions as observed in the long scan results presented in **Figure 27**. Under normal scanning conditions commonly employed for routine scans (short scan), no intercalates could be observed. Therefore, usage of XRD analysis as a detection method must only be performed bearing this into consideration. A more reliable and accurate method is SAXS analysis.

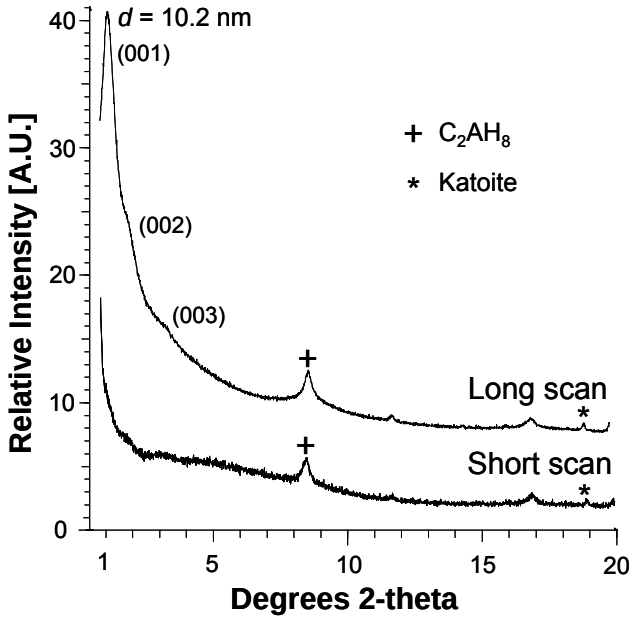

Figure 27. XRD diffractograms of a CAC sample hydrated in the presence of 0.05 % bwoc of PCE polymer 45PC6a at a w/c ratio of 0.52, reacted for 4 min, measured under two scanning conditions

9 Conclusion and Outlook

In this thesis, two main issues dealing with the dispersing effectiveness of PCEs with different cements (and contaminants) and the underlying mechanisms were highlighted.

In the first part of the investigations, we confirmed that clays diminished the effective dispersing power of polycarboxylate-based superplasticizers. This can be attributed to the consumption of PCEs by clay through intercalation via their side chains. With decreasing side chain length of PCEs, the role of electrostatic attraction of the anionic PCEs as mediated by a layer of Ca^{2+} adsorbed onto the negative clay surfaces increased. Accordingly, to combat this reduction in the dispersing power of PCEs as a result of the chemisorption, the best solution was to use PEG as a sacrificial agent for PCEs possessing high grafting density. Poly(methacrylate) or in combination with PEG was found ideal when PCEs exhibiting low grafting density were utilised.

Addition of polymers as sacrificial agents in combating this clay contaminant issue presents one potential solution, but it increases cost. Therefore, further alternatives should be evaluated. One method includes employing cheaper substituents such as polyelectrolytes possessing long chains with ionizing groups located along the entire chain length or proteins which exhibit a higher affinity to clay than PCEs. A second and better concept is to synthesize new superplasticizers which are clay tolerant. Recently, such new type of PCE had been presented in the literature which is based on hydroxyallyl side chains [106]. The unique functionality of the novel PCE render intercalation into clay impossible, thus decrease their consumption. Another potential synthesis route for new clay-tolerant PCEs which may be explored involves the ionization of the end groups in the PEO side chains so as to prevent onset of intercalation, the main driving detriment for the dispersion of cements.

In the second part of this thesis, an experimental proof for the formation of organo-mineral phases incorporating highly anionic PCEs during early hydration of CAC under typical field conditions was achieved. The high intercalating tendency of more anionic PCEs explained their poor dispers-

ing power as compared to the less anionic PCEs in CAC, which was contrary to that in OPC. Additionally, the added dosage of PCEs was an order of magnitude lower than that for OPC. From SAXS analysis, it was clearly evidenced that the intercalates formed possessed a wide range of *d*-values, as a result of the broad PDI of such copolymers and turbostratic disorders resulting from the short reaction time. XRD was shown to be a less favorable method because it can fail to detect intercalates with low stacking orders although they are clearly present according to SAXS measurement.

This study highlights a significant leap in the field of CAC research. For the first time, we have shown that intercalation of PCEs indeed occurred in an actual cement system, under actual application conditions, and that it greatly impacts the performance of such superplasticizers. Such chemical consumption is highly undesired. However, due to the fact that a very small amount of PCE was needed for effective dispersion, application of PCEs can still be favorable when only short duration of flowability is demanded. Also, the strong intercalation tendency of PCEs into CAC may be exploited to provide potential carriers of such PCE copolymers into other systems, where e.g. delayed dispersion, facilitated via anionic exchange mechanisms is needed.

Another lesson learnt from this work is careful consideration of the methodology and instruments for intercalate analysis. Due to the limitations and differences in experimental methods, it was observed that for the future determination of such intercalate compounds, much attention must be placed on the preparation and the choice of instrument. Whereby, SAXS analysis was found to present a much preferred method over XRD analysis. When higher resolution is needed, another potential method for the analysis of such intercalates is neutron and synchrotron X-ray diffraction.

References

[1] J. G. Cabrera, R. Rivera-Villarreal, The Role of Admixtures in High Performance Concrete, In: Proceedings of the International RILEM Conference, RILEM Publication (1999).

[2] V. S. Ramachandran, V. M. Malhotra, C. Jolicoeur, N. Spiratos, Superplasticizers: Properties and Applications in Concrete, CANMET Publication, Canadian Government Publishing Centre Supply & Services Canada, USA, ISBN 066017393X (1998).

[3] A. M. Paillere, Application of Admixtures in Concrete, RILEM Report 10, E & FN SPON Publishing, 1st Edition, London, UK (1995).

[4] S. N. Ghosh, Cement and Concrete Science & Technology, In: Progress in Cement and Concrete, Vol. 1, Part 1, 1st Edition, Abi Books Private Limited, New Delhi, India (1991).

[5] V. A. Fernandes, P. Purnell, G. T. Still, T. H. Thomas, The Effect of Sand Content used for Cementitious Materials in Developing Countries, Cem. Concr. Res., 37 (2007) 751–758.

[6] J. Plank, C. Liu, G. B. S. Ng, Interaction between Clays and Polycarboxylate Superplasticizers in Cementitious Materials, Malhotra V. M. Ed. 9th CANMET/ ACI International Conference on Superplasticizers and Other Chemical Admixtures in Concrete, Seville/Spain, American Concrete Institute, Supplementary volume (2009) 279–298.

[7] R. Bayer, H. Lutz, Dry Mortar in: Ullmann's Encyclopedia of Industrial Chemistry (2010) DOI: 10.1002/14356007.f16_f01.pub2.

[8] V. K. Singh, High Alumina Refractory Castables with Calcium Aluminate Binder, J. Mater. Sci. Lett., 8 (1989) 424–426.

[9] F. Massazza, U. Costa, A. Barrila, Interaction between Superplasticizers and Calcium Aluminate Hydrates, J. Am. Ceram. Soc. 65 (2006) 203–207.

[10] M. M. Alonso, T. Váquez, F. Puertas, M. Palacios, Compatibility between PCE Admixtures and Calcium Aluminate Cement, Proceedings of the 13th ICCC International Congress on the Chemistry of Cement, Abstract book, Madrid, Spain (2011) 382–388; full paper: ISBN: CD 978-84-7292-400-0 (7 pages).

[11] J. Plank, Z. Dai, P. R. Andres, Preparation and Characterization of New Ca-Al-Polycarboxylate Layered Double Hydroxides, Mater. Lett. 60 (2006) 3614–3617.

[12] G. R. Tucker, US 2,052,586, (1936), Dewy and Almy Chemical Company.

[13] Z. M. Wang, X. Liu, X. Cheng, Study on the Compatibility of a PCE with Raw Materials of

Concrete, Malhotra V. M. Ed. 10th CANMET/ ACI International Conference on Superplasticizers and Other Chemical Admixtures in Concrete, Prague/Czech Republic, American Concrete Institute, Supplementary volume (2009) 216–228.

[14] J. M. Zhu, Liaoning Oxiranchem. Inc., Presentation at 3rd National Conference on PCE Superplasticizers, Beijing, June 25–27 (2011) (In Chinese).

[15] T. Hirata, JP 84, 2022, S59-018338 (1981), Nippon Shokubai Co., Ltd.

[16] E. Sakai, A. Ishida, A. Ohta, New trend in the Development of Chemical Admixtures in Japan, J. Adv. Concr. Technol. 4 (2006) 211–223.

[17] K. Hattori, C. Yamakawa, S. Suzue, T. Azuma, T. Imamura, Y. Ejiri, Flowing concrete, Review of General Meeting, Technical Session – Cement Association of Japan, 30 (1976) 153–154.

[18] A. Aignesberger, P. Bornmann, H.-G. Rosenbauer, H. Theissig, DE 2,359,291, 1974, SKW Trostberg AG.

[19] A. Aignesberger, J. Plank, DE 3,144,673, 1981; J. Plank, A. Aignesberger, DE 3,344,291, 1981, SKW Trostberg AG.

[20] M. Pei, D. Wang, X. Hu, D. Xu, Synthesis of Sodium Sulfanilate-Phenol-Formaldehyde Condensate and its Application as a Superplasticizer in Concrete, Cem. Concr. Res. 30 (2000) 1841–1845.

[21] H. Uchikawa, S. Hanehara, D. Sawaki, The Role of Steric Repulsive Force in the Dispersion of Cement Particles in Fresh Paste prepared with Organic Admixture, Cem. Concr. Res. 27 (1997) 37–50.

[22] J. P. Guicquero, P. Maitrasse, M. Mosquet, A. Sers, Chryso SA, FR 2,776,285 (1998).

[23] S. Akimoto, S. Honda, T. Yasukohchi, EP 0,291,073 A2 (1988) Nippon Oil and Fats Company, Ltd.

[24] G. Albrecht, J. Weichmann, J. Penkner, A. Kern, EP 0,736,553 A2 (1996) SKW Trostberg AG.

[25] M. Yamamoto, T. Uno, Y. Onda, H. Tanaka, A. Yamashita, T. Hirata, N. Hirano, US 6,727,315 B2 (2004) Nippon Shokubai Co., Ltd.

[26] D. Hamada, F. Yamato, T. Mizunuma, H. Ichikawa, DE 10,048,139 A1 (2001) Nippon Shokubai Co., Ltd.

[27] H. Tahara, H. Ito, Y. Mori, M. Mizushima, US 5,476,885 (1995) Nippon Shokubai Co., Ltd.

[28] T. Amaya, A. Ikeda, J. Imamura, A. Kobayashi, K. Saito, W. Danzinger, T. Tomoyose, WO

00/39045 (2001) Sika Ltd and Toho Chemical Industry Co., Ltd.

[29] J. Witt, J. Plank, A Novel Type of PCE possessing Silyl Functionalities, Malhotra V. M. Ed. 10th CANMET/ ACI International Conference on Superplasticizers and Other Chemical Admixtures in Concrete, Prague/Czech Republic, American Concrete Institute, SP–288 (2012) 57–70.

[30] J. Plank, K. Pöllmann, N. Zouaoui, P. R. Andres, C. Schaefer, Synthesis and Performance of Methacrylic Ester based Polycarboxylate Superplasticizers Possessing Hydroxy Terminated Poly(ethylene glycol) Side Chains", Cem. Concr. Res. 38 (2008) 1210–1216.

[31] S. Pourchet, S. Liautaud, D. Rinaldi, I. Pochard, Effect of the Repartition of the PEG Side Chains on the Adsorption and Dispersion Behaviors of PCP in presence of Sulfate, Cem. Concr. Res., 42 (2012) 431–439.

[32] J. P. Guicquero, Ph. Maitrasse, M. A. Mosquet, A. Sers, A Water Soluble or Water Dispersible Dispersing Agent, FR 2,776,285 (1999).

[33] H. Okamura, M. Ouchi, Self-Compacting Concrete, J. Adv. Concr. Technol. 1 (2003) 5–15.

[34] S. Matsuo, M. Yaguchi, T. Sugiyama, H. Nagamine, Slump Retention of a Polycarboxylate-based AE High Range Water-Reducing Agent", Cem. Sci. Concr. Technol. 52 (1998) 242–247.

[35] M. Kinoshita, T. Suzuki, K. Soeda, T. Nawa, Properties of Methacrylic Water-Soluble Polymer as a Superplasticizer for Ultra High-Strength Concrete, Malhotra V. M. Ed. 5th CANMET/ ACI International Conference on Superplasticizers and Other Chemical Admixtures in Concrete, Rome, Italy, ACI, SP–173 (1997) 143–162.

[36] M. Shigemi, S. Takumi, S. Koei, G. Tsutomu, H. Kenji, Y. Hironobu, Workability Improving Superplasticizers 'RHEOBUILD SP8SV' and 'RHEOBUILD SP8RV', Trans. NMB Central Res. Lab.Annual Research Report, 14 (2002) 28–36 (In Japanese).

[37] M. Wallace, Flowing Concrete produced at the Batch Plant, Concrete Construction 30 (1985) 337–343.

[38] H. H. Murray, Applied Clay Mineralogy: Occurrence, Processing and Application of Kaolins, Bentonites, Palygorskite-Sepiolite, and Common Clays, In: Development of Clay Science 2, Elsevier B. V., Amsterdam, NL (2007).

[39] R. Suresh, S. N. Borkar, V. A. Sawant, V. S. Shende, S. K. Dimble, Nanoclay Drug Delivery System, Internat. J. Pharma. Sci. Technol., 3 (2010) 901–905.

[40] M. Q. Zhao, J. Q. Huang, Q. Zhang, W. L. Luo, F. Wei, Improve the Oil Adsorption Perform-

ance of Natural Vermiculites by Formation of a Sponge-like Hybrid with Aligned Carbon Nanotubes Intercalated among Clay Layers, 16th International Symposium on Intercalation Compounds, Seč-Ústupky/Czech Republic, 24th May 2011, 223. Abstract.

[41] P. S. C. Silva, S. M. B. Oliveira, L. Farias, D. I. T. Fávaro, B. P. Mazzilli, Chemical and Radiological Characterization of Clay Minerals used in Pharmaceutics and Cosmetics, Appl. Clay. Sci., 52 (2011) 145–149.

[42] G. W. Beall, The Use of Organo-Clays in Water Treatments, Appl. Clay Sci., 24 (203) 11–20.

[43] T. H. Cooper, Regents, Clay Minerals, Unit 12 Chapter 1, University of Minnesota, US (2008).

[44] F. Bergaya, G. Lagaly, General introduction: Clays, Clay Minerals, and Clay Science. In: Handbook of Clay Science. Developments in Clay Science, Vol. 1., Ed.: Bergaya, F., Theng, B. K. G., Lagaly, G., Elsevier Amsterdam, NL (2006) 1–18.

[45] B. Velde, Origin and Mineralogy of Clays: Clay and the Environment, Ed: B. Velde, Springer (1995).

[46] E. Tombácz, M. Szekeres, Colloidal Behavior of Aqueous Montmorillonite Suspensions: the Specific Role of pH in the Presence of Different Electrolytes, Applied Clay Sci. 27 (2004) 75–94.

[47] E. Tombácz, M. Szekeres, Surface Charge Heterogeneity of Kaolinite in Aqueous Suspension in Comparison with Montmorillonite, Applied Clay Sci. 34 (2006) 105–124.

[48] S. Karaborni, B. Smit, W. Heidug, J. Urai, E. Van Oort, The Swelling of Clays: Molecular Simulations of the Hydration of Montmorillonite, Science, 271 (1996) 1102–1105.

[49] H. van Olphen, An Introduction to Clay Colloid Chemistry, 2nd Edition, John Wiley & Son Inc., Canada, USA (1977).

[50] B. K. G. Theng, The Chemistry of Clay-Organic Reactions. Adam Hilger Ltd London. (1974).

[51] H.C.H. Darley, G. R. Gray, Composition and Properties of Drilling and Completion Fluids. Gulf Publishing Company (1988) 140–184.

[52] D.E. O'Brien, M.E. Chenevert, Stabilizing Sensitive Shales with Inhibited Potassium-Based Drilling Fluids, J. Petr. Tech. 25 (1973) 1089–1100.

[53] T. J. Pinnavaia, G. W. Beall, Polymer – Clay Nanocomposites, In: Wiley Series in Polymer Science, John Wiley & Son Ltd, New York, USA (2001).

[54] P. C. LeBaron, Z. Wang, T. J. Pinnavaia, Polymer–Layered Silicate Nanocomposites: An Overview, Applied Clay Sci., 15 (1999) 11–29.

[55] D. J. Greenland, Adsorption of Glycine and its Di-, Tri-, and Tetra- Peptides by Montmorillonite, Trans. Faraday Soc. 58 (1962) 829–841.

[56] B. K. G. Theng, Formation and Properties of Clay–Polymer Complexes, In: Development in Clay Science 4, 2nd Edition, Elsevier, Amsterdam, NL (2012).

[57] C. O. Oriakhi, M. M. Lerner, Poly(pyrrole) and Poly(thiophene)/Clay Nanocomposites via Latex Interaction, Mater. Res. Bull. 30 (1995) 723–739.

[58] H. R. Fischer, L. H. Gielgens, T. P. M. Koster, Nanocomposites from Polymers and Layered Minerals, Acta Polym. 50 (1999) 122–126.

[59] K. A. Carrado, P. Thiyagarajan, D. L. Elder, Polyvinyl Alcohol – Clay Complexes formed by Direct Synthesis, Clays Clay Miner. 44 (1996) 506–514.

[60] N. Takahashi, K. Kuroda, Materials Design of Layered Silicates through Covalent Modification of Interlayer Surfaces, J. Mater. Chem. 21 (2011) 14336–14353.

[61] K. A. Carrado, P. Thiyagarajan, R. E. Winans, R. E. Botto. Hydrothermal Crystallization of Porphyrin-Containing Layer Silicates, Inorg. Chem. 30 (1991) 794–799.

[62] J. L. Suter, P. V. Coveney, Computer Simulation Study of the Materials Properties of Intercalated and Exfoliated Poly(ethylene)glycol Clay Nanocomposites, Soft Matter, 5 (2009) 2239–2251.

[63] S. Rossi, P. F. Luckham, T. F. Tadros, Influence of Non-ionic Polymers on the Rheological Behaviour of Na^+-Montmorillonite Clay Suspensions – I Nonylphenol – Polypropylene Oxide – Polyethylene Oxide Copolymers, Colloid Surf. A, 201 (2002) 85–100.

[64] R. L. Parfitt, D. J. Greenland, The Adsorption of Poly(ethylene glycols) on Clay Minerals, Clay Miner. 8 (1970) 305–315.

[65] A. A. Jeknavorian, L. Jardine, C.C. Ou, H. Koyata, K.J. Folliard, Interaction of Superplasticizers with Clay-Bearing Aggregates, Special Publication ACI/ 7th CANMET Conference on Superplasticizers and Other Chemical Admixtures, Berlin, Germany, SP-217 (2003) 1293–1316.

[66] E. Sakai, D. Atarashi, M. Daimon, Interaction between Superplasticizers and Clay Minerals, Special Publication ACI/ 6th CANMET Conference on Superplasticizers and Other Chemical Admixtures, Xi' an, China (2006) 1560–1566.

[67] H. Kroyer, H. Lindgreen, H. J. Jakobsen, J. Skibsted, Hydration of Portland Cement in the Presence of Clay Minerals Studied by ^{29}Si and ^{27}Al MAS NMR Spectroscopy, Adv. Cem. Res., 15 (2003) 103–112.

[68] D. Atarashi, E. Sakai, R. Obinata, M. Daimon, Interactions between Superplasticizers and Clay Minerals, Cem. Sci. Concr. Technol. 58 (2004) 387–392.

[69] D. Atarashi, E. Sakai, R. Obinata, M. Daimon, Influence of Clay Minerals on Fluidity of $CaCO_3$ Suspension containing Comb-Type Polymer, Cem. Sci. Concr. Technol. 57 (2003) 386–391.

[70] L. A. Jardine, H. Koyata, K. J. Folliard, C. -C. Ou, F. Jachimowicz, B. -W. Chun, A. A. Jeknavorian, C. L. Hill, US 6,352,952 (2002) W. R. Grace & Co..

[71] Soc J&A, Fr. 320,290, Fr 391,454 (1908) Pavin de Lafarge.

[72] H.F.W. Taylor, Cement Chemistry, 2nd edition, Academic Press, London, UK (1990).

[73] G. C. Sang, J. P. Liu, Study of Properties of Portland and Aluminate Cementitious Composited Grouting Materials, Mater. Res. Innov., 14 (2010) 200–205.

[74] CERAM Research Ltd, http://www.azom.com/details.asp?ArticleID=1634, retrieved on 31st March 2009.

[75] K. Scrivener, Calcium Aluminate Cement, In: Advanced Concrete Technology, 1st Edition, Ed: J. Newman, B. S. Choo, Elsevier, Oxford, UK (2003).

[76] A. F. Wells, Structural Inorganic Chemistry, 5th Edition, Oxford University Press, Oxford, UK (1984).

[77] A. de Roy, C. Forano, K. E. Malki, Expanded Clays and Other Microporous Solids, 1st Edition, Vol. 2, Ed: M. L. Occelli, H. E., New York, USA (1992).

[78] R. J. M. Pellenq, J. M. Caillol, A. Delville, Electrostatic Attraction between two Charged Surfaces : A (N,V,T) Monte Carlo Simulation, J. Phys. Chem. B., 101 (1997) 8584–8594.

[79] P. P. Kumar, A. G. Kalinichev, R. J. Kirkpatrick, Hydration, Swelling, Interlayer Structure, and Hydrogen Bonding in Organolayered Double Hydroxides: Insights from Molecular Dynamics Simulation of Citrate-Intercalated Hydrotalcite, J. Phys. Chem. B Lett., 110 (2006) 3841–3844.

[80] A. Dubey, Synthesis and Catalytic Application of CMK-LDH (Layered Double Hydroxides) Nanocomposites Materials, Green Chem., 9 (2007) 424–426.

[81] D. P. Das, J. Das, K. Parida, Physicochemical Characterization and Adsorption Behavior of Calcined Zn/Al Hydrotalcite-like Compound (HTlc) Towards Removal of Fluoride from Aqueous Solution, J. Colloid Interface Sci. 261 (2003) 213–220.

[82] H. Chen, J. M. Wang, T. Pan, Y. L. Zhao, J. Q. Zhang, C. N. Cao, Physicochemical Properties and Electrochemical Performance of Al-substituted α-$Ni(OH)_2$ with Additives for Ni-Metal

Hydride Batteries, 150 (2003) 1399–1404.

[83] S. Aisawa, Y. Ohnuma, K. Hirose, S. Takahashi, H. Hirahara, E. Narita, Intercalation of Nucleotides into Layered Double Hydroxides by Ion-Exchange Reaction, Appl. Clay Sci., 28 (2005) 137–145.

[84] B. Lothenbach, L. Pelletier-Chaignat, F. Winnefeld, Stability in the System $CaO–Al_2O_3–H_2O$, Cem. Concr. Res., 42 (2012) 1621–1634.

[85] S. Stöber, H. Pöllmann, Synthesis of a Lamellar Calcium Aluminate Hydrate (AF_m phase) Containing Benzenesulfonic Acid Ions, Cem. Concr. Res. 29 (1999) 1841–1845.

[86] L. Raki, J. J. Beaudoin, L. Mitchell, Layered Double Hydroxide-Like Materials: Nanocomposites for Use in Concrete, Cem. Concr. Res. 34 (2004) 1717–1724.

[87] V. Fernon, A. Vichot, N. Le Goanvic, P. Colombet, F. Corazza, U. Costa, Interaction between Portland Cement Hydrates and Polynaphthalene Sulfonates, Malhotra V. M. Ed. 5th CANMET/ ACI International Conference on Superplasticizers and Other Chemical Admixtures in Concrete, ACI, Rome/Italy, SP–173 (1997) 225–248.

[88] C. Giradeau, J.-B. d'Espinose de Lacaillerie, Z. Souguir, A. Nonat, R. J. Flatt, Surface and Intercalation Chemistry of Polycarboxylate Copolymers in Cementitious Systems, J. Am. Ceram. Soc. 92 (2009) 2471–2488.

[89] J. Plank, H. Keller, P. R. Andres, and Z. M. Dai, Novel Organo-Mineral Phases Obtained by Intercalation of Maleic Anhydride-Allyl Ether Copolymers Into Layered Calcium Aluminum Hydrates, Inorg. Chim. Acta, 359 (2006) 4901–4908.

[90] J. Plank, Z. M. Dai, H. Keller, F. v. Hössle, W. Seidl, Fundamental Mechanisms for Polycarboxylate Intercalation into C_3A Hydrate Phases and the Role of Sulfate Present in Cement, Cem. Concr. Res 40 (2010) 45–57.

[91] Z. Wang, Z. Lu, F. Lu, H. Li, Relationship between Structure and Performance of Polycarboxylate Superplasticizer, Key Eng. Mater. 509 (2012) 57–64.

[92] S. Lv, R. Gao, J. Duan, Effects of Chemical Structure on Adsorption of polycarboxylate Superplasticizers on Cement Particles, Appl. Mech. Mater. 80–81 (2011) 185–189.

[93] S. Li, Q. Yu, J. Wei, Y. Ji, Effects of Molecular Structure of Polycarboxylate Water Reducers on their Performance in Cement Paste, Adv. Mater. Res. 168–170 (2011) 1854–1858.

[94] M. Hayakawa, Y. Yamamoto, K. Takeda, H. Tanaka, K. Natsuume, Effect of Polycarboxylate-based Superplasticizer on Properties of Flowing Concrete, Technology of Concrete When Pozzolans, Slags Chemical Admixtures are Used, Symposium, ACI–RILEM 85 (1985) 297–

290.

[95] A. Ohta, T. Sugiyama, Y. Tanaka, Fluidizing Mechanism and Application of Polycarboxylate-based Superplasticizers, Malhotra V. M. Ed. 5th CANMET/ ACI International Conference on Superplasticizers and Other Chemical Admixtures in Concrete, ACI, Rome/Italy, SP–173 (1997) 359–378.

[96] H. N. Zouaoui, Einfluss der Molekülarchitektur von Polycarboxylaten, hergestellt durch Blockcopolymerisation und Pfropfreaktion, auf die Wechselwirkung mit Fluoroanhydrit und Portlandzement; Dissertation, Technische Universität München, Lehrstuhl für Bauchemie (2009).

[97] K. Andersson, B. Allard, M. Bengtsson, B. Magnusson, Chemical Composition of Cement Pore Solutions, Cem. Concr. Res. 19 (1989) 327–332.

[98] G. H. Tattersall, P. F. G. Banfill, The Rheology of Fresh Concrete, Pitman Advanced Publishing, Boston, USA (1983).

[99] F. de Larrard, T. Sedran, Mixture-Proportioning of High-Performance Concrete, Cem. Concr. Res. 32 (2002) 1699–1704.

[100] F. de Larrard, C. F. Ferraris, T. Sedran, Fresh Concrete: a Herschel–Bulkley Material, Mat. Struct. 31 (1998) 494–498.

[101] I. Aiad, Influence of Time Addition of Superplasticizers on the Rheological Properties of Fresh Cement Pastes, Cem. Concr. Res. 33 (8) (2003) 1229–1234.

[102] N. Roussel, C. Stefani, R. Leroy, From Mini-Cone to Abrams Cone Test: Measurement of Cement-Based Materials Yield Stress using Slump Tests, Cem. Concr. Res., 35 (2005) 817–822.

[103] W. H. Zachariasen, Theory of X-Ray Diffraction in Crystals, Dover Phoenix Edition, New York, USA (2004).

[104] T. A. Ezquerra, M. Garciá-Gutiérrez, A. Nogales, M. Gomez, Applications of Synchrotron Light to Scattering and Diffraction in Materials and Life Sciences, 1st Edition, Springer, Madrid, Spain (2009).

[105] O. Glatter, O. Kratky, Small Angle X-Ray Scattering, Academic Press Inc. (London) Ltd., New York, USA (1982).

[106] L. Lei, J. Plank, A Concept For a Polycarboxylate Superplasticizer Possessing Enhanced Clay Tolerance, Cem. Concr. Res., 42 (2012) 1299–1306.

Paper 1

Interaction Mechanisms between Na montmorillonite Clay and MPEG-based Polycarboxylate Superplasticizers

S. Ng, J. Plank

Cement and Concrete Research 42 (2012) 847–854.

Cement and Concrete Research 42 (2012) 847–854

Contents lists available at SciVerse ScienceDirect

Cement and Concrete Research

journal homepage: http://ees.elsevier.com/CEMCON/default.asp

Interaction mechanisms between Na montmorillonite clay and MPEG-based polycarboxylate superplasticizers

S. Ng, J. Plank *

Technische Universität München, Chair for Construction Chemicals, 85747 Garching, Lichtenbergstraße 4, Germany

ARTICLE INFO

Article history:
Received 29 August 2011
Accepted 13 March 2012

Keywords:
Adsorption (C)
Cement (D)
Polymer (D)
Clay

ABSTRACT

Sodium montmorillonite clay is shown to negatively impact the dispersion force of two methacrylate based polycarboxylates (PCEs) in cement paste. The PCEs tested consist of methacrylic acid/MPEG methacrylate-ester with molar ratios of 6:1 and 1.5:1. It was found that the PCEs sorb both chemically and physically onto clay. The sorbed amounts are ~100 times more than on cement. Chemisorption occurs via intercalation of the poly(ethylene oxide) side chains into the interlayer region between the alumosilicate layers, while physisorption occurs on clay surfaces which are positively charged through uptake of Ca^{2+}. PCEs possessing high grafting density predominantly intercalate and show less surface adsorption, and vice versa. Also, the type of sorption is dosage dependent, whereby side chain intercalation dominates at higher PCE dosages, while electrostatic attraction via the anionic backbone prevails at lower dosages. Polyglycols can be utilised as sacrificial agents when highly grafted PCEs are employed at high dosages.

1. Introduction

Montmorillonite is a 2:1 smectite clay mineral, consisting of stacked octahedral aluminate layers sandwiched between two tetrahedral silicate layers (Fig. 1). The resulting alumosilicate layers measure about 1 nm in thickness [1]. The general composition of montmorillonite can be expressed as $M_x(Mg,Al,Fe)_2(OH)_2[Si_4O_{10}]\cdot nH_2O$, with $M^+ = Na^+$, K^+, 0.5 Mg^{2+} or 0.5 Ca^{2+}. Partial substitution of Si^{4+} by Al^{3+} generates an overall negative charge of the basal surfaces. This charge is balanced by intercalation of cations (M^+; hydrated or non-hydrated) in between the alumosilicate layers [2].

When clay is dispersed in electrolyte containing fluids such as cement pore solution, cations can also adsorb onto the permanently negatively charged basal surfaces of the clay platelets. Other anchoring sites for cations are the crystal edges where terminal –OH groups from aluminates and silicates are present [3,4]. Under high pH conditions, these terminal –OH groups are deprotonated and develop a negative charge (Fig. 2).

Montmorillonite is among the most researched clay minerals because of its natural abundance and its viscosifying property. Over the last two decades, novel nanocomposites comprising of polymer layered silicates (PLS) were developed whereby a wide range of monomers and polymers including glycols and polyimides intercalates into the galleries of montmorillonite clay. Such PLS nanocomposites, when compared to conventional materials based on glass or mineral fibre enforced polymers showed enhanced mechanical stiffness, strength and barrier properties [5–9]. Specifically, PLS nanocomposites provide enhanced thermal stability to the materials. In the construction field, applicators have observed that presence of certain clays may affect and can be detrimental to the initial workability of concrete [10–12]. Montmorillonite was found to be more harmful than other clays due to its expanding lattices which promote intercalation, swelling and cation exchange [13,14]. The extent of these interactions is dependent on many factors including pH and the type of polyelectrolyte present in the medium. The ability of this clay to sorb water and swell causes an increase in viscosity of the cement paste (a loss in workability) or a higher water demand to produce the same workability as before. This is detrimental for the mechanical properties and durability of concretes [15].

Some studies have shown that polymers can sorb on clay particles [16]. The impact of this process in the construction field is dependent on the type of admixtures used. For superplasticizers, polycondensates were shown to be less affected by the presence of clay than polycarboxylates [10,11,17,18]. This indicates that when concrete is contaminated by a significant quantity of montmorillonite, competing demands by different components (cement and clay) for the polycarboxylate can occur, thus reducing its availability for dispersion. In contrast to PCEs, polycondensates do not show this effect.

In the present study, the effect of clay addition to cement (dosage: 1% by weight of cement) on the behaviour of two polycarboxylate based superplasticizers was investigated. A naturally occurring sodium montmorillonite clay was employed. First, the influence of clay on the workability of cement pastes containing two different

* Corresponding author. Tel.: +49 89 289 13151; fax: +49 89 289 13152.
E-mail address: sekretariat@bauchemie.ch.tum.de (J. Plank).

0008-8846/$ – see front matter © 2012 Elsevier Ltd. All rights reserved.
doi:10.1016/j.cemconres.2012.03.005

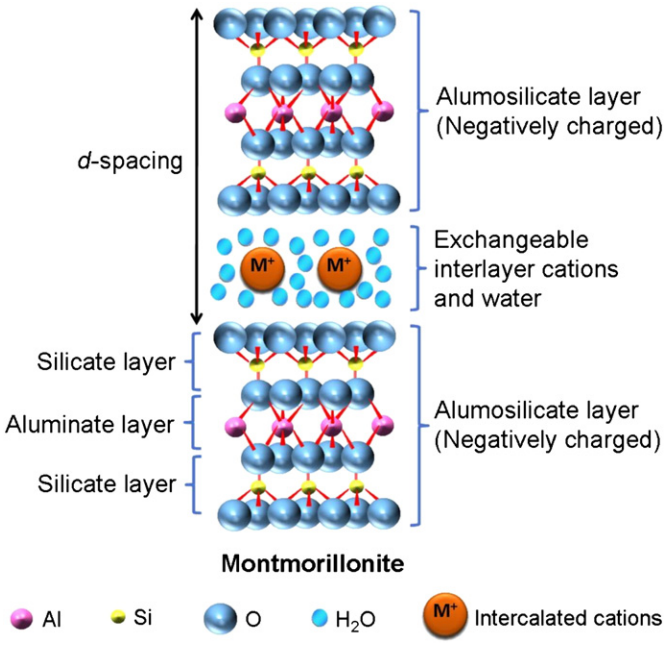

Fig. 1. Schematic illustration of the layer structure present in montmorillonite clay.

methacrylic acid–methacrylate ester based PCEs was determined by 'mini slump' test. The two PCEs varied by their grafting densities and correspondently anionic charge amounts. To ascertain the interaction of these PCEs with clay, their adsorption on the cement/clay mixture was measured via total organic carbon (TOC) method. A simplified system comprising only clay, PCE and synthetic cement pore solution was subsequently utilised to identify the sole effect of clay on PCE. First, the amount of PCE sorbed by clay was determined. XRD analysis was performed to probe a potential chemisorption of PCE by clay. For clarification of the specific interaction of individual PCE building blocks with clay, adsorption of the polymethacrylate backbone and of the poly(ethylene oxide) side chain were studied separately. This investigation was performed by using poly(methacrylic acid) (PMA) and polyethylene glycol (PEG). The individual amounts of side chain or backbone sorbed were used to calculate the idealised amount of PCE sorbed by clay. This way, the mechanism of interaction between PCE and clay in the cementitious system was sought to be clarified.

2. Materials and methods

2.1. Cement

A CEM I 52.5 R HS/NA (Holcim, Lägerdorf/Germany) was used. Its phase composition as obtained by quantitative X-ray diffraction (Bruker D8 advance instrument, software Topas 4.0) is presented in Table 1. The

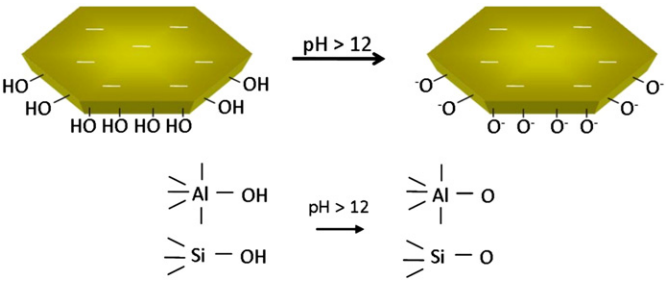

Fig. 2. Schematic illustration of charge distribution and deprotonation of terminal –OH groups present along crystal edges of a montmorillonite particle at high pH.

Table 1
Phase composition of CEM I 52.5 R HS/NA sample as determined by XRD using *Rietveld* refinement.

Phase	[wt.%]
C_3S, monoclinic	60.1
C_2S, monoclinic	19.0
C_3A, cubic	1.2
C_3A, orthorhombic	0.4
C_4AF, orthorhombic	14.5
Calcite	1.3
$CaSO_4 \cdot 1/2\ H_2O$[a]	2.2
$CaSO_4 \cdot 2\ H_2O$[a]	1.0
$CaSO_4$	0.4

[a] Determined by thermogravimetry.

specific surface area of 4300 cm^2/g was measured using a *Blaine* instrument (Toni Technik, Berlin/Germany). The particle size (d_{50} value) of 8.33 μm was obtained on a laser granulometer CILAS 1064 (Cilas, Marseille/France), while the density was 3.22 g/cm^2 measured by ultrapycnometry (Quantachrome, Odelzhausen/Germany).

2.2. Sodium montmorillonite clay

A commercial sodium montmorillonite clay sample (RXM 6020 supplied by Rockwood, Moosburg/Germany) was used as per obtained. This clay is a naturally occurring sodium montmorillonite clay. Its oxide composition is presented in Table 2. It develops a pH of ~9 when prepared as a 2 wt.% aqueous suspension. The XRD pattern of the dry clay reveals a *d*-spacing of 1.07 nm (Fig. 3).

2.3. Polycarboxylate samples

Two PCE superplasticizers and two polymers representing the poly(methacrylic acid) backbone and poly(ethylene oxide) side chain of the PCEs were utilised. The PCEs were synthesized according to a literature description by aqueous free radical copolymerization of methacrylic acid (MAA) and methoxy terminated poly(ethylene oxide) methacrylate (MPEG-MA) ester at molar ratios of 1.5 and 6 respectively [19]. Methallylsulfonic acid was used as chain transfer agent. Both copolymers have side chains made up of 45 ethylene oxide units (EOUs). They are denoted by 45PCx, where 45 refers to the number of EOUs in the side chain, and x corresponds to the molar ratio of MAA:MPEG-MA. The chemical formula of the PCEs is presented in Fig. 4. PMA was synthesized by aqueous free radical polymerization of MAA [20], while PEG-2000 was used as per obtained (Clariant, Frankfurt am Main/Germany).

For polymer characterisation, size exclusion chromatography (Waters Alliance 2695 from Waters, Eschborn/Germany) equipped with RI detector 2414 (Waters, Eschborn/Germany) and a 3 angle dynamic light scattering detector (mini Dawn from Wyatt Technologies, Santa Barbara, CA/USA) was used. Prior to application on the columns, the polymer solutions were filtered through a 0.2 μm filter. The polymers were separated on an Ultrahydrogel™ precolumn and three Ultrahydrogel™ (120, 250 and 500) columns (Waters, Eschborn/Germany) using 0.1 M aqueous $NaNO_3$ solution (adjusted to pH 12.0 with NaOH) as an eluant at a flow rate of 1.0 mL/min. From this separation, the molar masses (M_w and M_n), the polydispersity index (PDI) and the hydrodynamic radius ($R_{h(z)}$) of the polymers were

Table 2
Oxide composition of sodium montmorillonite clay sample, RXM 6020 as determined by X-ray fluorescence.

Oxide	SiO_2	Al_2O_3	CaO	MgO	Fe_2O_3	Na_2O	K_2O	TiO_2	LOI	Total
[wt.%]	59.7	18.4	0.8	2.3	4.0	2.3	0.1	0.1	12.1	99.8

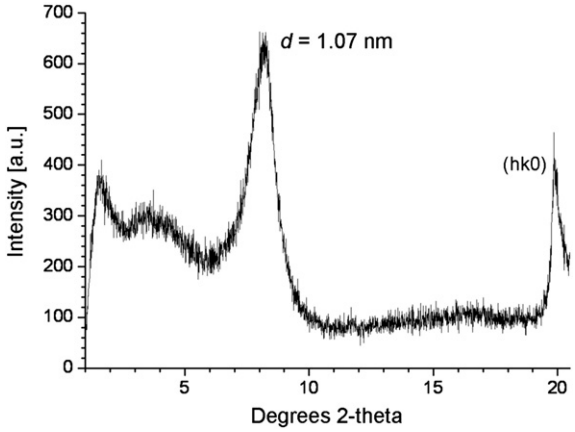

Fig. 3. X-ray diffraction pattern of dry sodium montmorillonite clay sample, RXM 6020.

determined. The value of dn/dc used to calculate M_w and M_n for all polymers was 0.135 mL/g (value for polyethylene oxide) [21].

Specific anionic charge amounts of the polymers were analysed by a particle charge detector (PCD 03 pH from Mütek Analytic Company, Herrsching/Germany). Solutions containing 0.02 wt.% of anionic polymer dissolved in synthetic cement pore solution were prepared and titrated against a 0.001 N solution of cationic polydiallyl dimethyl ammonium chloride (polyDADMAC) until charge neutralization was attained. The amount of negative charge per gram of polymer was calculated from the consumption of the cationic polyelectrolyte.

Purity of PEG-2000 was confirmed by ^{1}H NMR analysis using a Bruker DPX250 250 MHz instrument (Bruker, Ettlingen/Germany).

2.4. Zeta potential measurements

Zeta potentials of montmorillonite suspensions were determined as a function of pH in millipore water adjusted with 37 wt.% aqueous HCl and 19.5 wt.% aqueous NaOH, and in synthetic cement pore solution using a model DT 1200 Electroacoustic Spectrometer from Dispersion Technology, Inc. (Bedford Hills, NY/USA). The synthetic cement pore solution exhibited a pH of 12.8 and was prepared by dissolving 1.72 g $CaSO_4 \cdot 2H_2O$, 7.119 g KOH, 4.76 g K_2SO_4 and 6.956 g of Na_2SO_4 in 1 L of millipore water respectively. The ionic composition (mmol/L) of this synthetic cement pore solution ($Ca^{2+} = 10$; $Na^+ = 100$; $K^+ = 180$; $OH^- = 127$; $SO_4^{2-} = 86$) is typical for normal Portland cement dispersed in water at a w/c ratio of ~0.4 [22]. Particle size of clay was measured using a ZetaSizer from Malvern Instruments Ltd (Worcestershire/United Kingdom). The w/clay ratio was 53 to actualise the conditions in the 'mini slump' test where the w/c ratio was 0.53 and 1% by weight of cement of clay were present.

2.5. 'Mini slump' test

For determination of the paste flow, a "mini slump" test according to DIN EN 1015 was utilised and carried out as follows:

At first, the w/c ratio needed to attain a spread of 18 ± 0.5 cm for the neat cement paste was determined, and the dosage of PCE superplasticizer required to reach a spread of 26 ± 0.5 cm at this specific w/c ratio was established. The PCE solution was generally added to the mixing water placed in a porcelain cup and the amount of water introduced with the PCE solution was subtracted from the amount of mixing water required for a w/c ratio of 0.53. In a typical experiment, 300 g of solids (pure cement or cement blended with 1 wt.% of clay) were added to the mixing water, agitated for 1 min and left to stand for another minute. The cement paste was next stirred for 2 min before transferring into a Vicat cone placed on a glass plate. The dimensions of the Vicat cone were: height 40 mm, top diameter 70 mm, and bottom diameter 80 mm. The cement paste was filled to the brim of the cone and levelled before it was vertically lifted from the surface of the glass plate. The resulting spread of the paste was measured twice; the second measurement being perpendicular to the first. The final spread value was taken as the average of the two measured ones.

2.6. XRD analysis of clay hydrated in presence of PCE

0.025 g clay was added to 1.34 g of 0.93 wt.% polymer solution (w/clay ratio of 53). The suspension was manually mixed for 1 min, sonicated for 10 min and centrifuged at 14,600 rpm for another 10 min. The solid residue obtained was dried at 80 °C overnight before it was ground and analysed. XRD scans of all samples were taken at room temperature on a D8 Advance, Bruker AXS instrument (Bruker, Karlsruhe/Germany) utilising a Bragg–Bretano geometry. Samples were placed in a front mounted plastic sample holder. Step size was 0.15 s per step, and spin of sample during scanning was set at a revolution time of 4 s. Nickel filter was used for incident beam with an aperture slit of 0.3°. The scan range was set from 0.6° to 20° 2θ.

2.7. Sorption experiments

PCE sorption on clay or cement was determined by the depletion method, i.e. it was assumed that removal of PCE from the pore solution solely was the result of interaction with clay and/ or cement and that no precipitation had occurred. In sample preparation, 300 g of pure cement or cement blended with 1 wt.% of clay were added to 2.0 wt.% 45PC1.5 or 0.17 wt.% 45PC6 solutions over 1 min in a porcelain cup (PCE dosages and w/c ratio as determined in 'mini slump' test). The mixture was allowed to rest for another minute before it was stirred for 2 min. Thereafter, the paste was centrifuged at 8500 rpm for 15 min. The filtrate was recovered, diluted and acidified

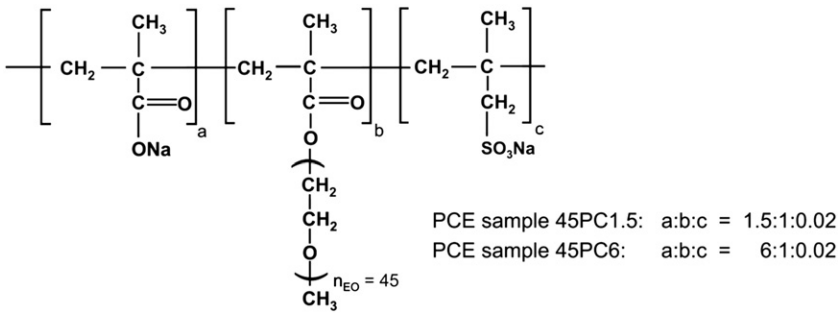

Fig. 4. Chemical structure of the PCE samples employed in the study.

with conc. HCl solution in a TOC sample flask. This final solution was then analysed by combustion at 890 °C on a HIGH TOC II instrument (Elementar Analysensysteme, Hanau/Germany). The sorbed amount of PCE was calculated from the difference between the TOC content in the stock solution and that left in the filtrate. In a separate experiment, 20 g/L of PCE was dissolved in the filtrate of clay suspended in synthetic cement pore solution and left to stand overnight. No precipitation was found, thus signifying that PCE depletion was solely a result of sorption by the cement or clay.

Sorption experiments of PCE, PMA and PEG-2000 on clay in synthetic cement pore solution were performed by using polymer solutions with concentrations ranging from 12.5 to 200% by weight of (bwo) clay. These polymer solutions were added to 0.025 g of clay, manually homogenized and sonicated for 10 min to achieve maximum dispersion of the clay particles and thus interaction with polymers. The mixture was then centrifuged at 14,600 rpm for 10 min. Thereafter, the filtrate was collected, diluted and acidified prior to further analysis by TOC measurement as before.

2.8. Theoretical calculation of PCE sorption

45PC1.5 consists of 11.6 wt.% PMA (backbone) and 88.4 wt.% PEG (side chain), while 45PC6 consists of 26.8 wt.% of PMA (backbone) and 73.2 wt.% PEG (side chain). From the experimental individual sorbed amounts of PEG-2000 and PMA, and from the relative percentage of each structural element present in the PCE, idealised amounts of 45PC1.5 and 45PC6 sorbed by clay were calculated as presented in Eqs. (1) and (2) and compared. Potential effects of different molecular architectures or sorbed conformations of the polymers were assumed to be negligible.

$$\text{PMA : Calculated amount of PCE sorbed} = \frac{\text{Exp.sorbed amount of PMA}}{\text{wt.\% of PMA present in PCE sample}}\,[\text{mg/g}] \quad (1)$$

$$\text{PEG : calculated amount of PCE sorbed} = \frac{\text{Exp.sorbed amount of PEG}}{\text{w.\% of PEG sample}}\,[\text{mg/g clay}] \quad (2)$$

Eqs. (1) and (2). Calculation of the sorbed amounts of PCEs based on the sorption profile of individual PMA and PEG respectively.

3. Results and discussion

3.1. Surface charge of montmorillonite

To assess the potential for electrostatic interaction between clay and PCE, its approximate overall surface charge as expressed by the zeta potential was measured. In deionised water, the zeta potential of the montmorillonite sample was found to be consistently negative due to its innate negative basal surface charge (Fig. 5). Till ~pH 5, the zeta potential of the clay suspension remained relatively constant at ~ −15 mV, but decreased sharply to ~−35 mV at pH 8 and stabilized thereafter. The transition in surface charge from pH 5 to 8 can be attributed to deprotonation of terminal silanol and aluminol groups present along the crystal edges of the clay platelets [23,24].

In synthetic cement pore solution (0.4 g/L Ca^{2+}), however, the clay suspension exhibited a zeta potential value of +15.1 mV, implying that cations such as Ca^{2+} adsorbed onto the clay surfaces. Through this mechanism, clay attains a positive surface charge and potential anchoring sites for incoming anionic polymers are formed.

3.2. Properties of PCE samples

The molecular characteristics and anionic charge amounts of the polymers are shown in Table 3. According to this data, the synthesized

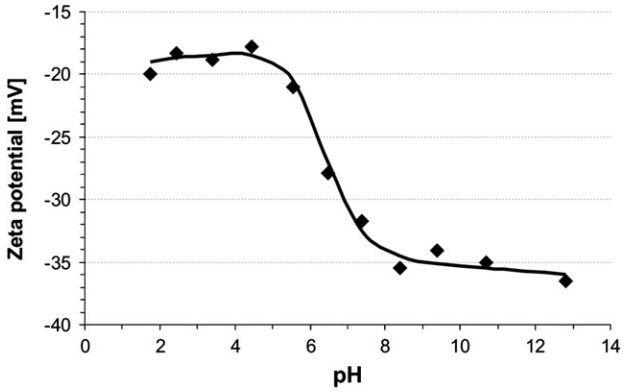

Fig. 5. Zeta potential of aqueous RXM 6020 montmorillonite suspension as a function of pH (w/clay ratio = 53).

poly(methacrylate) backbone on average consists of 33 methacrylate units while the PCE copolymers 45PC1.5 and 45PC6 contain 23 and 17 methacrylate functionalities respectively. The anionic charge amounts increase by the order as follows: PEG<45PC1.5<45PC6< PMA. ^{1}H NMR analysis (spectrum not shown here) confirmed purity of >99% for PEG-2000.

3.3. Dispersing performance of PCE in presence of clay

The w/c ratio of the neat cement paste for a spread of 18 ± 0.5 cm was determined to be 0.53. When 1 wt.% of clay was added, availability of water decreased due to consumption by hydration and swelling of the clay. Thus, the spread of the cement paste decreased to 15.3 cm (~−15%) as a result of increased viscosity.

In the absence of clay, the dosages of 45PC1.5 and 45PC6 required to obtain a spread of 26 ± 0.5 cm were 1.07 and 0.09% bwoc respectively. Obviously, PCE polymer 45PC6 is a much more effective dispersant due to its significantly higher anionic charge.

However, when 1 wt.% of clay was added, the spreads decreased by 41% and 58% to 22.3 cm and 21.3 cm for cement pastes with added 45PC1.5 and 45PC6 respectively (Fig. 6). These reductions in paste fluidity much exceed that observed in the absence of PCE which was 15% only. Thus, it indicates that besides water sorption, interaction of PCE with clay may also affect its dispersing effectiveness.

3.4. PCE sorption in cement/clay system

To ascertain the effect of clay on PCE, the sorbed amounts of 45PC1.5 and 45PC6 in cement paste with and without 1 wt.% of clay were investigated. Table 4 shows the sorbed amounts of the PCEs in presence or absence of clay.

When clay was present, then the sorbed amounts of the PCEs increased greatly. The effect was particularly strong with 45PC1.5 possessing high grafting density (sorbed amount increased from 25% to 55% of dosage added). Considering the small amount of clay present, this presents a huge increase in PCE sorption. Thus, it confirms strong interaction between this PCE and clay, plausibly higher

Table 3
Molecular properties and anionic charge amounts of 45PC1.5, 45PC6, PMA and PEG respectively, measured in synthetic cement pore solution.

Property	45PC1.5	45PC6	PMA	PEG
Molar mass M_w [g/mol]	196,300	156,400	26,200	2080
Molar mass M_n [g/mol]	51,900	43,680	7511	2090
Polydispersity index (PDI)	3.8	3.6	2.7	1.0
Molar ratio MAA : MPEG-MAA	1.5:1	6:1	–	–
Specific anionic charge amount $_{PS}$ [μeq/g]	175	1100	7900	0

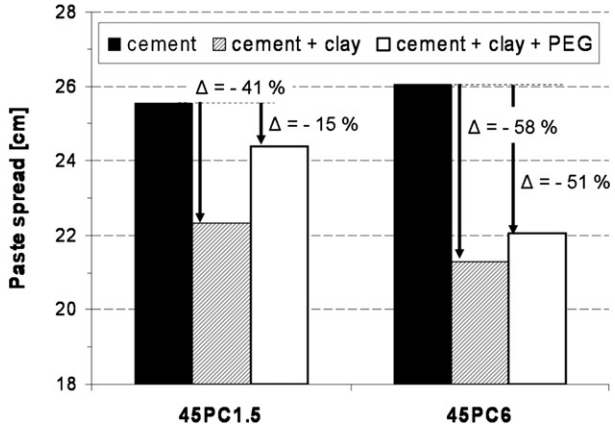

Fig. 6. Paste spread of cement slurries with and without 1 wt.% of clay added, in the presence of 1.07% bwoc of 45PC1.5 and 0.09% bwoc of 45PC6, with or without PEG-2000 added in equivalence to the PCE dosages (w/clay = 0.53).

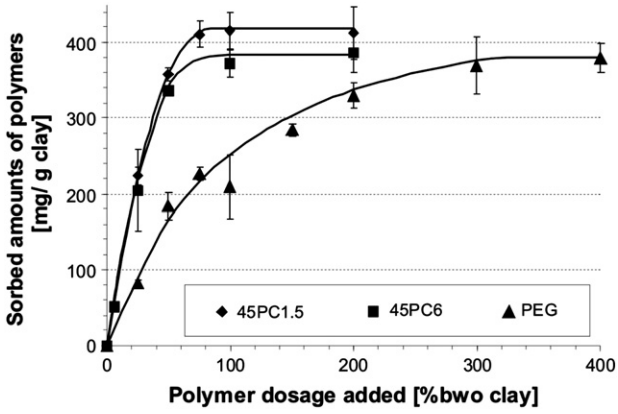

Fig. 7. Sorption isotherms of PCE polymers 45PC1.5, 45PC6 and PEG-2000 on montmorillonite dispersed in synthetic cement pore solution (Ca^{2+} concentration = 0.4 g/L, w/clay = 53).

than with cement. This result instigates that in a cementitious system, a considerable amount of PCE can be consumed by a relatively minor amount of clay contaminant.

To examine the effect of clay only on PCE and to eliminate the effect from cement, a simplified system consisting of only clay and PCE in synthetic cement pore solution was utilised next.

3.5. PCE sorption by montmorillonite

The sorption isotherms of 45PC1.5 and 45C6 on clay in synthetic cement pore solution are displayed in Fig. 7. The isotherms are *Langmuirian* L type as characterised by the steep initial increase of the adsorbed amounts. This montmorillonite exhibits an extremely high affinity for both PCE polymers, showing maximum sorbed amounts of 415 mg/g and 380 mg/g for 45PC1.5 and 45PC6 respectively. Such sorbed amounts are ~100 times higher than for an ordinary Portland cement (OPC), thus confirming the high affinity of PCE for clay [25–27].

3.6. Interaction of PEO side chain with clay

PCE consists of two main structural elements, the polymethacrylate backbone and the poly(ethylene oxide) side chain. The main question is thus which one interacts with clay, and to which extent.

Theoretically, two possibilities exist: first, in synthetic cement pore solution, due to the uptake of Ca^{2+} cations by the clay surface, electrostatic interaction between cationic clay surfaces sites and the anionic PCE backbone may occur. Second, the poly(ethylene oxide) side chains present in PCE have similar chemical composition as polyglycols. Polyglycols, especially those possessing high molecular weight, are known to be readily sorbed by this clay in large amounts [28]. The mechanism behind glycol sorption is intercalation between the alumosilicate layers occurring via H-bonding of the partially polarized oxygen atoms present in the polyethylene oxide chains and water molecules anchored by the silanol groups present on the surfaces of the alumosilicate layers (Fig. 8) [29,30]. Thus, a side chain interaction of PCE with clay is plausible. To discern between these two possibilities, the PCEs were studied in two portions, first the poly(ethylene glycol) side chain made up of 45 ethylene oxide units and second, the anionic backbone consisting of repeating units of methacrylic acid. Each building block can be represented by PEG and PMA respectively, and sorption studies of these two polymers were performed.

Table 4
Sorption of 45PC1.5 and 45PC6 on cement in presence or absence of clay (w/c = 0.53).

System	PCE dosages [% bwoc][a]	Sorbed amount of PCE [mg/g of solid]	Sorption [% of PCE dosage added]
CEM I 52.5 R + 45PC1.5	1.07	2.63	24.6
CEM I 52.5 R + 45PC1.5 + 1 wt.% clay	1.07	5.84	54.6
CEM I 52.5 R + 45PC6	0.09	0.42	46.4
CEM I 52.5 R + 45PC6 + 1 wt.% clay	0.09	0.59	65.0

[a] bwoc = by weight of cement.

First, it was found that a very high amount of PEG-2000 (at saturated equilibrium condition: 380 mg/g clay) was sorbed due to the high affinity of the PEO chain to clay (Fig. 7). Comparing the PEG and PCE sorbed amounts, it can be observed that the maximum sorbed amounts of the PCE polymers are in the same order (380–420 mg/g clay). The only difference being that the PCEs reach the point of saturated adsorption at lower addition. Therefore, it can be concluded that side chain interaction plays a significant role in the interaction between PCE and clay.

To confirm the mechanistic role of the side chain in the uptake of PCE by clay, XRD analysis was performed. Here, clay was mixed with PCE, PEG and PMA at a w/clay ratio of 53 and polymer dosages of 50% bwo clay respectively. According to Fig. 9, when hydrated, pure clay shows a *d*-spacing of 1.23 nm. A shift in the *d*-spacing from 1.23 nm to 1.77 nm was observed when PEG was added to the montmorillonite. This *d* value is characteristic for montmorillonite intercalated with polyglycols [31,32]. Likewise, when 45PC1.5 and 45PC6 were added to the clay, a shift in *d*-spacing from 1.23 nm to 1.77 nm was also detected. However, no significant change in *d*-value was observed when PMA was added to the clay. These results signify that intercalation of the PEO side chain of PCE in between the alumosilicate layers occurs. Whereas the polymethacrylate backbone does not incorporate into the interlayer region.

A second observation was the change in width of the reflection characteristic for the *d*-spacing of 1.77 nm. An increase in broadness of the characteristic reflections was observed as the side chain density of the polymers decreased, i.e. PEG<45PC1.5<45PC6. This can be explained by their different ability to form ordered layers during intercalation. In the absence of a backbone, the pure polyglycol (PEG-2000) can intercalate in between the clay layers with ease and generate highly ordered layer structures, thus producing sharper reflections. On the other hand, when PCEs are incorporated into the clay, turbostratic disorderness due to electrostatic repulsion of the anionic backbone by the negatively charged alumosilicate layers occurs. The extent of the disruption is a function of the grafting

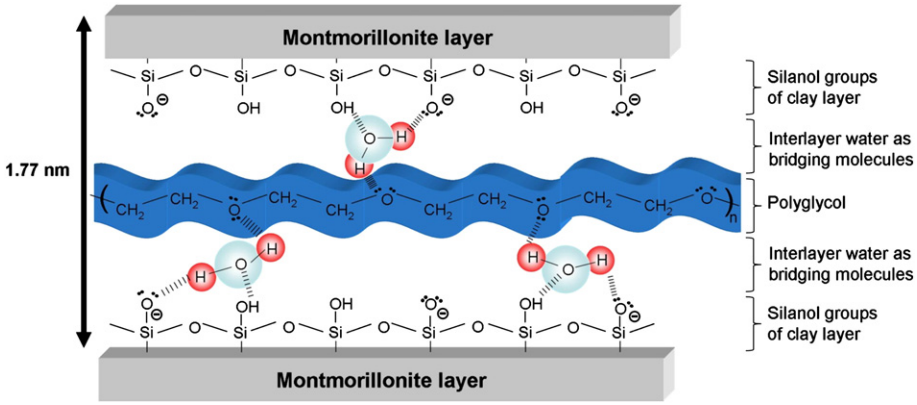

Fig. 8. Conceptual illustration of polyglycol intercalation between the alumosilicate layers of montmorillonite.

density; 45PC6 with its lower grafting density and higher anionic charge showed a more diffused reflection, thus greater disturbance in the layer structure. On the other hand, 45PC1.5, with its higher grafting density and lower anionic charge showed a more ordered intercalate product.

3.7. Interaction of PMA backbone with clay

The data presented so far clearly indicate that the PEO side chain of PCE constitutes the one structural element which facilitates PCE intercalation into the clay layer structure. However, according to Fig. 7, it becomes evident that in addition to this side chain interaction, another mode of interaction between PCE and clay must prevail as the amount of PEG sorbed cannot account for the relatively small difference in the sorbed amounts of 45PC1.5 and 45PC6, which possess significantly different amounts of PEO side chains. Additionally, according to Fig. 7, PCEs were consumed by clay at a much faster rate than individual PEG. Therefore, another mechanism of different nature must be at play. To investigate, the sorption of pure PMA backbone by clay was studied next.

According to Fig. 10, clay also sorbed PMA via electrostatic attraction mediated by the monolayer of Ca^{2+} cations formed on the clay surface in synthetic cement pore solution. This mechanism was confirmed by a dosage dependent decrease of zeta potential of the clay suspension when PMA was added until an equilibrium value representing the state of saturated adsorption was reached (curve not shown here). The fact that PMA adsorbs on clay signifies that PCEs can also be consumed through mere surface adsorption. However, the maximum adsorbed amount of PMA is only 32.5 mg/g clay. This value is much lower than those for PEG and PCEs (see Fig. 7) and can be attributed to the absence of graft chains.

3.8. Comparison of experimental sorption data with theoretical calculations

From the experimental sorption isotherms of individual PMA and PEG, the total amounts of PCE sorbed can be calculated, considering the overall composition of the PCEs as presented in Section 2.8. These calculations were performed and the results obtained were compared with those attained in earlier experiments (see Fig. 7).

Fig. 11 displays the calculated sorbed amounts of 45PC1.5 and 45PC6 based on experimental data on PEG sorption. The maximum sorbed amounts of 510 mg/g clay and 420 mg/g clay for samples with added 45PC1.5 and 45PC6 were attained only after adding 300% bwo clay of PCE, indicating a much slower sorption rate than experimentally determined (Fig. 7). However, when the point of saturated sorbed amount (equilibrium state) was reached, the trend in the difference in sorbed amount of the PCEs (calculated versus actual) was comparable, suggesting that the poly(ethylene oxide) side chain steers the sorption process at higher PCE dosages.

Likewise, the same calculations were performed based on experimental sorption data of PMA presented in Fig. 10. From this, the

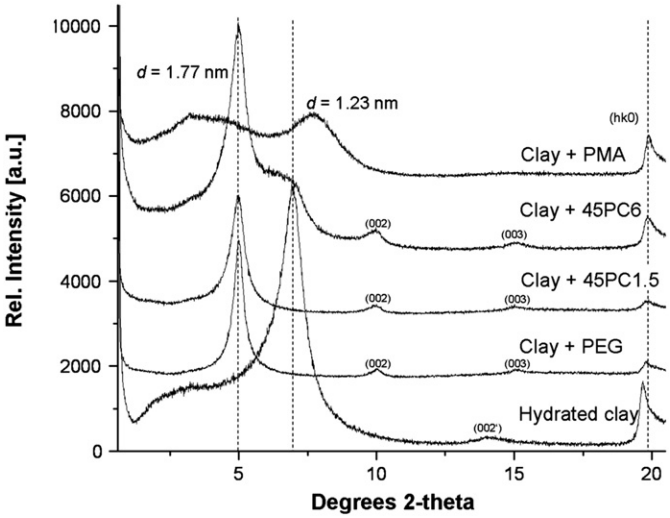

Fig. 9. XRD patterns of montmorillonite dispersed in synthetic cement pore solution, holding 50% bwo clay of PMA, PEG, 45PC1.5 and 45PC6 respectively (w/clay = 53).

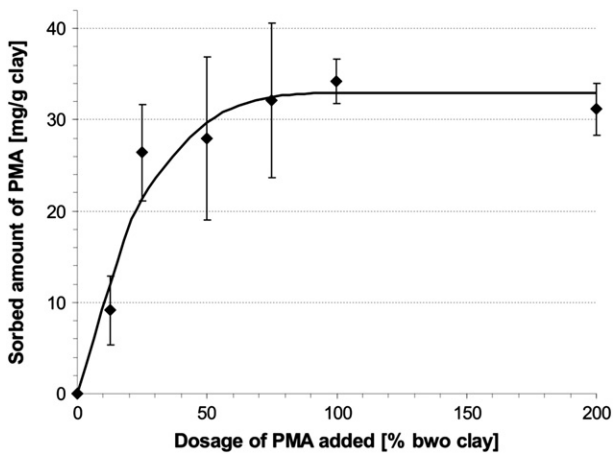

Fig. 10. Sorption isotherm of PMA on montmorillonite dispersed in synthetic cement pore solution as a function of PMA dosage (Ca^{2+} = 0.4 g/L, w/clay = 53).

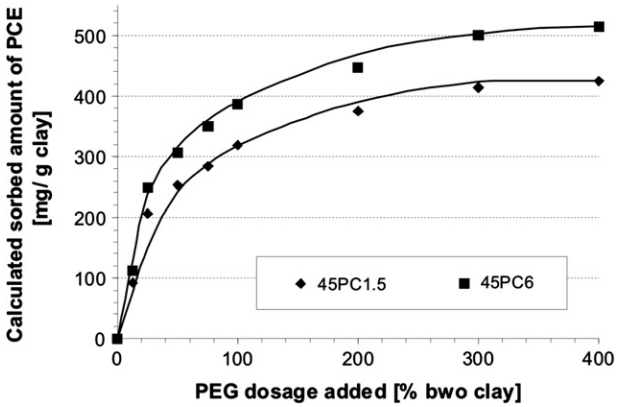

Fig. 11. Idealised sorption isotherms of the PCEs, calculated from sorption data of individual PEG on clay, assuming that PCE sorption solely occurs through PEO side chain interaction.

theoretical maximum amounts of PCE which can adsorb onto clay solely via electrostatic attraction were calculated as ~290 mg/g clay for 45PC1.5 and 120 mg/g clay for 45PC6 respectively (Fig. 12). These values do not fit the experimentally found sorbed amounts of 415 mg/g clay and 380 mg/g clay for 45PC1.5 and 45PC6 samples. However, the initial steep increase in sorbed amounts of PCE is similar to that obtained experimentally (Fig. 7). This signifies that at lower dosages, the PCE–clay interaction is mainly driven by electrostatic attraction.

To summarize, the mechanism of interaction between PCE and clay depends not only on the PEO content of PCE, but is also dosage dependent. At lower PCE dosages, backbone interaction with montmorillonite clay surfaces via electrostatic attraction dominates, while at higher dosages, intercalation of the poly(ethylene oxide) side chain prevails.

3.9. PEG as sacrificial agent

To confirm our concept of side chain interaction, pure PEG was added to cement/clay pastes holding both PCE polymers, and the paste spread was measured by 'mini slump' tests. The results are presented in Fig. 6. Both pastes incorporating pure PEG showed less decrease in workability than in the absence of this agent (spread value 24.4 cm instead of 22.3 cm for 45PC1.5, and 22.1 cm instead of 21.3 cm for 45PC6). This demonstrates that due to the similarity in chemical composition with the PCE side chain, polyglycols such as PEG can work as a sacrificial agent to reduce the amount of PCE consumed by clay, thus softening the negative impact on PCE

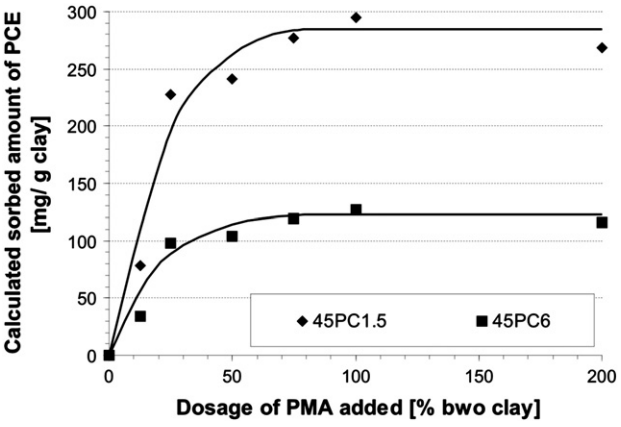

Fig. 12. Idealised adsorption isotherms of PCE samples, calculated from sorption data of PMA on clay, assuming that the PCE molecules only sorb via their backbone.

performance in the presence of clay contaminants. Additionally, the higher regain in spread for 45PC1.5 confirms that for this PCE (employed at a higher dosage of 1.07% bwoc), interaction with clay is more driven by side chain interaction, which is a result of its higher grafting density. On the other hand, in 45PC6, the trunk plays a more important role in its consumption by clay, especially due to the lower dosage of 0.09% bwoc required to fluidize this cement.

These results instigate that the usage of glycols as sacrificial agents generally is suitable for PCEs possessing higher side chain density such as 45PC1.5 (ready-mix type PCE) which in actual field applications are utilised at fairly high dosages (~0.3–0.5%). However, for PCEs with high anionic charge amounts (precast type) where added dosages are usually much less (~0.05–0.1%), the improvement in flow is not as desirable. Therefore, an alternative remedy, possibly interfering with their electrostatic preference for clay surfaces is required.

4. Conclusions

This work confirms that sodium montmorillonite clay exhibits a much higher affinity for PCE than cement. When only very minor amounts of montmorillonite clay are introduced into cement pastes, they reduce the availability and thus dispersing effectiveness of PCE superplasticizers. The effect on clay can be correlated to the specific molecular composition and the dosages of PCE employed. Generally, the affinity of PCE to clay originates from two different mechanisms: first, the intercalating ability of the poly(ethylene oxide) side chain of PCE into the interlayer space of the alumosilicate layers. Second, especially for PCEs possessing increased anionic charge density, electrostatic attraction mediated by surface adsorbed Ca^{2+} cations occurs. Theoretical calculations demonstrate that electrostatic attraction plays a more prevalent role at lower PCE dosages while side chain intercalation dominates at high PCE dosages. Therefore, the total amount of a PCE sorbed by clay is the result of a delicate balance between PCE dosage added, amount of PEO side chains available for intercalation, and anionic charge density of the PCE which promotes surface adsorption.

The failure of PCE to fluidize in concrete can have many reasons. It is known that SO_4^{2-} can greatly affect the performance of PCEs by competitive adsorption onto the surfaces of cement particles [33], or it may arise from incompatibility with other admixtures, or even the overall composition of cements. The latter influences are not well understood as of today. As shown here, another potential reason for failure is interaction with clays such as montmorillonite. Therefore, when a PCE fails during application, a methylene blue test for clay might help to identify the root cause (such as contamination from sand, gravel or limestone) for the problem, from which a suitable remedy such as addition of a glycol can thus be devised.

Acknowledgments

The authors would like to thank Dr. Coutelle from Rockwood (Moosburg/Germany) for supplying the clay sample. Also, Serina Ng would like to thank Jürgen Manchot Stiftung for generous funding of this research.

References

[1] D. Manning, Handbook of Clay Science (Developments in Clay Science, 1, in: F. Bergaya, B.K.G. Theng, G. Lagaly (Eds.), Elsevier's Science & Technology, 2007.
[2] B. Velde, Origin and Mineralogy of Clays: Clay and the Environment, in: B. Velde (Ed.), Springer, 1995.
[3] E. Tombácz, M. Szekeres, Colloidal behavior of aqueous montmorillonite suspensions: the specific role of pH in the presence of indifferent electrolytes, Appl. Clay Sci. 27 (2004) 75–94.
[4] E. Tombácz, M. Szekeres, Surface charge heterogeneity of kaolinite in aqueous suspension in comparison with montmorillonite, Appl. Clay Sci. 34 (2006) 105–124.

[5] E.P. Giannelis, Polymer layered silicate nanocomposites, Adv. Mater. 8 (1996) 29–35.
[6] M. Alexandre, P. Dubois, Polymer-layered silicate nanocomposites: preparation, properties and uses of a new class of materials, Mater. Sci. Eng. 28 (2000) 1–63.
[7] P.C. LeBaron, Z. Wang, T.J. Pinnavaia, Polymer-layered silicate nanocomposites: an overview, Appl. Clay Sci. 15 (1999) 11–29.
[8] H.C. Greenwell, A.A. Bowden, B. Chen, P. Boulet, J.R.G. Evans, P.V. Coveney, A. Whiting, Intercalation and in situ polymerization of poly(alkylene oxide) derivatives within M^+-montmorillonite (M = Li, Na, K), J. Mater. Chem. 16 (2006) 1082–1094.
[9] H.C. Greenwell, W. Jones, P.V. Coveney, S. Stackhouse, On the application of computer simulation techniques to anionic and cationic clays: a materials chemistry perspective, J. Mater. Chem. 16 (2006) 708–723.
[10] A.A. Jeknavorian, L. Jardine, C.C. Ou, H. Koyata, K.J. Folliard, Interaction of Superplasticizers with Clay-Bearing Aggregates, Special Publication ACI/ 7th CANMET Conference on Superplasticizers and Other Chemical Admixtures, Berlin, Germany, 2003, pp. 1293–1316, SP-217.
[11] E. Sakai, D. Atarashi, M. Daimon, Interaction between Superplasticizers and Clay Minerals, Special Publication ACI/ 6th CANMET Conference on Superplasticizers and Other Chemical Admixtures, Xi' an, China, 2006, pp. 1560–1566.
[12] H. Kroyer, H. Lindgreen, H.J. Jakobsen, J. Skibsted, Hydration of portland cement in the presence of clay minerals studied by ^{29}Si and ^{27}Al MAS NMR spectroscopy, Adv. Cem. Res. 15 (2003) 103–112.
[13] T. Mandalia, F. Bergaya, Organo clay mineral-melted polyolefin nanocomposites: effect of surfactant/CEC ratio, J. Phys. Chem. Solids 67 (2006) 836–845.
[14] M. Gay-Duchosal, D.H. Powell, R.E. Lechner, Benoit Rufflé, QINS studies of water diffusion in Na–montmorillonite, Physica B 276–278 (2000) 234–235.
[15] J. Kropp, Performance of Concrete as a Criterion of its Durability, in: H. Hilsdorf, J. Kropp (Eds.), RILEM Technical Committee TC 116-PCD, Spon Press, 1995.
[16] L. Jaernstrom, P. Stenius, Adsorption of polyacrylate and carboxy methyl cellulose on kaolinite: salt effects and competitive adsorption, Colloids Surf. 50 (1990) 47–73.
[17] D. Atarashi, E. Sakai, R. Obinata, M. Daimon, Interactions between superplasticizers and clay minerals, Cem. Sci. Concr. Technol. 58 (2004) 387–392.
[18] D. Atarashi, E. Sakai, R. Obinata, M. Daimon, Influence of clay minerals on fluidity of $CaCO_3$ suspension containing comb-type polymer, Cem. Sci. Concr. Technol. 57 (2003) 386–391.
[19] J. Plank, K. Pöllmann, N. Zouaoui, P.R. Andres, C. Schaefer, Synthesis and performance of methacrylic ester based polycarboxylate superplasticizers possessing hydroxy terminated poly(ethylene glycol) side chains, Cem. Concr. Res. 39 (2009) 1–5.
[20] H. N. Zouaoui, Einfluss der Molekülarchitektur von Polycarboxylaten, hergestellt durch Blockcopolymerisation und Pfropfreaktion, auf die Wechselwirkung mit Fluoroanhydrit und Portlandzement; Dissertation, Technische Universität München, Lehrstuhl für Bauchemie (2009).
[21] S. Kawaguchi, K. Aikaike, Z.M. Zhang, K. Matsumoto, K. Ito, Water soluble bottlebrushes, Polym. J. 30 (1998) 1004–1007.
[22] K. Andersson, B. Allard, M. Bengtsson, B. Magnusson, Chemical composition of cement pore solutions, Cem. Concr. Res. 19 (1989) 327–332.
[23] G. Lagaly, From clay mineral crystals to colloidal clay mineral dispersions, Surfact. Sci. Series, Vol. 126, Coagulation and Flocculation (2nd Edition), General Review (2005) 519–600.
[24] L.M. Vane, G.M. Zang, Effect of aqueous phase properties on clay particle zeta potential and electro-osmotic permeability: implications for electrokinetic remediation processes, J. Hazard. Mater. 55 (1997) 1–22.
[25] C.Z. Li, N.Q. Feng, Y.D. Li, R.J. Chen, Effects of polyethylene oxide chains on the performance of polycarboxylate-type water-reducers, Cem. Concr. Res. 35 (2005) 867–873.
[26] A. Zingg, F. Winnefeld, L. Holzer, J. Pakusch, S. Becker, R. Figi, L. Gauckler, Interaction of polycarboxylate-based superplasticizers with cements containing different C_3A amounts, Cem. Concr. Com. 31 (2009) 153–162.
[27] J. Plank, G. Bassioni, Z. Dai, H. Keller, B. Sachsenhauser, N. Zouaoui, Neues zur Wechselwirkung von Zementen und Fließmitteln, 16th Ibausil, Bauhaus-Universität Weimar, Tagungsband 1, Weimar, Germany, 2006, pp. 579–598.
[28] S. Liu, X. Mo, C. Zhang, D. Sun, C. Mu, Swelling inhibition by polyglycols in montmorillonite dispersions, J. Disper. Sci. Technol. 25 (2004) 63–66.
[29] P.M. Amarasinghe, K.S. Katti, D.R. Katti, Nature of organic fluid–montmorillonite interactions: an FTIR spectroscopic study, J. Colloid Interface Sci. 337 (2009) 97–105.
[30] S. Burchill, P.L. Hall, R. Harrison, M.H.B. Hayes, J.I. Langford, W.R. Livingston, R.J. Smedley, D.K. Ross, J.J. Tuck, Smectite–polymer interactions in aqueous systems, Clay Miner. 18 (1983) 373–397.
[31] P.D. Svensson, S. Hansen, Intercalation of smectite with liquid ethylene glycol — resolved in time and space by synchrotron X-ray diffraction, Appl. Clay Sci. 48 (2010) 358–367.
[32] J.L. Suter, P.V. Coveney, Computer simulation study of the materials properties of intercalated and exfoliated poly(ethylene) glycol clay nanocomposites, Soft mater. 5 (2009) 2239–2251.
[33] K. Yamada, S. Ogawa, S. Hanehara, Controlling of the adsorption and dispersing force of polycarboxylate-type superplasticizer by sulfate ion concentration in aqueous phase, Cem. Concr. Res. 31 (2001) 375–383.

Paper 2

Study on the Interaction of Na-montmorillonite Clay with Polycarboxylates

S. Ng, J. Plank

V. M. Malhotra (Ed.) 10th CANMET/ACI Conference on Superplasticizers and Other Chemical Admixtures in Concrete
SP–288, ACI, Prague (2012) 407–420.

Study on the Interaction of Na-montmorillonite Clay with Polycarboxylates

Serina Ng and Johann Plank

SYNOPSIS:

The negative impact of sodium montmorillonite clay on dispersion effectiveness of two polycarboxylates consisting of methacrylate acid : MPEG methacrylate ester at molar ratios of 6:1 and 1.5:1 was investigated. When 1 % by weight of cement (bwoc) of clay was present, cement spreads decreased by up to 60 % while PCE sorption soared to ~ 400 mg/g clay (~ 100 times higher than on Portland cement). The PCEs mainly undergo chemisorption by intercalation between the alumosilicate layers via their poly(ethylene oxide) side chains. Additionally, to a minor extent (~ 15 %), adsorption via electrostatic attraction to the positively charged clay surfaces takes place. Polyglycols can be effectively used as a sacrificial agent to protect PCEs possessing high grafting density from the negative effects of clay, while more anionic PCEs benefit, however to a certain extent only, from the addition of highly anionic polyelectrolytes such as poly(methacrylic acid).

Keywords: cement; clay; montmorillonite; polycarboxylate; interaction

Serina Ng studied Industrial Chemistry (M.Sc.) within the frame of a joint program between Technische Universität München, Germany and National University of Singapore. She is currently a Ph.D. student at the Chair for Construction Chemicals in Munich, researching on mechanisms of superplasticizer interaction with calcium aluminate cements and clays.

Johann Plank is full Professor at the Institute of Inorganic Chemistry of Technische Universität München, Germany. Since 2001, he holds the Chair for Construction Chemicals there. Research interests include cement chemistry, concrete admixtures, organic-inorganic composite and nano materials, concrete, dry-mix mortars and oil well cementing.

INTRODUCTION

Polycarboxylates (PCEs) is a class of superplasticizers with exceptional fluidizing ability. They can maintain workability of concrete mixtures over extended periods of time (~ 2 hrs slump retention) [1]. The main benefit of using PCE over other conventional superplasticizers lies in their relatively low dosage due to the steric repulsive forces arising from their long side chains [2]. While the benefits of PCEs are plentiful, applicators have observed that unlike for polycondensates, presence of clay contaminants can negatively impact their effectiveness [3-5] and generally impede the properties of concrete [6]. Montmorillonite (MMT), a 2:1 smectite clay of general composition $M_x(Mg,Al,Fe)_2(OH)_2[Si_4O_{10}]\cdot nH_2O$ where $M^+ = Na^+$, K^+, 0.5 Mg^{2+} or 0.5 Ca^{2+} is more harmful than other clay minerals due to its expanding lattices which allow intercalation, swelling and cation exchange [7]. Generally, the capacity of MMT to sorb water and swell viscosifies cement pastes. This effect results in a loss in workability or a higher water demand to achieve the same workability as in the absence of clay.

In a previous paper [8], we have presented the negative effect of MMT on two methacrylic acid-methacrylate ester based PCEs which are sorbed in high amount by this clay (~ 100 times more than on cement). There, we found that the main driving force for sorption of PCE is side chain intercalation in between the alumosilicate layers. Additionally, a minor amount of PCE is sorbed by electrostatic attraction mediated by a layer of Ca^{2+} ions present on the surfaces of the clay platelets. It also became apparent that the mode of interaction is dosage dependent: at lower PCE dosages, its adsorption is electrostatic driven, while intercalation dominates at higher PCE dosages.

This study here complements those previous results by focussing on the electrostatic interaction between PCE and clay. At first, the uptake of Ca^{2+} by MMT was quantified via zeta potential measurement. This was followed by measurement of poly(methacrylic acid) (PMA) sorption on this clay to present the interaction between the anionic PCE backbone and MMT. In the second part, different strategies to mitigate the negative effects of clay on PCE were probed. First, addition of K^+ which is known to occupy and thus block the interlayer spaces of MMT was explored as a method to prevent side chain intercalation. Secondly, in reference to a US patent filed in 1998, non-ionic polyglycol (PEG) were probed as a sacrificial agent to reduce PCE-clay interaction [9]. And lastly, anionic PMA and PCE polymer 24PC18 were also studied as other potential sacrificial agents.

RESEARCH SIGNIFICANCE

The issue of occasional performance failure of PCE superplasticizers in concrete is addressed. Limestone, sand and gravel used in concrete can be loaded with clay impurities which normally are removed by washing. However, this procedure is now often omitted to reduce the amount of waste water. We confirm that montmorillonite clay presents a key contaminant which diminishes the dispersing effectiveness of common PCE superplasticizers. Additionally, the mechanism underlying the interaction between clay and PCE is clarified here, and potential mitigation strategies are proposed.

EXPERIMENTAL PROCEDURES

Cement

A CEM I 52.5 R HS/NA (Holcim, Lägerdorf/Germany) was used. Its phase composition as obtained by quantitative X-ray diffraction (Bruker D8 advance instrument, software Topas 4.0) is presented in **Table 1**. Specific surface area was 4,300 cm^2/g (*Blaine* instrument, Toni Technik, Berlin/Germany), particle size (d_{50} value) was 8.33 µm (laser granulometer CILAS 1064, Cilas, Marseille/France) and density was 3.22 g/cm^2 (ultrapycnometry, Quantachrome, Odelzhausen/Germany).

Clay

A commercial naturally occurring sodium montmorillonite clay sample (RXM 6020 supplied by Rockwood, Moosburg/Germany) was used as per obtained. Its oxide composition is presented in **Table 2**. It develops a pH of ~ 9 when prepared as a 2 wt. % aqueous suspension. The XRD pattern of the dry clay reveals a *d*-spacing of 1.07 nm.

Polycarboxylates

Two PCE samples and two polymers representing the poly(methacrylic acid) backbone (PMA) and poly(ethylene glycol) side chain (PEG) of the PCEs were utilised. The PCEs were synthesized according to a literature description by aqueous free radical copolymerization of methacrylic acid (MAA) and methoxy terminated poly(ethylene glycol) methacrylate (MPEG-MA) ester at molar ratios of 1.5 and 6 respectively [10]. Methallylsulfonic acid was used as chain transfer agent. Both copolymers have side chains made up of 45 ethylene oxide units (EOUs). They are denoted by 45PCx, where 45 refers to the number of EOUs in the side chain, and x corresponds to the molar ratio of MAA:MPEG-MA. The chemical formula of the PCEs is presented in **Fig. 1**. PMA was synthesized by aqueous free radical polymerization of MAA [11], while PEG–2000 (n_{EO} = 45) with a purity of > 99 % was used as per obtained (Clariant, Frankfurt am Main/Germany). As sacrificial agent, PCE polymer 24PC18 (n_{EO} = 24, MAA:MPEG-MA = 18) was synthesized as above.

Polymer characterisation

Size exclusion chromatography (SEC; Waters Alliance 2695) equipped with RI detector 2414 (both from Waters, Eschborn/Germany) and a 3 angle dynamic light scattering detector (mini Dawn from Wyatt Technologies, Santa Barbara, CA/USA) was used. The polymer solutions were first filtered through a 0.2 µm filter and then separated on a precolumn and three columns (120, 250 and 500; Ultrahydrogel™, Waters, Eschborn/Germany) using 0.1 M aqueous $NaNO_3$ solution (adjusted to pH 12.0 with NaOH) as an eluant at a flow rate of 1.0 mL/min. From this separation, the molar masses (M_w, M_n) and the polydispersity index (PDI) of the polymers were determined. The value of dn/dc used to calculate M_w and M_n was 0.135 mL/g (value for polyethylene oxide) [12].

Specific anionic charge amounts of the polymers were analysed by a particle charge detector (PCD 03 pH from Mütek Analytic Company, Herrsching/Germany). Solutions containing 0.02 wt. % of anionic polymer dissolved in synthetic cement pore solution [ionic composition (mmol/L): Ca^{2+} = 10; Na^+ = 100; K^+ =180; OH^- = 127; SO_4^{2-} = 86] were prepared and titrated against a 0.001N solution of cationic poly(diallyl dimethyl ammonium chloride) (polyDADMAC) until charge neutralization was attained. The amount of negative charge per gram of polymer was calculated from the consumption of the cationic polyelectrolyte.

Zeta potential measurements

pH dependent zeta potentials of MMT dispersed in water were determined in the range of pH 1.5 – 13 using 37 wt. % aqueous HCl or 19.5 wt. % aqueous NaOH for pH adjustment, and in synthetic cement pore solution, employing a model DT 1200 Electroacoustic Spectrometer (Dispersion Technology Inc., Bedford Hills, NY/USA). Particle size was measured on a ZetaSizer from Malvern Instruments Ltd (Worcestershire/United Kingdom). The w/clay ratio was 53 to actualise the conditions in the 'mini slump' tests where the w/c ratio was 0.53 and 1 % by weight of cement (bwoc) of clay were present. For titration studies, a 40 g/L Ca^{2+} solution prepared from $CaCl_2$, and a 10 wt. % PMA solution were used respectively. In a separate experiment, 20 g/L of PMA were dissolved in the filtrate of clay suspended in synthetic cement pore solution and left to stand

overnight. No precipitation was found, showing that PMA depletion was solely a result of sorption by the cement or clay.

'Mini Slump' test

For determination of paste flow, a 'mini slump' test according to DIN EN 1015 was conducted. At first, the w/c ratio needed to attain a spread of 18 ± 0.5 cm (~ 22 Pa) for the neat cement paste was established, and the PCE dosages required to reach a spread of 26 ± 0.5 cm (~ 3.3 Pa) at this specific w/c ratio were determined. The PCE solution generally was added to the mixing water placed in a porcelain cup, and the amount of water introduced with the PCE solution was subtracted from the amount of mixing water required for a w/c ratio of 53. 300 g of solids (pure cement or cement blended with 1 wt. % of stirred for 2 minutes before transferring into a Vicat cone on a glass plate. The dimensions of the Vicat cone were: height 40 mm, top diameter 70 mm, and bottom diameter 80 mm (1.57, 2.76 and 3.15 in. respectively). The cement paste was filled to the brim of the cone and levelled before it was vertically lifted from the surface of the glass plate. The resulting paste spread was measured twice; the second measurement being perpendicular to the first. The final spread value was taken as the average of the two measured ones.

PEG and PCE polymer 24PC18 were added in equal amounts as PCE, while PMA was added in two forms: equal amount or five times the dosage of PCE added.

XRD analysis

0.025 g clay were added to 1.34 g of 0.93 wt. % polymer solution (w/clay ratio of 53). The suspensions were manually mixed for 1 minute, sonicated for 10 minutes and centrifuged at 14,600 rpm for a further 10 minutes. The solid residues obtained were dried at 80 °C overnight and ground. XRD scans of all samples were taken at room temperature on a D8 Advance, Bruker AXS instrument (Bruker, Karlsruhe/Germany) utilising Bragg-Bretano geometry. Samples were placed in a front mounted plastic sample holder. The conditions were as follows: step size 0.15 s/ step, scan spin at a revolution time of 4 sec, nickel filter as incident beam, aperture slit 0.3°, scan range from 0.6° to 20 ° 2θ.

Sorption experiments

PCE sorption was determined by the depletion method, i.e. it was assumed that removal of PCE from the pore solution solely was the result of interaction with clay and that no precipitation had occurred. In sample preparation, over 1 minute 300 g of pure cement or cement blended with 1 wt. % of clay were added to 159 mL of 2.0 wt. % 45PC1.5 or 0.17 wt. % 45PC6 solutions (with or without the equivalent amount of PEG) in a porcelain cup (w/c ratio 0.53). The mixture was allowed to rest for one minute, stirred for another 2 minutes and centrifuged at 8,500 rpm for 10 minutes. The filtrate was recovered, and evaluated by SEC analysis. In a separate experiment, 20 g/L of PCE were dissolved in the filtrate of clay suspended in synthetic cement pore solution and left to stand overnight. No precipitation was found, showing that PCE depletion was solely a result of sorption by the cement or clay.

Sorption of PCE samples on clay alone, with or without saturated KOH, was performed employing PCE solutions of concentrations between 12.5 to 200 % by weight of (bwo) clay. These solutions were added to 0.025 g of clay, manually homogenized, sonicated for 10 minutes and centrifuged at 14,600 rpm for 10 minutes. The filtrate were recovered, diluted and acidified with conc. HCl in a TOC sample flask. This final solution was analysed by combustion at 890 °C on a HIGH TOC II instrument (Elementar Analysensysteme, Hanau/Germany). The sorbed amount of PCE was calculated from the difference between the TOC content in the stock solution and that left in the filtrate.

Sorption of PCE on clay alone with equivalence amount of PEG added was performed with PCE solutions of concentrations between 12.5 % bwo clay and 200 % bwo clay. These solutions were added to 0.24 g of clay, manually homogenized, sonicated for 10 minutes and centrifuged at 8,500 rpm for 10 minutes. The concentration of unadsorbed PCE contained in the filtrates and in the starting solution holding PEG and PCE were quantified via SEC.

EXPERIMENTAL RESULTS AND DISCUSSION

Impact of Ca^{2+} on surface charge of montomorillonite

The zeta potential of the clay sample was found to be consistently negative, due to the innate negative basal surface charge (**Fig. 2**). Till pH 5, the zeta potential of the clay suspension remained relatively constant at ~ – 15 mV. It decreased sharply to ~ – 35.2 mV at pH 8 and stabilized thereafter. The transition in surface charge from pH 5 to 8 can be attributed to deprotonation of terminal silanol and aluminol groups along the crystal edges of clay platelets.

However, when a 40 g/L Ca^{2+} solution was titrated against the native MMT suspension at pH 12.8, its zeta potential increased strongly from – 35 mV to 0 mV after addition of ~ 0.8 g/L of Ca^{2+}. Thereafter, the zeta potential increased to + 21 mV with further titration of Ca^{2+} solution, confirming adsorption of a large amount of Ca^{2+} onto the negative surfaces of MMT (**Fig. 3**). Likewise, in synthetic cement pore solution (0.4 g/L Ca^{2+}), the clay suspension registered a positive and stable zeta potential value of + 15.1 mV within the first 5 minutes after mixing. These results signified that in the presence of cement, charge reversal of MMT occurs as a result of rapid Ca^{2+} uptake.

Properties of PCE samples

The molecular characteristics and anionic charge amounts of the polymers are shown in **Table 3**. According to this data, the synthesized poly(methacrylate) backbone on average consists of 33 methacrylate units while the PCE copolymers 45PC1.5 and 45PC6 contain 23 and 17 methacrylate functionalities. The specific anionic charge amounts increase as follow: PEG < 45PC1.5 < 45PC6 < PMA.

Dispersing performance of PCE in presence of clay

The w/c ratio of the neat cement paste for a spread of 18 ± 0.5 cm (~ 22 Pa; [13]) was determined to be 0.53. When 1 % bwoc of clay was added, the spread of the cement paste decreased to 15.3 cm (- 15 %), as availability of water decreased from clay flocculation.

In the absence of clay, the dosages of 45PC1.5 and 45PC6 required to obtain a spread of 26 ± 0.5 cm (~ 3.3 Pa) were 1.07 % bwoc and 0.09 % bwoc respectively. Thus, 45PC6 is a much more effective dispersant due to its significantly higher anionic charge. However, when 1 % bwoc of clay was added, the respective spreads decreased by 41 % and 58 % to 22.3 cm (7.4 Pa, 45PC1.5) and 21.3 cm (9.4 Pa, 45PC6), as shown in **Fig. 4**. These reductions in paste fluidity much exceed that observed in the absence of PCE, indicating that interaction of PCE with clay affects its dispersing effectiveness.

PCE sorption in cement/clay system

To confirm the effect of clay on PCE, the sorbed amounts of 45PC1.5 and 45PC6 in cement paste with or without 1 wt. % clay were investigated. According to **Table 4**, when clay was added, the sorbed amount of PCE increased greatly and was particularly strong with 45PC1.5 possessing high grafting density (from 24.6 to 54.6 %). Considering the small amount of clay added, this presents a huge increase in PCE sorption, thus confirming strong interaction between PCE and clay. This result instigates that in a cementitious system, a considerable amount of PCE can be consumed by a relatively minor amount of clay contaminant. To examine the effect of clay only on PCE and to eliminate the effects of cement, a simplified system consisting of only clay and PCE in synthetic cement pore solution was utilized next.

Sorption of PCE on clay

The sorption isotherms of 45PC1.5 and 45C6 on MMT in synthetic cement pore solution are illustrated in **Fig. 5**. The clay had an extremely high affinity for both polymers, showing maximum sorbed amounts of 415 mg/g clay (8.87 mg/m^2 clay) for 45PC1.5 and 380 mg/g clay (8.14 mg/m^2 clay) for 45PC6. Such sorbed amounts are ~ 100 times higher than on OPC [14].

When MMT was suspended in the same alkaline solution but holding no Ca^{2+}, sorbed amounts of 45PC1.5 and 45PC6 decreased to 360 mg/g clay (7.71 mg/m^2 clay) and 345 mg/g clay (7.39 mg/m^2 clay) respectively (**Fig. 6**). This decrease signifies that the presence of Ca^{2+} accounts for 10 – 15 % uptake of PCE by clay. It also becomes

clear that in the absence of Ca^{2+}, the anionic charge of PCE no longer impacts its sorption on clay. This confirms that in such systems, interaction between PCE and clay is solely the result of side chain interaction.

Electrostatic interaction PCE–clay

To confirm occurrence of electrostatic interaction between PCE and clay loaded with Ca^{2+}, anionic PMA which represents the backbone of PCE was added to the clay suspended in synthetic cement pore solution. As a result, the zeta potential value decreased from + 15.1 mV to + 6.8 mV (**Fig. 7**), showing that PMA has adsorbed onto clay surfaces by electrostatic attraction, mediated by a monolayer of Ca^{2+} ions sorbed on the alumosilicate surfaces. In the equilibrium state, this clay adsorbs a high amount (~ 70 % of its own weight or 70 mg/g clay) of PMA. This signifies strong electrostatic attraction between PCE and clay. According to this principle, PCEs can adsorb onto clay via their anionic polymethacrylate based backbone.

The difference in sorbed amounts of the two PCEs in the two aqueous systems demonstrates that electrostatic attraction accounts for ~ 10 % of 45PC1.5 sorption and ~ 15 % of 45PC6 sorption in the static synthetic cement pore solution. In a cement paste, the actual adsorbed amount of PCEs via electrostatic attraction may be higher due to the continuous dissolution of Ca^{2+} from the clinker phases, thus providing a surface possessing enhanced anchoring capability for incoming anionic PCEs. As expected, the more anionic 45PC6 exhibited higher preference for electrostatic attraction than the less anionic 45PC1.5. On the other hand, the main mode of PCE sorption can be attributed to interaction of the PCE side chain with clay, as was confirmed by the high sorbed amount of 380 mg/g clay (8.14 mg/m^2 clay) of PEG (**Fig. 5**).

Side chain interaction PCE–clay

Interaction of PCE and of pure polyethylene glycol (PEG–2000, $n_{EO} = 45$) with MMT was investigated via XRD analysis. For sample preparation, 0.025 g clay were added to 1.34 g of 0.93 wt. % polymer solution. According to **Fig. 8**, a characteristic *d*-spacing of 1.77 nm was observed when PEG was added to the MMT. This result came as expected, because glycols, which possess similar chemical composition as the PCE side chain, are known to intercalate readily into the MMT structure [15]. Likewise, when 45PC1.5 and 45PC6 were added, a shift in *d*-spacing from 1.23 nm (for hydrated clay) to the same value of 1.77 nm was detected. Also, an increase in broadness of the reflection characteristics for the *d*-spacing of 1.77 nm was observed as side chain density of the polymers decreased, i.e. PEG < 45PC1.5 < 45PC6. These findings signify that the PCEs intercalates mainly via their PEO side chains, while the anionic backbone apparently disturbs the stacking order of the MMT layers. Pure PEG, which does not possess an anionic backbone can intercalate in between the clay layers with ease and generate highly ordered structures, thus producing sharper reflections. Consequently, 45PC1.5, with its higher grafting density and lower anionic charge showed a more ordered intercalate product than 45PC6.

Effect of K^+ on PCE sorption by clay

The effect of K^+ on the amount of 45PC1.5 sorbed by clay was analysed next. This experiment was performed to verify PCE incorporation into the layered structure of MMT. It is well established that K^+ readily occupies the interlayer region between the alumosilicate layers [16] and thus potentially can block the chemical uptake of PCE. According to **Fig. 9**, a huge decrease in sorbed amount of 45PC1.5 from 415 mg/g clay (8.89 mg/m^2 clay) to 110 mg/g clay (2.36 mg/m^2 clay) occurred when K^+ was added. This reduction in sorbed amount of PCE (~ 75 %) shows that PCE and K^+ compete for the same sorption site in the MMT structure, thus confirming that PCE intercalates between the alumosilicate layers. The stabilization of clay layers reduces exfoliation and decreases the effective surfaces for PCE adsorption. However, this accounts only for a minor portion as the remaining sorbed amount of PCEs indicates that PCE still sorbs on clay via electrostatic attraction. Accordingly, addition of K^+ provides a method to remedy the negative impact of clay on PCE.

PEG as sacrificial agents

Another strategy to minimise side chain interaction is the addition of PEG. 'Mini slump' tests with PEG–2000 added (dosage equal to that of PCE) were performed (**Fig. 4**). Cement pastes containing 45PC1.5 increased in spread from 22.3 cm (7.4 Pa) to 24.4 cm (4.6 Pa.), while that with 45PC6 rose from 21.3 cm (9.4 Pa) to 22.1 cm (7.7 Pa). Corresponding sorption studies revealed that the sorbed amount of 45PC1.5 decreased from 54.6 % to 28.0 %, while that of 45PC6 fell from 65.0 % to 60.6 % only (**Table 4**). Accordingly, PEG generally can protect PCE from consumption by clay, but its effect varies with PCE composition. It is more effective in reducing the

sorption of higher grafted, ready–mix type PCEs such as 45PC1.5, than that of PCEs commonly used to manufacture precast concrete (e.g. 45PC6).

Anionic PCE polymers as sacrificial agents

Finally, more anionic PCEs were explored as potential sacrificial agents. Focussing on the electrostatic adsorption behaviour of PCE, PMA and PCE polymer 24PC18 were tested as sacrificial agents via 'mini slump' test (**Table 5)**. Addition of PMA at low dosage (0.09 % bwoc) improved the dispersing effectiveness of 45PC6 more than PEG, indicating that this polymer undergoes considerable electrostatic interaction with clay. At high PMA addition (0.45 % bwoc), this polymer flocculated the suspension and thus viscosified the paste. Effectiveness of highly anionic PCE polymer 24PC18 to improve performance of 45PC6 was less than that of PMA. Contrary to this, addition of PMA to the paste holding 45PC1.5 showed no benefit at all with respect to improved fluidity, thus confirming that this PCE interacts with clay almost exclusively through its side chain. On the other hand, addition of PCE polymer 24PC18 greatly increased the spread of the paste containing 45PC1.5. This effect however is owed to the high dispersing power of 24PC18. When 24PC18 is used as a dispersant alone, only 0.06 % bwoc of this PCE was required to achieve a cement spread of 26 ± 0.5 cm (~ 3 Pa). Therefore, when such a high dosage of 24PC18 (1.07 % bwoc) was added, this more anionic copolymer acts as the main dispersing agent while the higher grafted 45PC1.5 becomes the sacrificial agent for clay.

The results indicate that PMA can function as a potential sacrificial agent when applied at low dosages. However, its effectiveness is limited. It seems to be more difficult to shield highly anionic PCEs from the negative effects of clay than to protect PCEs possessing high grafting density.

CONCLUSIONS

This work confirms that sodium montmorillonite negatively impacts the dispersing effectiveness of PCEs on cement. When present in only very minor quantity, this clay sorbed large amounts of PCEs and thus reduces their availability for dispersion. Affinity of PCE for clay occurs mainly through chemisorption of their PEO side chains between the alumosilicate layers of the clay. PEG addition presents a potential remedy to maintain the dispersing ability of highly grafted PCEs. For PCE possessing high anionic charge (low grafting density), strongly anionic polyelectrolytes employed as sacrificial agents provided only minor improvement, indicating that for this type of PCE, mitigation of the negative impacts of clay is more difficult.

ACKNOWLEDGMENTS

SERINA NG WOULD LIKE TO THANK JÜRGEN MANCHOT STIFTUNG FOR GENEROUS FUNDING OF THIS RESEARCH.

REFERENCES

[1] Matsuo S., Yaguchi M., Sugiyama T., Nagamine H. "Slump retention of a polycarboxylate-based AE high range Water-reducing agent", *Cement Science and Concrete Technology*, V. 52, 1998, pp. 242–247.

[2] Yoshioka K., Sakai E., Daimon M., Kitahara A., "Role of Steric Hindrance in the Performance of Superplasticizers for Concrete", *Journal of American Ceramic Society*, V. 80, 1997, pp. 2667–2671.

[3] Jeknavorian A. A., Jardine L., Ou C. C., Koyata H., Folliard K. J., "Interaction of Superplasticizers with Clay-Bearing Aggregates", Malhotra V. M. Ed. 7th CANMET/ ACI International Conference on Superplasticizers and Other Chemical Admixtures in Concrete, Berlin/Germany, American Concrete Institute, SP–217, 2003, pp. 1293–1316.

[4] Sakai E., Atarashi D., Daimon M., "Interaction between Superplasticizers and Clay Minerals", 6th CANMET/ACI International Symposium on Concrete Technology for Sustainable Development, Xi'an/China, American Concrete Institute, 2006, pp. 1560–1566.

[5] Atarashi D., Sakai E., Obinata R., Daimon M., "Interactions between Superplasticizers and Clay minerals", *Cement Science Concrete Technology*, V. 58, 2004, pp. 387–392.

[6] Li B., Zhou M., Wang J., "Effect of the Methylene Blue Value of Manufactured Sand on Performances of Concrete", *Journal of Advanced Concrete Technology*, V. 9, 2011, pp. 127–132.
[7] Manning D., "Handbook of Clay Science (Developments in Clay Science, 1)", Bergaya F., Theng B. K. G., Lagaly G. Ed., Elsevier's Science & Technology, 2007, pp. 19–86.
[8] Ng S., Plank J., "Interaction Mechanisms Between Na Montmorillonite Clay and MPEG-Based Polycarboxylate Superplasticizers", *Cement and Concrete Research*, DOI: 10.1016/j.cemconres.2012.03.005.
[9] L. A. Jardine, H. Koyata, K. J. Folliard, C. -C. Ou, F. Jachimowicz, B. -W. Chun, A. A. Jeknavorian, C. L. Hill, US 6,352,952, 2002, W. R. Grace & Co..
[10] Plank J., Pöllmann K., Zouaoui N., Andres P. R., Schaefer C., "Synthesis and Performance of Methacrylic ester based Polycarboxylate Superplasticizers possessing hydroxy terminated Poly(ethylene glycol) side chains", *Cement and Concrete Research*, V. 39, 2009, pp. 1–5.
[11] Zouaoui H. N., Einfluss der Molekülarchitektur von Polycarboxylaten, hergestellt durch Blockcopolymerisation und Pfropfreaktion, auf die Wechselwirkung mit Fluoroanhydrit und Portlandzement; Dissertation, Technische Universität München, Lehrstuhl für Bauchemie, 2009.
[12] Kawaguchi S., Aikaike K., Zhang Z. M., Matsumoto K., Ito K., "Water Soluble Bottlebrushes", *Polymer Journal*, V. 30, 1998, pp. 1004–1007.
[13] Roussel N., Stefani C., Leroy R., "From mini-cone to Abrams cone test: measurement of cement-based materials yield stress using slump tests", *Cement and Concrete Research*, V. 35, 2005, pp. 817–822.
[14] Zingg A., Winnefeld F., Holzer L., Pakusch J., Becker S., Figi R., Gauckler L., "Interaction of Polycarboxylate–based Superplasticizers with Cements containing different C_3A amounts", *Cement and Concrete Composite*, V. 31, 2009, pp. 153–162.
[15] Liu S., Mo X., Zhang C., Sun D., Mu C., "Swelling Inhibition by Polyglycols in Montmorillonite Dispersions", *Journal of Dispersion Science and Technology*, V. 25, 2004, pp. 63–66.
[16] Sydansk, Robert D., "Stabilizing Clays With Potassium Hydroxide", *Journal of Petroleum Technology*, V. 36, 1984, pp. 1366–374.

TABLES AND FIGURES

List of Tables:

Table 1 – Phase composition of CEM I 52.5 R HS/NA sample as determined by XRD using *Rietveld* refinement

Table 2 – Oxide composition of montmorillonite as determined by X-ray fluorescence

Table 3 – Molecular properties and anionic charge amounts of 45PC1.5, 45PC6, PMA and PEG respectively, measured in synthetic cement pore solution

Table 4 – Sorption of 45PC1.5 and 45PC6 on cement in presence or absence of clay and PEG (w/c = 0.53)

Table 5 – Paste spreads of cement slurries holding 1 wt. % clay, in presence of 1.07 % bwoc of 45PC1.5 and 0.09 % bwoc of 45PC6, with PMA (added in equal or 5 times of PCE dosage), and PEG–2000 or 24PC18 added in equal amount as PCE (w/clay = 0.53)

List of Figures:

Fig. 1 – Chemical structure of the PCE samples employed in the study.

Fig. 2 – Zeta potential of aqueous montmorillonite suspension as a function of pH (w/clay = 53).

Fig. 3 – Zeta potential of aqueous montmorillonite suspension as a function of Ca^{2+} dosage in alkaline solution (pH = 12.8, w/clay = 53).

Fig. 4 – Paste spread of cement slurries with and without 1 wt. % of clay added, in the presence of 1.07 % bwoc of 45PC1.5 and 0.09 % bwoc of 45PC6, with or without PEG–2000 added in equivalence to the PCE dosages (w/clay = 0.53).

Fig. 5 – Sorption isotherm of 45PC1.5, 45PC6 and PEG on clay as a function of PCE–2000 sample dosage in synthetic cement pore solution (Ca^{2+} = 0.4 g/L, w/clay = 53).

Fig. 6 – Sorption isotherm of 45PC1.5 and 45PC6 on clay as a function of PCE dosage in alkaline solution (pH 12.8, w/clay = 53).

Fig. 7 – Zeta potential of aqueous clay suspension as a function of PMA dosages in synthetic cement pore solution (Ca^{2+} = 0.4 g/L, w/clay = 53).

Fig. 8 – XRD patterns of clay dispersed in synthetic cement pore solution holding 50 % bwo clay of PEG, 45PC1.5 and 45PC6 respectively (Ca^{2+} = 0.4 g/L, w/clay = 53).

Fig. 9 – Sorption isotherms of 45PC1.5 on clay treated or untreated with saturated KOH solution in synthetic cement pore solution (Ca^{2+} = 0.4 g/L, w/clay = 53).

Table 1 – Phase composition of CEM I 52.5 R HS/NA sample as determined by XRD using *Rietveld* refinement

Phase	[wt. %]
C_3S, monoclinic	60.1
C_2S, monoclinic	19.0
C_3A, cubic	1.2
C_3A, orthorhombic	0.4
C_4AF, orthorhombic	14.5
$CaSO_4$	1.3
$CaSO_4$. ½ H_2O*	2.2
$CaSO_4$. 2 H_2O*	1.0
Calcite	0.0
Quartz	0.4

*Determined by thermogravimetry

Table 2 – Oxide composition of montmorillonite as determined by X-ray fluorescence

Oxide	SiO_2	Al_2O_3	CaO	MgO	Fe_2O_3	Na_2O	K_2O	TiO_2	LOI	Total
[wt. %]	59.7	18.4	0.8	2.3	4.0	2.3	0.1	0.1	12.1	99.8

Table 3 – Molecular properties and anionic charge amounts of 45PC1.5, 45PC6, PMA and PEG respectively, measured in synthetic cement pore solution

Property	45PC1.5	45PC6	PMA	PEG
Molar mass M_w [g/mol]	196,300	156,400	26,200	2,080
Molar mass M_n [g/mol]	51,900	43,680	7,511	2,090
Polydispersity index (PDI)	3.8	3.6	2.7	1.0
Molar ratio MAA : MPEG-MAA	1.5 : 1	6 : 1	-	-
Specific anionic charge amount $_{PS}$ [µeq/g]	175	1,100	7,900	0

Table 4 – Sorption of 45PC1.5 and 45PC6 on cement in presence or absence of clay and PEG (w/c = 0.53)

System	PCE dosage [% bwoc]	Sorbed amount of PCE [mg/g of solid]	Sorption [% of PCE added]
CEM I 52.5 R + 45PC1.5	1.07	2.63	24.6
CEM I 52.5 R + 45PC1.5 + 1 wt.% clay	1.07	5.84	54.6
CEM I 52.5 R + 45PC1.5 + 1 wt.% clay + PEG	1.07	2.99	28.0
CEM I 52.5 R + 45PC6	0.09	0.42	46.4
CEM I 52.5 R + 45PC6 + 1 wt.% clay	0.09	0.59	65.0
CEM I 52.5 R + 45PC6 + 1 wt.% clay + PEG	0.09	0.55	60.6

Table 5 – Paste spreads of cement slurries holding 1 wt. % clay, in presence of 1.07 % bwoc of 45PC1.5 and 0.09 % bwoc of 45PC6, with PMA (added in equal or 5 times of PCE dosage), and PEG–2000 or 24PC18 added in equal amount as PCE (w/clay = 0.53)

			PCE only	PMA	PMA x 5	PEG	24PC18
Paste with 45PC1.5	Spread	[cm]	22.3	14.8	-	24.4	28.2
Paste with 45PC6	Spread	[cm]	21.3	22.8	19.5	22.1	22.1

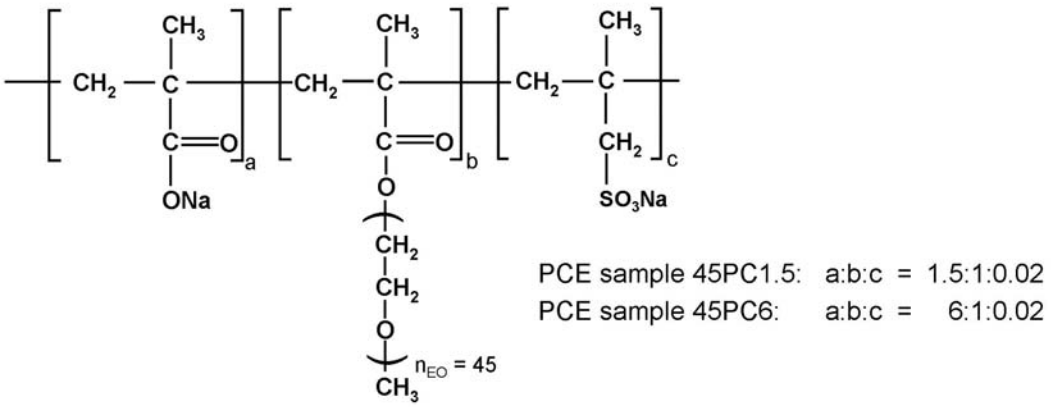

Fig. 1 – Chemical structure of the PCE samples employed in the study.

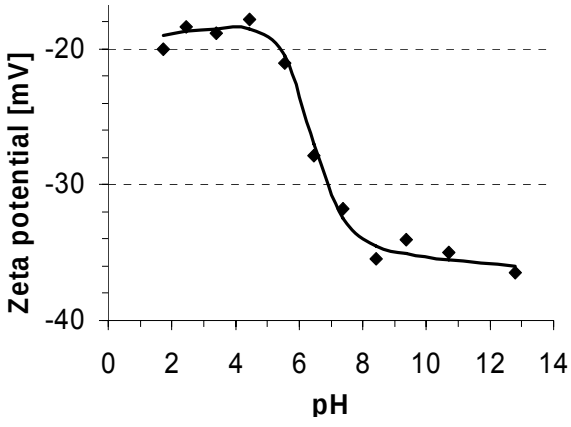

Fig. 2 – Zeta potential of aqueous montmorillonite suspension as a function of pH (w/clay = 53).

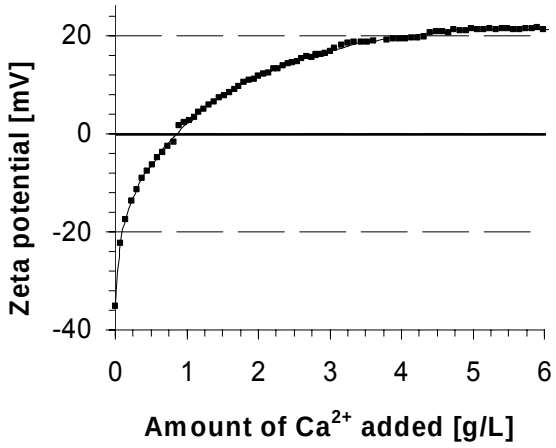

Fig. 3 – Zeta potential of aqueous montmorillonite suspension as a function of Ca^{2+} dosage in alkaline solution (pH = 12.8, w/clay = 53).

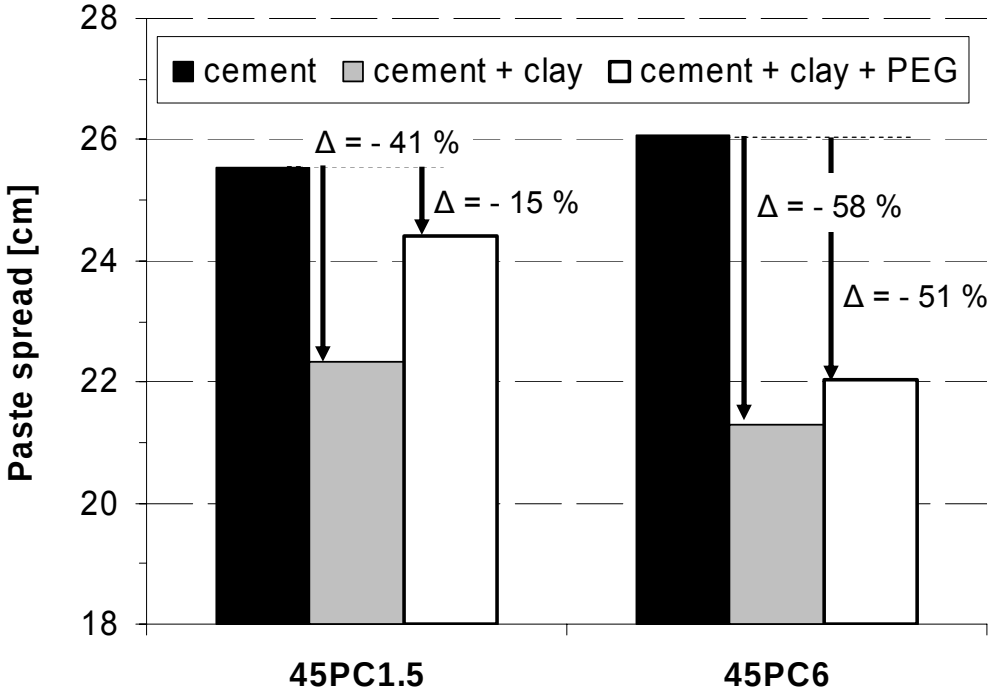

Fig. 4 – Paste spread of cement slurries with and without 1 wt. % of clay added, in the presence of 1.07 % bwoc of 45PC1.5 and 0.09 % bwoc of 45PC6, with or without PEG–2000 added in equivalence to the PCE dosages (w/clay = 0.53).

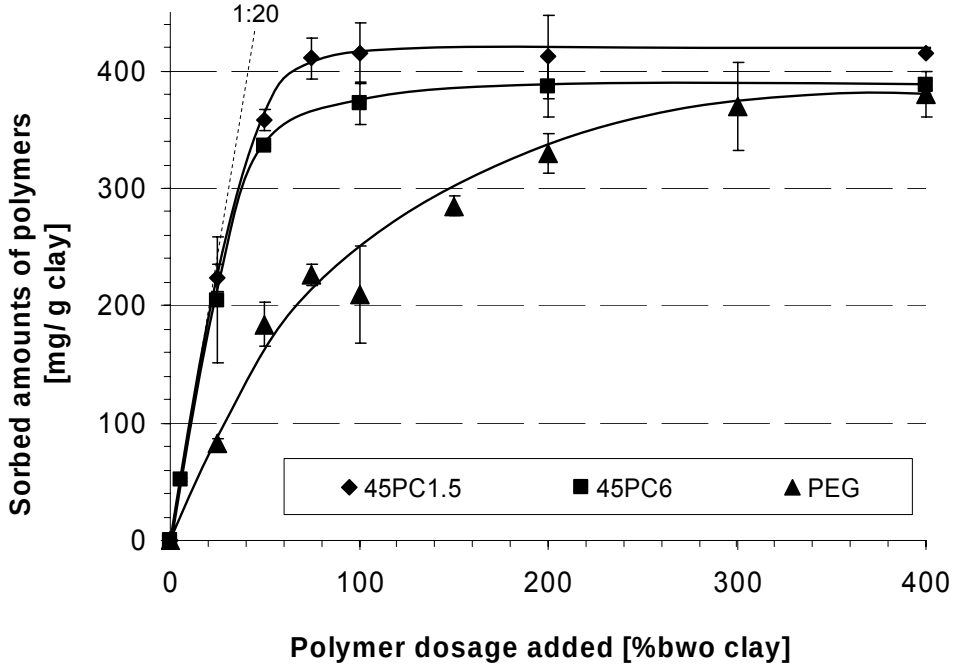

Fig. 5 – Sorption isotherm of 45PC1.5, 45PC6 and PEG–2000 on clay as a function of PCE sample dosage in synthetic cement pore solution (Ca^{2+} = 0.4 g/L, w/clay = 53).

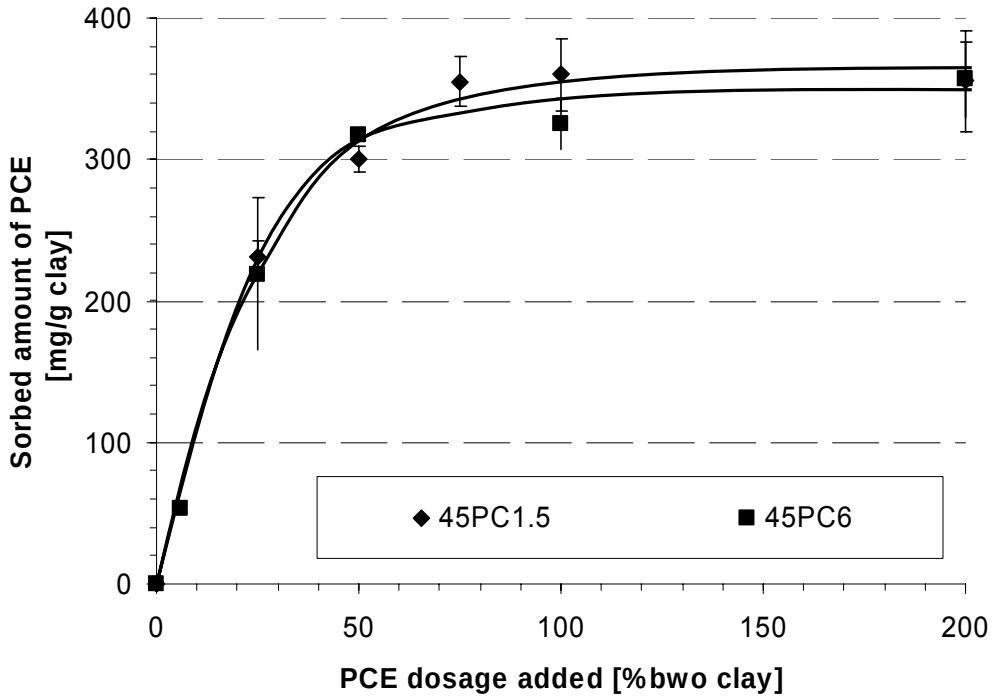

Fig. 6 – Sorption isotherm of 45PC1.5 and 45PC6 on clay as a function of PCE dosage in alkaline solution (pH 12.8, w/clay = 53).

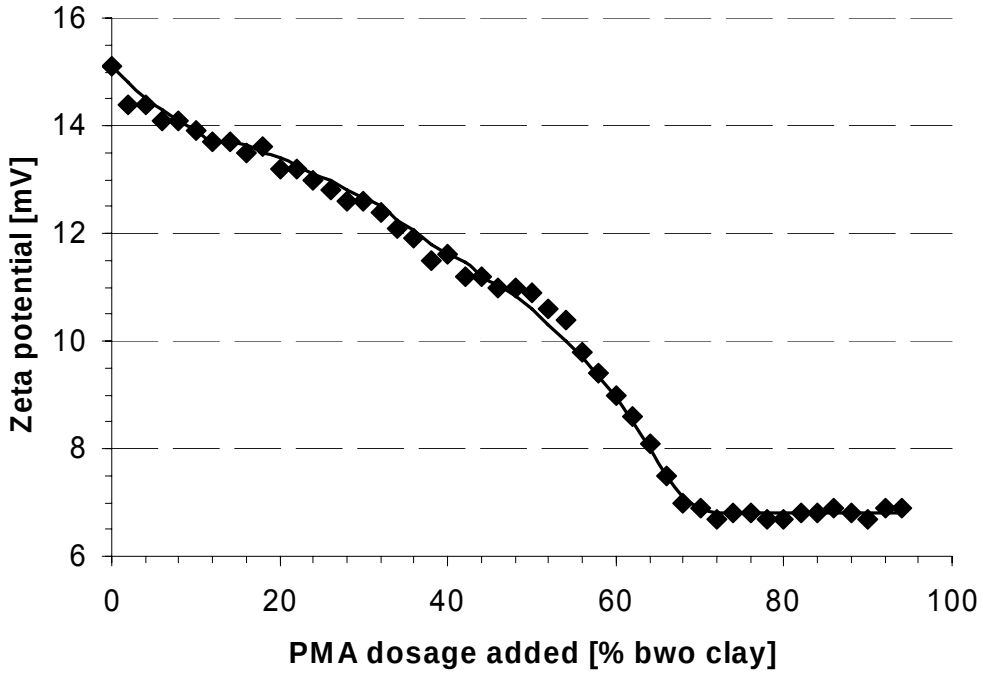

Fig. 7 – Zeta potential of aqueous clay suspension as a function of PMA dosages in synthetic cement pore solution (Ca^{2+} = 0.4 g/L, w/clay = 53).

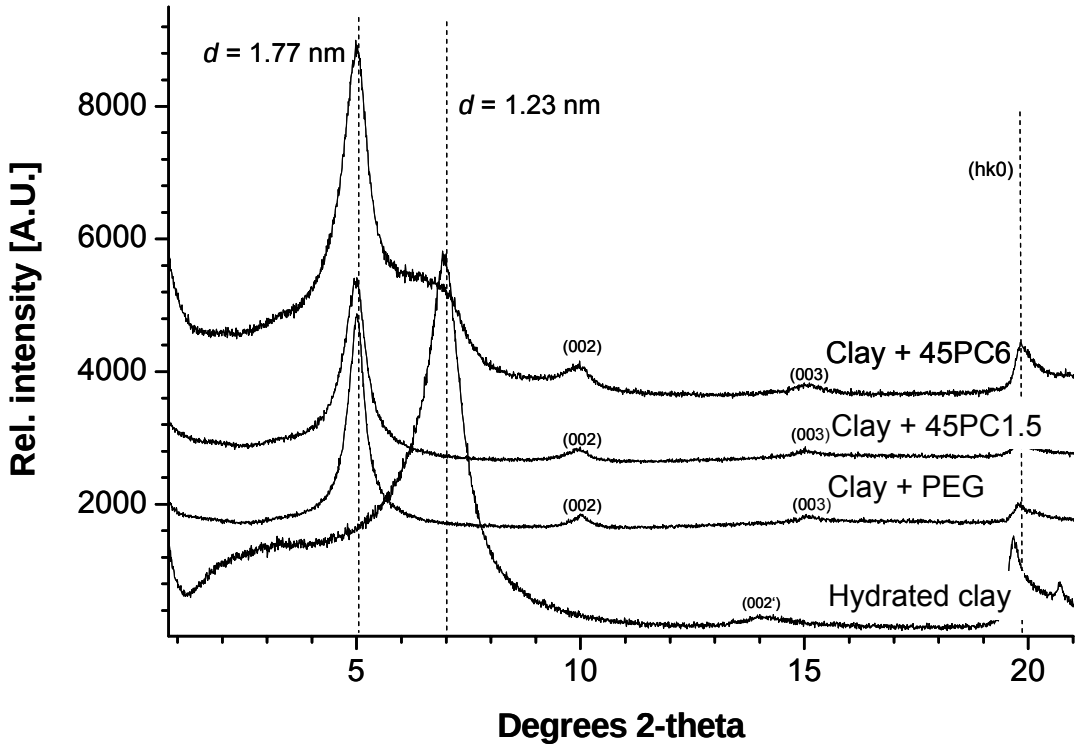

Fig. 8 – XRD patterns of clay dispersed in synthetic cement pore solution holding 50 % bwo clay of PEG, 45PC1.5 and 45PC6 respectively (Ca^{2+} = 0.4 g/L, w/clay = 53).

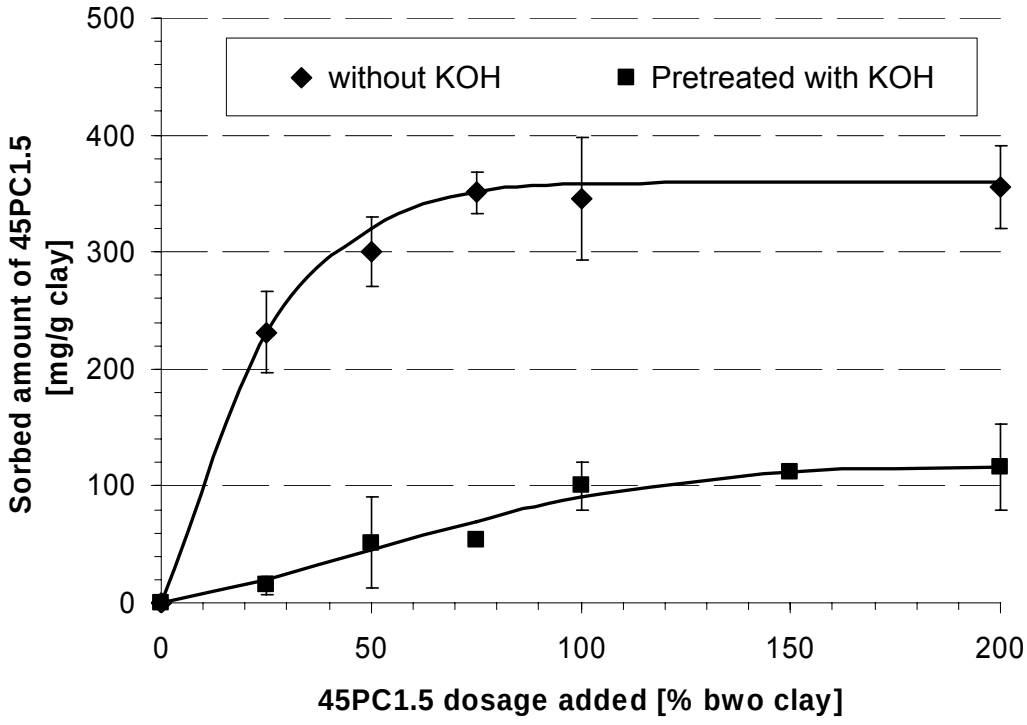

Fig. 9 – Sorption isotherms of 45PC1.5 on clay treated or untreated with saturated KOH solution in synthetic cement pore solution (Ca^{2+} = 0.4 g/L, w/clay = 53).

Paper 3

Effect of Graft Chain Length of Methacrylate Ester Based PCE Superplasticizers on their Interactions with Na-Montmorillonite Clay

S. Ng, J. Plank

Applied Clay Science

(Submitted on 25th August 2012)

Effect of Graft Chain Length of Methacrylate Ester Based PCE Superplasticizers on Their Interactions with Na-montmorillonite Clay

S. Ng, J. Plank*

Technische Universität München

Chair for Construction Chemicals,

85747 Garching, Lichtenbergstraße 4, Germany

*: Corresponding author
Tel.: +49 (0)89 289 13151
Fax.: +49 (0)89 289 13152
E-mail address: sekretariat@bauchemie.ch.tum.de (J. Plank).

Abstract

The negative impact of sodium montmorillonite clay on the dispersing effectiveness of three polycarboxylate (PCE) concrete superplasticizers prepared from methacrylic acid and methoxy polyethylene glycol (MPEG) methacrylate ester (molar ratio of 6:1), with different graft chain lengths of 45, 17 and 8.5 ethylene oxide units (EOUs) was investigated. Only 1 % of clay added to cement decreased cement spreads by up to 60 %. This indicates strong interaction between clay and PCE. Clay alone sorbed up to ~ 600 mg/g of polycarboxylates which is ~ 100 times higher than by Portland cement. For the polycarboxylate possessing the longest graft chain (45 EOUs), sorption by clay was found to occur mainly via intercalation of the poly(ethylene oxide) side chain between the alumosilicate layers. While for PCEs with shorter graft chains (8.5 and 17 EOUs), electrostatic adsorption onto the positively charged clay surfaces became significant. For PCEs holding shorter lateral chains, poly(methacrylic acid) can be used as sacrificial agent to mitigate the negative effect of clay.

Keywords: Clay, Montmorillonite, Polycarboxylate, Interaction, Cement

1. Introduction

Many different chemical reactions can occur during the process of cement hydration, especially with the addition of admixtures such as polycarboxylate based superplasticizers (PCEs). The failure of this class of superplasticizers to fluidize concrete can have many reasons. It is known that SO_4^{2-} can greatly affect the performance of PCEs [Hiroyoshi and Kazuhiro, 1998; Magarotto *et al.*, 2003; Plank *et al.*, 2010]. Alternatively, it may arise from

incompatibility with other admixtures [Bedard and Mailvaganam, 2005], or even from the overall composition of cements [Dodson and Hayden, 1989].

Recently, contamination by clay in concrete has been identified as another potential source of PCE failure [Jeknavorian *et al.*, 2003; Atarashi *et al.*, 2004]. Montmorillonite was found to be most harmful due to its expanding lattices which promote intercalation, swelling and cation exchange [Greenwell *et al.*, 2006; Bergaya and Lagaly, 2006]. This character of montmorillonite promotes high consumption of water which increases the viscosity of the cement paste. It causes a loss in workability or higher water demand to produce the same workability as before, thus decreasing the mechanical properties and durability of concretes. Moreover, it has been found that anionic polymers can adsorb onto clay particles [Jaernstrom and Stenius, 1990]. The extent of adsorption is dependent on the anionic character, chemical composition and molecular architecture of the polymers present. For superplasticizers, polycondensates were shown to be less affected by the presence of clay than PCEs [Atarashi *et al.*, 2003]. This result is surprising, because polycondensates typically are more anionic polymers than PCEs. It gives a hint that besides electrostatic attraction, another mechanism must be involved in the interaction between PCE and clay.

In a previous study on the effect of clay on PCEs we have shown that montmorillonite has a high affinity for PCEs, whereby the dispersing effectiveness of PCEs in cement pastes is greatly perturbed by the presence of this clay [Ng and Plank, 2012]. Two mechanisms were found to govern the consumption of PCEs by clay: (1) chemisorption (intercalation) of the poly(ethylene oxide) graft chains of the PCE via hydrogen bonding with water molecules anchored by the silanol groups between the alumosilicate layers [Amarasinghe *et al.*]; and (2) electrostatic attraction of the anionic trunk of a PCE molecule to the clay surface which is

positively charged due to the adsorption of Ca^{2+} ions from cement pore solution [Durand-Piana *et al.*, 1987].

In this present study, the affinity of clay for PCEs possessing varying graft chain lengths was investigated. Three different PCEs consisting of methacrylic acid and MPEG methacrylate ester at a molar ratio of 6:1, but with different graft chain lengths (45, 17 and 8.5 ethylene oxide units) were utilized. To study this interaction, a naturally occurring sodium montmorillonite clay was employed. First, the influence of clay on the workability of cement pastes containing these three different methacrylic acid-methacrylate ester based PCEs was determined by 'mini slump' test. To ascertain the type of interaction of these PCEs with clay, at first their adsorption on the cement/clay mixture was measured via total organic carbon (TOC) method. Next, adsorption on clay only dispersed in synthetic cement pore solution was investigated to identify the sole effect of clay on PCE. Also, to differentiate between surface adsorbed and intercalated PCE, the amount of PCE sorbed by clay in cement paste was compared to that sorbed in alkaline solution only (no Ca^{2+} ions present). Finally, XRD analysis and measurement of PEG sorption by clay were performed to access the chemisorption capacity of clay for PCE. From this data, it was aimed to develop an understanding on how much PCE is sorbed by surface interaction with clay and by chemical intercalation. This way, the effect of varying graft chain lengths of PCEs on their type of interaction with clay in cementitious systems and a possible remedy was sought to be clarified.

2. Materials and methods

2.1. Cement

A CEM I 52.5 R HS/NA (Holcim, Lägerdorf/Germany) was used. Its phase composition as obtained by quantitative X-ray diffraction (Bruker D8 advance instrument, software Topas 4.0) is presented in **Table 1**. The specific surface area was 4,300 cm^2/g (*Blaine* instrument, Toni Technik, Berlin/Germany), average particle size (d_{50} value) was 8.33 µm (laser granulometer CILAS 1064, Cilas, Marseille/France), and the density was 3.22 g/cm^3 (ultrapycnometry, Quantachrome, Odelzhausen/Germany).

Table 1. Phase composition of CEM I 52.5 R HS/NA sample as determined by XRD using *Rietveld* refinement

Phase	[wt. %]
C_3S, monoclinic	60.1
C_2S, monoclinic	19.0
C_3A, cubic	1.2
C_3A, orthorhombic	0.4
C_4AF, orthorhombic	14.5
$CaSO_4 \cdot ½\ H_2O$*	2.2
$CaSO_4 \cdot 2\ H_2O$*	1.0
$CaSO_4$	0.4
Calcite	1.3
Total	100.1

* Determined by thermogravimetry

2.2. Sodium montmorillonite clay

A commercial sodium montmorillonite clay sample (RXM 6020 supplied by Rockwood, Moosburg/Germany) was used as per obtained. This clay is a naturally occurring sodium montmorillonite clay with a specific surface area of 46.7 m^2/kg measured on the BET (N_2) instrument. Its oxide composition is presented in **Table 2**. It develops a pH of ~ 9 when prepared as a 2 wt. % aqueous suspension. At pH 12.8 (pH value of the cement pore solution), the clay registers a zeta potential value of ~ - 35 mV which increased to ~ + 15 mV in synthetic cement pore solution [Ng and Plank, 2012]. In its dry state, the native dry clay reveals an interlayer spacing of 1.07 nm.

Table 2. Oxide composition of sodium montmorillonite clay sample, RXM 6020 as determined by X-ray fluorescence

Oxide	SiO_2	Al_2O_3	CaO	MgO	Fe_2O_3	Na_2O	K_2O	TiO_2	LOI	Total
[wt. %]	59.7	18.4	0.8	2.3	4.0	2.3	0.1	0.1	12.1	99.8

2.3. Polycarboxylate samples

Three PCE superplasticizers were synthesized by aqueous free radical copolymerization of methacrylic acid (MAA) and methoxy terminated poly(ethylene oxide) methacrylate (MPEG-MA) ester at a molar ratio of 6:1 following a description from previous literature [Plank *et al.*, 2009]. Methallylsulfonic acid was used as chain transfer agent. The synthesized copolymers differ by the length of their graft chains which consist of varying numbers of ethylene oxide units, namely 45, 17 and 8.5 respectively. The polymers were denoted by xPC6, where x refers to the number of EOUs in the lateral chain, and 6 corresponds to the molar ratio of MAA:MPEG-MA ester. The chemical formula of the synthesized PCEs is presented in **Fig. 1**.

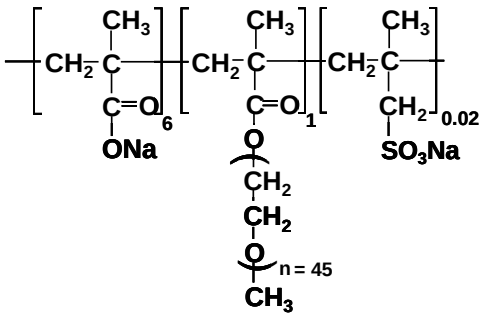

PCE Samples:

45PC6 : n = 45
17PC6 : n = 17
8.5PC6 : n = 8.5

Fig. 1. Chemical structure of the PCE samples employed in the study

For polymer characterisation, size exclusion chromatography (Waters Alliance 2695 from Waters, Eschborn/Germany) equipped with RI detector 2414 (Waters, Eschborn/Germany) and a 3 angle dynamic light scattering detector (mini Dawn from Wyatt Technologies, Santa Barbara, CA/USA) was used. Prior to application on the columns, the polymer solutions were filtered through a 0.2 µm filter. The polymers were separated on an Ultrahydrogel™ precolumn and three Ultrahydrogel™ columns (120, 250 and 500; Waters, Eschborn/Germany) using 0.1 M aqueous $NaNO_3$ solution (adjusted to pH 12.0 with NaOH) as an eluant at a flow rate of 1.0 mL/min. From this separation, the molar masses (M_w and M_n), the polydispersity index (PDI) and the hydrodynamic radius ($R_{h(z)}$) of the polymers were determined. The value of dn/dc used to calculate M_w and M_n for all polymers was 0.135 mL/g (value for polyethylene oxide) [Kawaguchi *et al.*, 1998].

Specific anionic charge amounts of the polymers were analysed by a particle charge detector (PCD 03 pH from Mütek Analytic Company, Herrsching/Germany). Solutions containing 0.02 wt. % of anionic polymer dissolved in synthetic cement pore solution were prepared and titrated against a 0.001N solution of cationic polydiallyl dimethyl ammonium chloride (polyDADMAC) until charge neutralization was attained. The amount of negative charge per gram of polymer was calculated from the consumption of the cationic polyelectrolyte.

Polymethacrylic acid (PMA) was synthesized by aqueous free radical polymerization of MAA [Zouaoui, 2009], while PEG–2000 (n_{EO} = 45) with a purity of > 99 % was used as per obtained (Clariant, Frankfurt am Main/Germany).

2.4. 'Mini Slump' test

For determination of the paste flow, a "mini slump" test according to DIN EN 1015 was utilized and carried out as follows:

At first, the w/c ratio needed to attain a spread of 18 ± 0.5 cm for the neat cement paste was determined, and the dosage of PCE superplasticizer required to reach a spread of 26 ± 0.5 cm at this specific w/c ratio was established. The PCE solution was generally added to the mixing water placed in a porcelain cup and the amount of water introduced with the PCE solution was subtracted from the amount of mixing water required for a w/c ratio of 0.53. In a typical experiment, 300 g of solids (pure cement or cement blended with 1 wt. % of clay) were added to the mixing water, agitated for 1 minute and left to stand for another minute. The cement paste was next stirred for 2 minutes before transferring into a Vicat cone placed on a glass plate. The dimensions of the Vicat cone were: height 40 mm, top diameter 70 mm, and bottom diameter 80 mm. The cement paste was filled to the brim of the cone and levelled before it was vertically lifted from the surface of the glass plate. The resulting spread of the paste was measured twice; the second measurement being perpendicular to the first. The final spread value was taken as the average of the two measured ones.

2.5. Sorption experiments

PCE sorption on clay or cement was determined by the depletion method, i.e. it was assumed that removal of PCE from the pore solution solely was the result of interaction with clay and/ or cement and that no precipitation had occurred. In sample preparation, 300 g of pure cement or cement blended with 1 wt. % of clay were added to 0.09 % by weight of cement (bwoc) 45PC6, 0.07 % bwoc 17PC6 or 0.07 % bwoc 8.5PC6 solutions over 1 minute in a porcelain cup (PCE dosages and w/c ratio as determined in 'mini slump' test). The mixture was allowed to rest for another minute before it was stirred for 2 minutes. Thereafter, the paste was centrifuged at 8,500 rpm for 15 minutes. The filtrate was recovered, diluted and acidified with conc. HCl solution in a TOC sample flask. This final solution was then analysed by combustion at 890 °C on a HIGH TOC II instrument (Elementar Analysensysteme, Hanau/Germany). The sorbed amount of PCE was calculated from the difference between the TOC content in the stock solution and that left in the filtrate. In a separate experiment, 20 g/L of PCE were dissolved in the filtrate of clay suspended in synthetic cement pore solution and left to stand overnight. No precipitation was found, thus signifying that PCE depletion was solely a result of sorption by the cement or clay.

Sorption experiments of PCE or PEG on clay in synthetic cement pore solution and alkaline solution (adjusted to pH 12.8 with aqueous NaOH) were performed by using polymer solutions with concentrations ranging from 12.5 to 300 % by weight of (bwo) clay. The synthetic cement pore solution exhibited a pH of 12.8 and was prepared by dissolving 1.72 g $CaSO_4 \cdot 2H_2O$, 7.119 g KOH, 4.76 g K_2SO_4 and 6.956 g of Na_2SO_4 in 1 L of millipore water respectively. The ionic composition (mmol/L) of this synthetic cement pore solution (Ca^{2+} = 10; Na^+ = 100; K^+ =180; OH^- = 127; SO_4^{2-} = 86) is typical for normal Portland cement

dispersed in water at a w/c ratio of ~ 0.4 [Andersson *et al.*, 1989]. These polymer solutions were added to 0.025 g of clay at a w/clay ratio of 53 (to actualise the conditions in the 'mini slump' test where the w/c ratio was 0.53 and 1 % bwoc of clay were present), manually homogenized and sonicated for 10 minutes to achieve maximum dispersion of the clay particles and thus interaction with the polymers. The mixture was then centrifuged at 14,600 rpm for 10 minutes. Thereafter, the filtrate was collected, diluted and acidified prior to further analysis by TOC measurement as before.

2.6. XRD analysis of clay hydrated in presence of PCE

0.025 g clay were added to 1.34 g of 0.93 wt. % polymer solution (w/clay ratio of 53). The polymer solution was prepared with synthetic cement pore solution. The suspension was manually mixed for 1 minute, sonicated for 10 minutes and centrifuged at 14,600 rpm for another 10 minutes. The solid residue obtained was dried at 80 °C overnight before it was ground and analysed. XRD scans of all samples were taken at room temperature on a D8 Advance, Bruker AXS instrument (Bruker, Karlsruhe/Germany) utilising a Bragg-Bretano geometry. Samples were placed in a front mounted plastic sample holder. Step size was 0.15 sec per step, and spin of sample during scanning was set at a revolution time of 4 sec. Nickel filter was used for incident beam with an aperture slit of 0.3°. The scan range was set from 0.6 ° to 20 ° 2θ.

2.7. Calculation of the sorbed amount of EO from PCE

The weight percentage of EO contained in PCE polymers 45PC6, 17PC6 and 8.5PC6 was calculated from their chemical formulae (**Fig. 1**) as 77.2 %, 56.1 % and 39.0 % respectively. Using the experimentally determined sorbed amounts of the PCEs in synthetic cement pore

solution and in alkaline solution, the sorbed amount of EO was calculated according to **Equation 1**. The results obtained were compared with experimental data on the sorbed amount of PEGs.

$$\text{Amount of EO sorbed on clay [mg/g clay]} = \text{wt. \% of EO from PCE} \times \text{Experimentally determined amount of PCE sorbed on clay} \quad \text{(Equ. 1)}$$

Equations 1. Calculation of amount of EO sorbed on clay for the different PCEs, based on the sorption profile of the PCEs

3. Results and discussion

3.1. Properties of PCE samples

The molecular characteristics and anionic charge amounts of the PCE polymers are shown in **Table 3**.

Table 3. Molecular properties and anionic charge amounts of PCE copolymers 45PC6, 17PC6 and 8.5PC6 respectively and of poly(methacrylic acid) (PMA), measured in synthetic cement pore solution

Property	45PC6	17PC6	8.5PC6	PMA
Molar mass, M_w [g/mol]	156,400	80,700	151,800	26,200
Molar mass, M_n [g/mol]	43,700	27,100	29,300	7,511
Polydispersity index, PDI	3.6	3.0	5.1	2.7
Graft chain length [nm]	16.7	4.7	2.4	-
Specific anionic charge amount* [µeq/g]	1,100	4,700	6,100	7,900

*measured in cement pore solution

The anionic charge amounts increase by the order as follows: 45PC6 < 17PC6 < 8.5PC6. The graft chain length of the PCE polymers was calculated by multiplying the number of EO units contained in each chain with the length of an EO unit arranged in a helical mode which according to literature is 2.78 Å [Takahashi and Tadokoro, 1973].

3.2. Dispersing performance of PCE in presence of clay

The w/c ratio of the neat cement paste for a spread of 18 ± 0.5 cm was determined to be 0.53. When 1 wt. % of clay was added, availability of water decreased due to consumption by hydration and swelling of the clay. Thus, the spread of the cement paste decreased to 15.3 cm (~ - 15 %) as a result of increased viscosity.

In the absence of clay, the dosages of 45PC6, 17PC6 and 8.5PC6 required to obtain a cement paste spread of 26 ± 0.5 cm were 0.09 % bwoc, 0.07 % bwoc and 0.07 % bwoc respectively (**Fig. 2**). Obviously, all three PCE polymers are highly effective cement dispersants. However, when 1 wt.% of clay was added, the spreads decreased by 59 %, 47 % and 41 % to 21.3 cm, 22.1 cm and 22.7 cm respectively. These reductions in paste fluidity appear to be related to the graft chain length of these PCEs; the longer the side chain, the higher the impact on flow spread. Additionally, they much exceed that observed in the absence of PCE which was 15 % only. Thus, it confirmed that besides water consumption by clay, a specific interaction of the PCE with clay occurs which also affects its dispersing effectiveness.

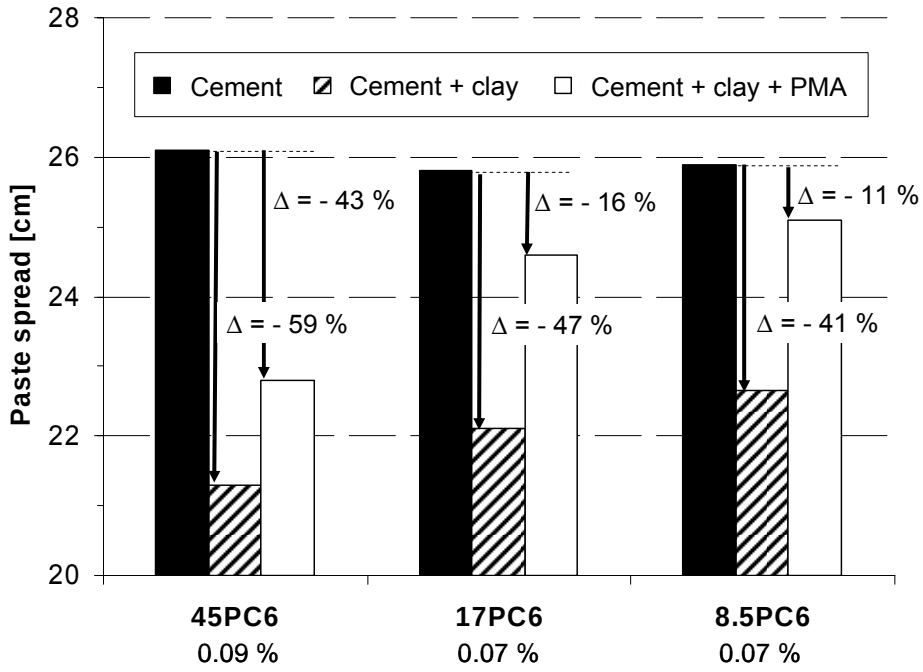

Fig. 2. Paste spread of cement slurries with and without 1 wt. % of clay added, in the presence of 0.09 % bwoc of 45PC6, 0.07 % bwoc of 17PC6 and 0.07 % bwoc of 8.5PC6, with or without 0.1 % bwoc of polymethacrylic acid (PMA, w/c = 0.53)

3.3. PCE sorption in cement/clay system

To ascertain the negative impact of clay on PCE, the sorbed amounts of 45PC6, 17PC6 and 8.5PC6 in cement paste with and without 1 wt. % of clay were investigated. **Table 4** shows the sorbed amounts of the PCEs in presence or absence of clay. When clay was present, the sorbed amounts of the PCEs increased significantly by ~ 30 – 50 %. Considering the small amount of clay present, these increases signify a strong impact of clay on PCE. Obviously, interaction between PCE and clay is much stronger than with cement. Interestingly, the amount of polymer 45PC6 consumed by the cement/clay blend is higher than for 17PC6 and 8.5PC6 respectively. This implies that at these PCE dosages (~ 0.1 % bwoc), clay may have a preference for 45PC6, followed by 17PC6 and 8.5PC6. The result instigates that in a

cementitious system, a considerable amount of PCE can be consumed by a relatively minor amount of clay contaminant.

Table 4. Sorption of PCE polymers 45PC6, 17PC6 and 8.5PC6 on cement in presence or absence of clay (w/c = 0.53)

System	PCE dosages [% bwoc]	Sorbed amount of PCE [mg/g of solid]	Sorption [% of PCE dosage added]
CEM I 52.5 R + 45PC6	0.09	0.42	46.4
CEM I 52.5 R + 45PC6 + 1 wt.% clay	0.09	0.59	65.0
CEM I 52.5 R + 17PC6	0.07	0.33	47.7
CEM I 52.5 R + 17PC6 + 1 wt.% clay	0.07	0.42	60.3
CEM I 52.5 R + 8.5PC6	0.07	0.29	41.0
CEM I 52.5 R + 8.5PC6 + 1 wt.% clay	0.07	0.40	57.0

To examine the effect of individual clay on PCE and to eliminate the effect from cement, a model system consisting of clay dispersed in synthetic cement pore solution holding PCE was utilised next.

3.4. PCE sorption by montmorillonite clay

First, the sorption behaviour of PCE polymers 45PC6, 17PC6 and 8.5PC6 on clay was measured in synthetic cement pore solution. The result is displayed in **Fig. 3**.

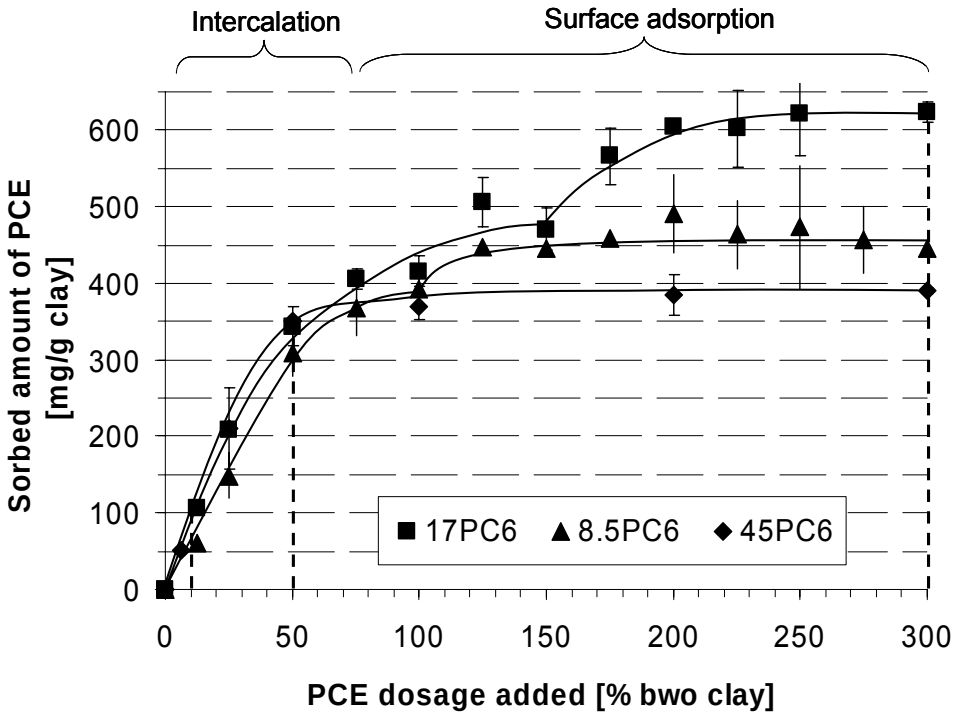

Fig. 3. Sorption behaviour of PCE polymers 45PC6, 17PC6 and 8.5PC6 on montmorillonite clay dispersed in synthetic cement pore solution (Ca^{2+} concentration = 0.4 g/L, w/clay = 53)

According to this, montmorillonite clay exhibits an extremely high affinity for all three PCE polymers. At dosages of 0.1 % bwoc of PCE (~ 10 % bwo clay), the sorbed amounts of the PCEs are comparable. However, this trend differentiates at higher PCE dosages. For example, at a PCE dosage of 50 % bwo clay, the montmorillonite clay has sorbed 360 mg/g clay for 45PC6; 340 mg/g clay for 17PC6 and 300 mg/g clay for 8.5PC6 respectively. Such sorbed amounts are ~ 100 times higher than those for a neat ordinary Portland cement (OPC) [Li *et al.*, 2005; Zingg *et al.*, 2009], thus confirming the high affinity of PCE for clay. Interestingly, at even higher PCE dosages of up to 300 % bwo clay, the three PCE polymers exhibit different behaviours: While the sorbed amount of 45PC6 practically has reached a plateau at ~ 380 mg/g clay, the other copolymers showed further increments in their sorbed amounts to 610 mg/g clay (17PC6) and 465 mg/g clay (8.5PC6) respectively. Obviously, these two polymers are involved in an additional interaction with clay which occurs after an initial

sorption has reached the saturation point, and which is dependent on the polymer composition. Plausibly, the two types of interaction which can occur between clay and PCE are (a) surface adsorption, facilitated by electrostatic attraction, and (b) chemisorption via intercalation of the PCE polymer into the layered structure of clay.

3.5. Surface adsorption of PCE

To determine the portion of PCE sorbed electrostatically on clay, its sorbed amount in alkaline solution (pH 12.8 w/NaOH) instead of synthetic cement pore solution was determined next. The rationale behind this experiment was that in alkaline solution, the negatively charged clay surfaces cannot adsorb anionic PCE polymer. Hence, the sorbed amounts of PCEs here were solely attributed to chemisorption into the layered structure of clay.

It was found that in alkaline solution holding no Ca^{2+}, the sorbed amount of 45PC6 was the highest, followed by 17PC6 and 8.5PC6 (**Fig. 4**). This corroborates that intercalation of the PCEs into the clay structure clearly is dependent on the graft chain length. PCE polymers possessing longer graft chains intercalate to a higher extent than those with short lateral PEO chains. Also, compared to the sorbed amounts of the PCEs in synthetic cement pore solution (**Fig. 3**), the amount of 45PC6 sorbed by clay decreased from 380 mg/g clay to ~ 360 mg/g clay, showing that only ~ 5 % of this copolymer were consumed by clay through an interaction which occurs in addition to this intercalation, plausibly electrostatically induced surface adsorption. Opposite to this, decreases in PCE sorption were observed for 17PC6 (- 50 %) and 8.5PC6 (- 40 %), confirming that for such short-chained PCEs, electrostatic adsorption played an almost equally important role as intercalation.

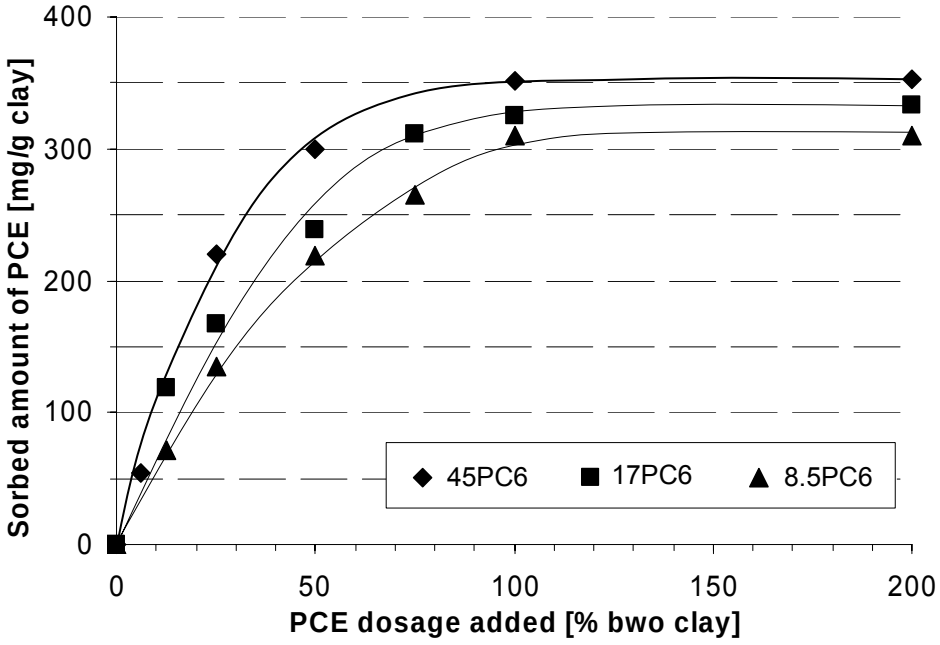

Fig. 4. Sorption isotherms of PCE polymers 45PC6, 17PC6 and 8.5PC6 on montmorillonite clay dispersed in alkaline solution at pH 12.8, adjusted with NaOH (w/clay = 53)

3.6. Chemisorption of PCE

In addition to the electrostatic attraction of the anionic trunk chain of the PCE onto the Ca^{2+} enriched clay surfaces, montmorillonite also has a high affinity for the PEO side chain, resulting in intercalation [Jaknavorian *et al.*,, 2003; Atarashi *et al.*, 2003]. To confirm the role of the side chains in the uptake of PCE by clay, an XRD analysis was performed. Here, clay was mixed with the three different PCEs, with polymethacrylic acid (PMA) and three polyethylene glycols possessing 45 EOUs (PEG–2000), 17 EOUs (PEG–750) and 8.5 EOUs (PEG–350) at a w/clay ratio of 53 and polymer dosages of 50 % bwo clay respectively. These PEGs represent the side chains of the PCE polymers studied here. According to **Fig. 5**, when hydrated, pure clay exhibits a *d*-spacing of 1.23 nm. When PEG–2000 was added to the montmorillonite, a characteristic shift in the *d*-spacing from 1.23 nm to 1.77 nm was observed. This *d* value (1.77 nm) is typical for montmorillonite intercalated with polyglycols [Svensson

and Hansen, 2010; Suter and Coveney, 2009]. When PEG–750 and PEG–350 were added to the montmorillonite, a similar *d*-value was observed. However, the reflections were broader, confirming higher disorderness in the layer structures when PEGs with lower molecular weights intercalate [Alemdar *et al.*, 2005; Chen and Evans, 2005].

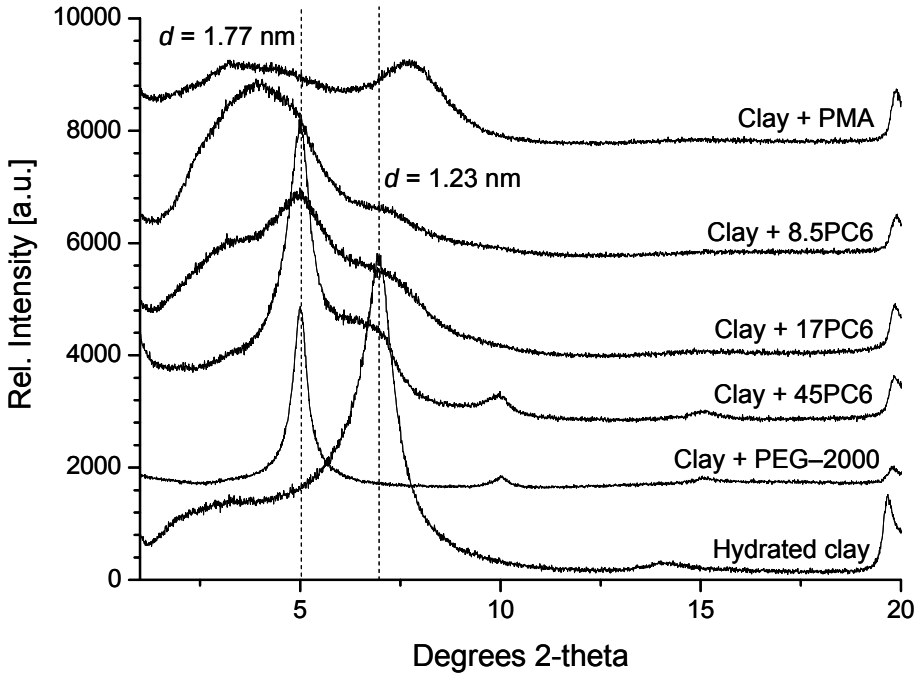

Fig. 5. XRD patterns of montmorillonite clay dispersed in synthetic cement pore solution, holding 50 % bwo clay of PEG–2000 and of PCE polymers 45PC6, 17PC6, 8.5PC6 and PMA respectively (w/clay = 53)

When PCE polymer 45PC6 was added to the clay, a shift in *d*-spacing from 1.23 nm to 1.77 nm was detected, confirming the intercalation of the long PEO side chain of 45PC6 into the clay structure. When 17PC6 was added, the characteristic reflection (d = 1.77 nm) decreased in intensity and broadened. Also, a slight shoulder formed at higher 2-theta degrees angles (3.2 °2θ). An even more pronounced broadening in reflection was observed when 8.5PC6 was added. This corroborates that the intercalates formed decrease in orderness when PCEs possessing shorter side chains are utilised, indicating that the tendency for intercalation is

dependent on the graft chain length of a PCE used. Opposite to this, when PMA was added to the clay, no significant change in *d*-value was observed, thus signifying that the chemical interaction of PCE was solely owed to its lateral PEO chains. These results corroborate that the intercalating ability of PCEs can vary between that of pure PEG and pure PMA. For PCEs possessing long side chains, their intercalating behaviour is more similar to that of PEG, while PCEs possessing short side chains behave more like pure PMA.

To quantify the intercalation ability of the PEO side chains of PCEs, the amounts of sorbed PEGs by clay in synthetic cement pore solution were next measured (**Fig. 6**). For PEG–2000 (possessing the same length as the side chain in 45PC6), a maximum sorbed amount of 340 mg/g clay was attained. In the case of PEG–750 (17PC6) and PEG–350 (8.5PC6), the maximum sorbed amounts were only 145 mg/g clay and 65 mg/g clay respectively (as shown in **Fig. 6**). These sorbed amounts of the PEGs appear to explain the relative intercalating ability of the PCEs well. However, when comparing the amounts of PEG (**Fig. 6**) and PCE sorbed by clay in alkaline solution (**Fig. 4**), for PCEs possessing shorter side chains, a discrepancy in the sorbed amounts was observed. This may indicate a disparity in the intercalation ability of PCEs from PEGs. Therefore, to fully quantify the sorption behavior of PCEs on clay, a quantitative analysis of the sorbed amount of EO contained in PCE was performed and compared with the experimentally determined sorbed amounts of PEG.

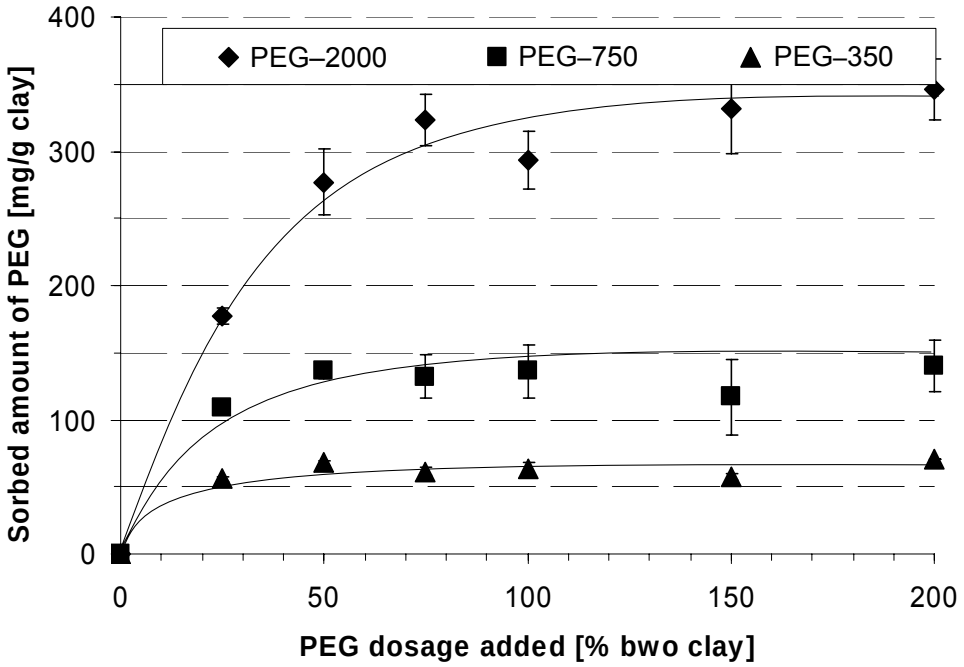

Fig. 6. Sorption isotherms of PEG–2000, PEG–750 and PEG–350 on montmorillonite clay dispersed in synthetic cement pore solution (Ca^{2+} concentration = 0.4 g/L, w/clay = 53)

3.7. Sorbed amount of EO from PCE

Fig. 7 shows the amounts of EO from PCE sorbed on clay in alkaline solution derived from the sorbed amounts of the PCEs (**Fig. 4**). Knowing the amount of EO from PCE sorbed in alkaline solution allows to assess the affinity of a PCE polymer for clay with respect to graft chain intercalation. Comparing this calculation profile to the experimentally determined sorption profile for pure PEG (**Fig. 6**) revealed that in both cases, similar results were obtained. This confirmed that the intercalation behaviour of PCE is similar to that of PEG and that no discrepancy exists. PCEs possessing longer graft chains intercalate in greater quantity than those with shorter graft chains, similar to PEGs possessing higher molecular weights which can intercalate more as compared to their counter PEGs possessing lower molecular weights. This behaviour has been reported before by another group [Zhao *et al.*, 1989].

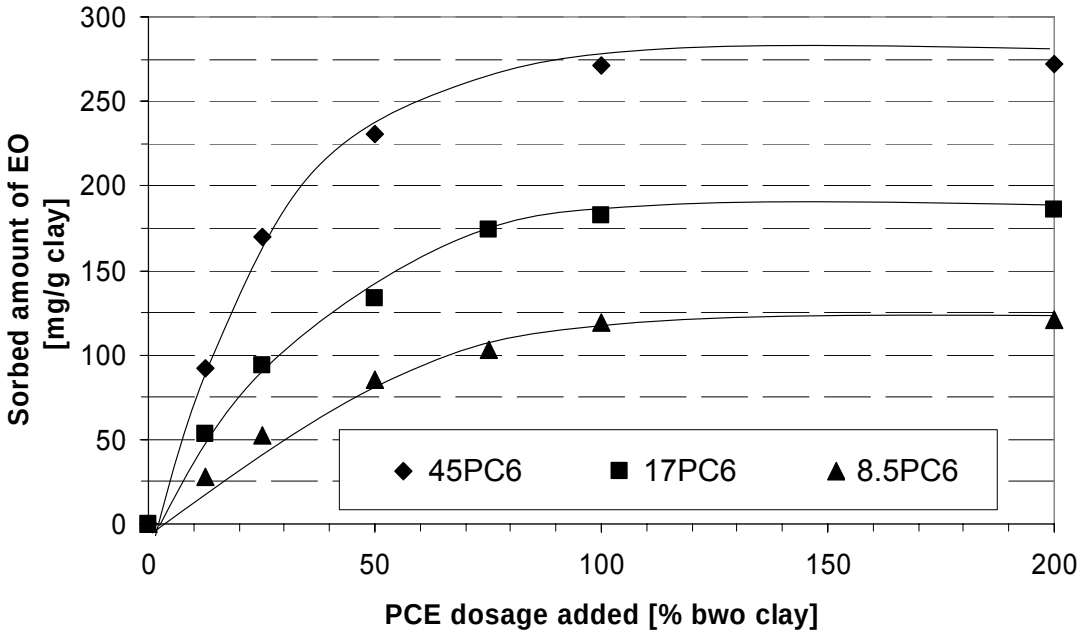

Fig. 7. Calculated amount of EO from PCE sorbed on clay as a function of PCE dosage added, measured in alkaline solution at pH 12.8 (adjusted by NaOH addition, w/clay = 53)

However, when this calculation was conducted for PCEs sorbed by clay in synthetic cement pore solution, a totally different trend was observed (**Fig. 8**). The sorbed amount of EO for 45PC6 remained at ~ 295 mg/g clay (compared to 275 mg/g clay in alkaline solution), confirming that for this polymer, chemisorption (intercalation) was by far the main driving force for interaction with clay (also see **Fig. 3**). However, for the PCE polymers 8.5PC6 and 17PC6, much higher sorbed amounts of EO (up to 45 % more) were found, as compared to in alkaline solution. This confirmed that in the consumption of such PCEs, electrostatic attraction plays a significant role. It also signifies that when the PEO graft chains are shorter, more PCE adsorbs onto the clay surfaces.

From this data, ranges for the dosage-dependent portions of chemisorptive interaction, facilitated by the PEO side chain of PCE, and adsorptive interaction owed to the anionic trunk chain of PCE were developed as displayed in **Fig. 8**. It corroborates that at low PCE dosages

(up to 50 % bwo clay for all PCEs), only PEO side chain intercalation and little surface adsorption occurs. At higher dosages, PCEs with short side chains begin to interact with clay through surface adsorption. While for PCEs holding long PEO side chains, surface adsorption is almost negligible.

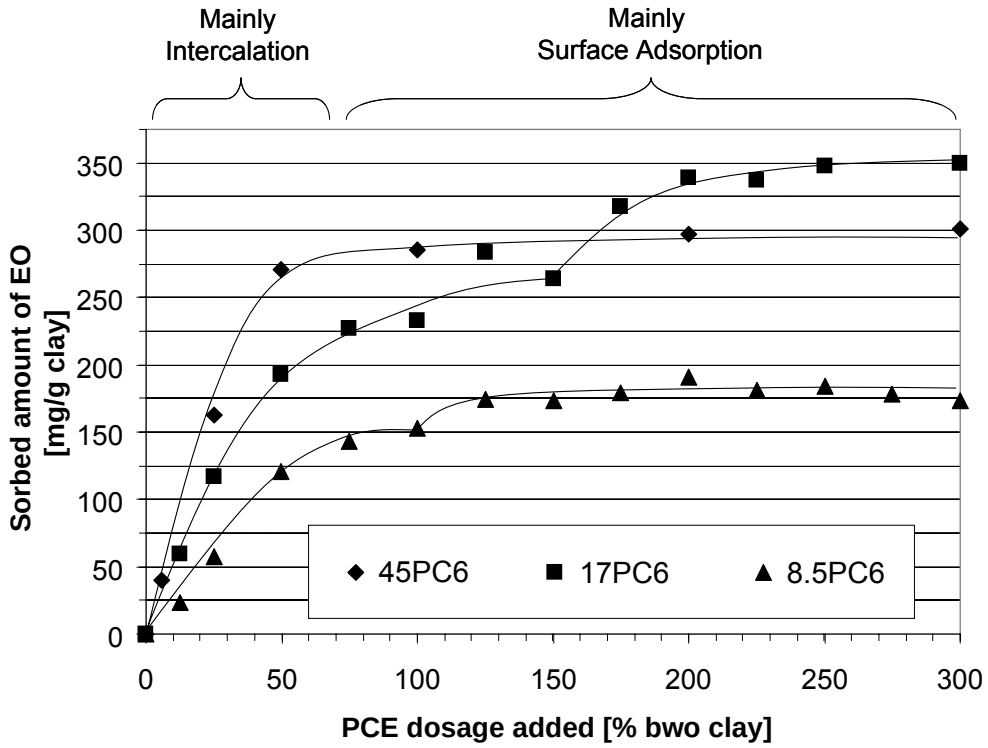

Fig. 8. Calculated amount of EO from PCE sorbed on clay as a function of PCE dosage added, measured in synthetic cement pore solution (w/clay = 53)

3.8. PMA as an anionic sacrificial agent

It can be clearly stated that at low dosages, intercalation of PCEs is the main reaction occurring between PCEs and clay. However, at medium to high dosages, for PCEs possessing short PEO side chains electrostatic attraction must also be considered when searching for remedies. To prevent surface adsorption of such PCEs, pure PMA (dosage: 0.1 % bwoc) was

added as a sacrificial agent to cement/clay pastes holding the three PCE polymers, and the paste spread was measured by 'mini slump' tests. The results are presented in **Fig. 2**.

All three pastes incorporating pure PMA showed less decrease in workability than in the absence of this agent (spread value 22.1 cm instead of 21.3 cm for 45PC6, 24.6 cm instead of 22.1 cm for 17PC6, and 25.1 cm instead of 22.7 cm for 8.5PC6). This demonstrates that due to the similarity in chemical composition with the PCE anionic backbone, polymethacrylic acid can act as a sacrificial agent to reduce the amount of PCE consumed by clay, thus softening the negative impact on PCE performance in the presence of clay contaminants. Additionally, the higher regain in spread for 8.5PC6 confirmed that for this PCE, interaction with clay was particularly owed to backbone interaction with the clay surface, as a result of its shorter side chains. On the other hand, dispersing effectiveness of 45PC6 was not much improved by PMA, because it exhibits only a weak surface interaction with clay. The behavior of PCE polymer 17PC6 was found to lie in between these two PCE polymers.

These results suggest that the usage of an anionic polymer such as polymethacrylic acid as sacrificial agent generally is suitable for PCEs possessing short side chains (e.g. 8.5PC6) or low grafting density. However, for PCEs holding longer side chains such as 45PC6 (precast type), the improvement in flow is not as desirable with sole usage of PMA as a sacrificial agent. There, a potential sacrificial agent mainly needs to prevent side chain intercalation to be effective.

4. Conclusions

PCE copolymers, regardless of their side chain length, possess a higher affinity for sodium montmorillonite clay than for cement. When only very minor amounts of montmorillonite clay are introduced into cement or concrete, availability and thus dispersing effectiveness of the PCE superplasticizer is greatly reduced. Generally, the extent at which PCEs are affected by clay is correlated to their side chain lengths. The longer the side chain of a PCE, the greater is the loss in dispersing capacity. Generally, PCEs possessing longer side chains are sorbed by clay mainly through intercalation via their poly(ethylene oxide) side chains into the interlayer space of the alumosilicate layers. While for PCEs with shorter side chains, electrostatic attraction mediated by surface adsorbed Ca^{2+} cations becomes significant. Therefore, the total amount of a PCE sorbed by clay is the result of a delicate balance between PCE dosage added, amount of EO contained in the side chains of the PCE which can intercalate, and the anionic charge density along the PCE trunk chain which promotes surface adsorption. For optimal usage of highly anionic PCEs in cement contaminated with clay, PMA has proven to be an effective remedy.

Acknowledgments

The authors would like to thank Dr. Coutelle from Rockwood (Moosburg/Germany) for supplying the clay sample. Also, Serina Ng would like to thank Jürgen Manchot Stiftung for generous funding of this research.

References

- Alemdar, A., Güngör, N., Ece, O. I., Atici, O., 2005. The Rheological Properties and Characterization of Bentonite Dispersions in the Presence of Non-ionic Polymer PEG. J. Mater. Sci. 40, 171–177.
- Amarasinghe, P.M., Katti, K.S., Katti, D.R., 2009. Nature of Organic Fluid–Montmorillonite Interactions: An FTIR Spectroscopic Study, J. Colloid Interface Sci. 337, 97–105.
- Andersson, K., Allard, B., Bengtsson, M., Magnusson, B., 1989. Chemical Composition of Cement Pore Solutions. Cem. Concr. Res. 19, 327–332.
- Atarashi, D., Sakai, E., Obinata, R., Daimon, M., 2003. Influence of Clay Minerals on Fluidity of $CaCO_3$ Suspension containing Comb-type Polymer, Cem. Sci. Concr. Technol. 57, 386–391.
- Atarashi, D., Sakai, E., Obinata, R., Daimon, M., 2004. Interactions between Superplasticizers and Clay Minerals. Cem. Sci. Concr. Technol. 58, 387–392.
- Bedard, P. E., Mailvaganam, N. P., 2005. The Use of Chemical Admixtures in Concrete: Part II: Admixture-Admixture Compatibility and Practical Problems. ASCE J. Performance Constr. Facil. 263–266.
- Bergaya, F., Lagaly, G., 2006. General introduction: Clays, Clay Minerals, and Clay Science. In: Handbook of Clay Science. Developments in Clay Science, Vol. 1., Ed.: Bergaya, F., Theng, B. K. G., Lagaly, G., Elsevier Amsterdam, Netherlands. 1–18.
- Chen, B., Evans, J. RG, 2005. X-ray Diffraction Studies and Phase Volume Determinations in Poly(ethylene glycol)–Montmorillonite Nanocomposites. Polym. Int. 54, 807–813.
- Dodson, V. H., Hayden, T.D., 1989. Another Look at the Portland Cement / Chemical Admixture Incompatibility Problem. Cem. Concr. Res. 19, 52–56.

- Durand-Piana, G., Lafuma, F., Audebert, R., 1987. Flocculation and Adsorption Properties of Cationic Polyelectrolytes toward Na-Montmorillonite Dilute Suspensions, J. Colloid Inter. Sci.. 119, 474–480.
- Greenwell, H. C., Bowden, A. A., Chen B., Boulet, P., Evans, J. R. G., Coveney, P. V., 2006. A. Whiting, Intercalation and In Situ Polymerization of Poly(alkylene oxide) Derivatives within M^{+}–Montmorillonite (M = Li, Na, K). J. Mater. Chem. 16, 1082–1094.
- Hiroyoshi, K., Kazuhiro, Y., 1998. Influence of Sulfate Ion on the Fluidity of Cement Paste containing Polycarboxylic Type Superplasticizer. JCA Proceedings of Cement & Concrete. 52, 144–151.
- Jaernstrom, L., Stenius, P., 1990. Adsorption of Polyacrylate and Carboxy Methyl Cellulose on Kaolinite: Salt Effects and Competitive Adsorption. Colloids Surf. 50, 47–73.
- Jeknavorian, A.A., Jardine, L., Ou, C.C., Koyata, H., Folliard, K.J., 2003. Interaction of Superplasticizers with Clay-Bearing Aggregates. Special Publication ACI/ 7th CANMET Conference on Superplasticizers and Other Chemical Admixtures, Berlin, Germany, SP-217, 1293–1316.
- Kawaguchi, S., Aikaike, K., Zhang, Z.M., Matsumoto, K., Ito, K., 1998. Water Soluble Bottlebrushes. Polym J. 30, 1004–1007.
- Li, C. Z., Feng, N. Q., Li, Y. D., Chen, R. J., 2005. Effects of Polyethylene Oxide Chains on the Performance of Polycarboxylate-type Water-Reducers. Cem. Concr. Res. 35, 867–873.
- Magarotto, R., Torresan, I., Zeminian, N., 2003. Effect of Alkaline Sulfates on Performance of Superplasticizers. In: Proceedings of the 11th International Congress on the Chemistry of Cement: Cement's Contribution to Development in the 21st Century, V. 2, Ed: G. Grieve, G. Owens, Durban, South Africa, 569–580.
- Ng, S., Plank, J., 2012. Study on the Interaction of Na-montmorillonite clays with Polycarboxylate based superplasticizers. V. M. Malhotra (Ed.) 10th CANMET/ACI

Conference on Superplasticizers and Other Chemical Admixtures in Concrete (Proceeding Papers), ACI, Prague, Czech Republic.

- Plank, J., Pöllmann, K., Zouaoui, N. Andres, P.R., Schaefer, C., 2009. Synthesis and Performance of Methacrylic Ester based Polycarboxylate Superplasticizers possessing Hydroxy terminated Poly(ethylene glycol) Side Chains, Cem. Concr. Res. 39, 1–5.
- Plank, J., Dai, Z., Keller, H., von Hoessle, F., Seidl, W., 2010. Fundamental Mechanisms for Polycarboxylate Intercalation into C_3A Hydrate Phases and the Role of Sulfate present in Cement. Cem. Concr. Res. 40, 45–57.
- Suter, J. L., Coveney, P. V., 2009. Computer Simulation Study of the Materials Properties of Intercalated and Exfoliated Poly(ethylene) Glycol Clay Nanocomposites. Soft Mater. 5, 2239–2251.
- Svensson, P. D., Hansen, S., 2010. Intercalation of Smectite with Liquid Ethylene Glycol — Resolved in Time and Space by Synchrotron X-ray Diffraction. Appl. Clay Sci. 48, 358–367.
- Takahashi, Y., Tadokoro, H., 1973. Structural Studies of Polyethers, $(-(CH_2)_m\text{-}O\text{-})_n$. X. Crystal Structure of Poly(ethylene oxide). Macromol. 6, 672–675.
- Zhao, X., Urano, K., Ogasawara, S., 1989. Adsorption of Polyethylene Glycol from Aqueous Solution on Montmorillonite Clays. Colloid Polym. Sci. 267, 899–906.
- Zingg, A., Winnefeld, F., Holzer, L., Pakusch, J., Becker, S., Figi, R., Gauckler, L., 2009. Interaction of Polycarboxylate–based Superplasticizers with Cements containing Different C_3A amounts. Cem. Concr. Com. 31, 153–162.
- Zouaoui, H. N., 2009. Einfluss der Molekülarchitektur von Polycarboxylaten, hergestellt durch Blockcopolymerisation und Pfropfreaktion, auf die Wechselwirkung mit Fluoroanhydrit und Portlandzement. Dissertation, Technische Universität München, Lehrstuhl für Bauchemie.

Paper 4

Formation of Organo-mineral Phases Incorporating PCE Superplasticizers During Early Hydration of Calcium Aluminate Cement

S. Ng, J. Plank

Proceedings of the 13th ICCC International Congress on the Chemistry of Cement

Abstract book p. 251, Madrid/Spain (2011)

ISBN: CD 978-84-7292-400-0.

Formation of Organo-Mineral Phases Incorporating PCE Superplasticizers During Early Hydration of Calcium Aluminate Cement

Ng S, Plank J*
Technische Universität München, Lehrstuhl für Bauchemie, Lichtenbergstr. 4, 85747 Garching b. München, Germany

Abstract
Organic admixtures, particularly those possessing highly anionic character, may intercalate into calcium aluminate hydrates and form layered organo-mineral phases of the general composition $[Ca_2Al(OH)_6](A)_x \cdot (OH)_y \cdot nH_2O$. The formation of intercalates has been analytically proven in model systems such as hydrating C_3A, but not in real Portland cement. This can be attributed to the nano crystallinity of the XRD amorphous intercalates and the presence of sulfates which may entirely prevent intercalation. Here, for the first time, we present experimental evidence confirming the formation of organo-mineral phases incorporating PCEs in calcium aluminate cement (CAC) during its early hydration. A comprehensive study using a commercially available CAC (~ 70% Al_2O_3) undergoing early hydration in the presence of three different PCEs revealed that aside from surface adsorption, intercalation plays a key role. Generally, the intercalation ability of PCEs is dependent on the methacrylate (MA): MPEG-MA ester molar ratio. When CAC was hydrated with PCEs for 2 h, suspensions containing PCEs possessing a molar ratio of 1.5:1 failed to display intercalates. However, nano crystalline, colloidal particles were recovered when PCEs possessing a molar ratio of 6:1 were utilized. Under XRD analysis, these particles displayed the characteristic reflections of organo-mineral phases with a d-spacing of ~ 6.4 nm. This layered structure was further confirmed by TEM imaging. During CAC hydration, direct formation of the organo-mineral phases occurs via co-precipitation and nucleation where self-assembly of dissolved Ca^{2+} and $Al(OH)_4^-$ occurs in the presence of PCE as template. Another mechanism is indirect formation via anion exchange between the interlayer OH^- and dissolved PCE in the initially formed C_2AH_8. This exchange process, however, is relatively slow and probably consumes insignificant amounts of PCE. Slump flow tests revealed that PCEs composed of MA: MPEG-MA ester at molar ratio of and 1.5:1 respectively disperse this CAC very well. Lower effectiveness was obtained for PCEs with higher molar ratios (3:1 and 6:1 respectively). This behaviour is contrary to what is known for Portland cement. Apparently, a link exists between the dispersing force of PCE and intercalation tendency. PCEs possessing high anionic charge (3:1 and 6:1 molar ratios) are very prone to intercalation. Thus, for an added dosage, these PCEs are consumed and become less effective as dispersant. PCEs exhibiting low anionic charge are fully available for the dispersion effect as none is wasted in the intercalation reaction. This mechanism explains the difference in dispersing force for these PCEs in Portland cement and CAC.

Originality
This work addresses the mechanism behind the reactions occurring during early hydration of a high alumina cement in the presence of polycarboxylate-based (PCE) superplasticizers. In literature, little work has been presented on the interaction of high alumina cement with superplasticizers. Even less has been proposed on the mechanism of interaction, with focus on the chemical absorption. Here, we confirm the formation of intercalates from high alumina cement in the presence of PCEs during early hydration. The intercalates formed after 2 h at room temperature are nano crystalline and form a colloidal suspension which can be obtained as a gel precipitate under prolonged hydration of up to 2 days. This confirms the formation of intercalates via co-precipitation during early hydration of this cement, followed by subsequent growth of the Ca-Al-PCE-LDH nuclei. We believe that the proof for existence of intercalates in cement to be of great significance as it can explain numerous phenomenons such as the differences in performance of PCEs under conditions of delayed addition.

Chief contributions
PCE is a commonly used high-performance superplasticizer in the field of construction chemistry due to the low dosages required for the same effectiveness as its counterparts such as the polycondensates. These superplasticizers may intercalate into the layered structures of calcium aluminate hydrates, mainly C_2AH_8, thus rendering the polycarboxylate ineffective as dispersing agent during early hydration. Despite the importance, intercalation in cementitious materials has only been reported using simplified systems involving the hydration of pure C_3A over a hydration period of 2 days or 2 h at elevated temperatures. These conditions are not ideal representations of actual cement systems where workability of the PCEs is required. Here, we provide experimental proof that organo-mineral phases incorporating highly anionic PCEs are being formed during early hydration of CAC under typical field conditions. Thus, for the first time, the formation of organo-mineral phases from PCE and a cement under realistic conditions of applications is shown to occur. This can then be directly correlated to the dispersing force of different PCE molecules.

Keywords: *Calcium aluminate cement, polycarboxylate, organo-mineral phases, intercalation, dispersing force*

* **Corresponding author: Email-** sekretariat@bauchemie.ch.tum.de, **Tel-** + (49) 8928913151, **Fax-** +(49) 8928913152

1. Introduction

Anionic organic admixtures are widely used in modern concrete technology for improving workability and compressive strength. Commonly used SPs including polycondensates and PCEs interact strongly with cement through an adsorptive mechanism and develop dispersion either by electrostatic repulsion or steric effect between cement particles (Ramachandran *et al.*, 1995; Rixom *et al*., 1999; Uchikawa *et al*., 1997; Yoshioka *et al.*, 2002). Their workabilities had been investigated in OPC and PCEs were found to be the most effective. In CAC, however, the performance of SP is far inferior to that in OPC. This discrepancy can be attributed to the behaviour of SPs in cement. During early hydration of CAC at room temperature, formation of C_2AH_8 predominates. This metastable phase undergoes gradual conversion to katoite (C_3AH_6) via a "through solution" mechanism. It is thermodynamically favored by an increase in temperature and kinetically governed by the availability of free (liquid) water within the cement microstructure (Bradbury *et al.*, 1976). Conversion thus rarely occurs during early hydration, leading to the domination of interaction between the C_2AH_8 phase and SPs such as PCEs.

SPs may intercalate into calcium aluminate hydrates and form layered organo-mineral phases of the general composition $[Ca_2Al(OH)_6](A)_x \cdot (OH)_y \cdot nH_2O$ (Stöber *et al.*, 1999). The formation of intercalates has been analytically proven in model systems such as hydrating C_3A, but not in cements (Fernon *et al.*, 1997, Raki *et al.*, 2004). This can be attributed to the nano crystallinity of intercalates, the relatively small amount of intercalates being formed, or the presence of dissolved sulfates which may entirely prevent intercalation. Plank *et al.* have shown that hydrating C_3A with PCEs leads to the formation of organo-mineral phases of Ca-Al-PCE-LDH type (Plank *et al.*, 2006; Plank *et al.*, 2006, Plank *et al.*, 2010). Sequestration of PCE into AF_m crystallites depletes the dispersant from the pore solution and can reduce its effectiveness. C_3A hydrates in a similar manner as the monocalcium aluminate (CA) present in CAC. The poor performance of some SPs in CAC may stem from partial intercalation. The aim here is thus to determine whether or not chemical absorption of PCE occurs and to extrapolate the findings to the dispersing effectiveness of the PCEs on CAC. For this purpose, a commercial white CAC was selected. First, a parametric study via 'mini slump' test was conducted to determine the dispersing effect of three different PCEs on this cement. This was followed by further studies using XRD, TEM, SEM and elemental analysis to determine the mode of sorption of the PCE molecules on CAC (chemical absorption/ intercalation or physical surface adsorption).

2. Materials

Calcium aluminate cement -- A cement containing ~ 70 % Al_2O_3 (Ternal White® from Kerneos®, Neuilly Sur Seine Cedex/ France) was used in this study. The phase composition was quantified by Rietveld method with TOPAS software using X-ray diffractometry at room temperature (D8 Advance instrument from Bruker AXS, Karlsruhe/Germany) with Bragg-Bretano geometry. Samples were prepared in a front mount plastic holder and analysed with a scan range of 3 to 70 °2θ; step size 0.15 sec/step; spin revolution time 4 sec; aperture slit 0.5 °; and nickel filter for the incident beams. The oxide composition (determined via XRF) is shown in Table 1. Specific surface area was measured with a Blaine instrument (Toni Technik, Berlin/Germany) to be 3,800 cm^2/g, while particle size was determined to be 7.76 µm via Laser granulometry on a Cilas 1064 instrument (Cilas Company, Orleans/France). Density was 2.89 g/cm^3 as measured on the Helium pycnometer.

Table 1. Phase content and oxide composition of the commercial CAC sample

Phase	CA		CA_2		$C_{12}A_7$	
wt%	65.8		33.4		0.8	
Oxide	CaO	Al_2O_3	Na_2O	SiO_2	MgO	FeO
wt%	27.1	71.6	0.3	0.2	0.4	0.1

Polycarboxylates -- Three PCE samples were synthesized by aqueous free radical copolymerization of MAA with MPEG-MA ester following a procedure described before (Plank *et al.*, 2009). The

copolymers were composed of different molar ratios of monomers and contain side chains each made of 45 ethylene oxide units (EOUs, side chain length = 12.5 nm). The PCEs were denoted as 45PCx, where 45 refers to EOUs, and x corresponds to the molar ratio of MAA: MPEG-MA ester. The 3 polymers were thus labeled as 45PC6, 45PC3 and 45PC1.5 and their general chemical composition is presented in Figure 1. These PCE compositions were selected as they represent the types of PCEs commonly used in precast (45PC6) and ready-mix concrete (45PC1.5). All three PCEs were neutralized with NaOH and dialyzed against a membrane with a M_w cutoff of 8k Da (provided by Spectra® Laboratories, Kehl, Rhein/Germany) before further usage.

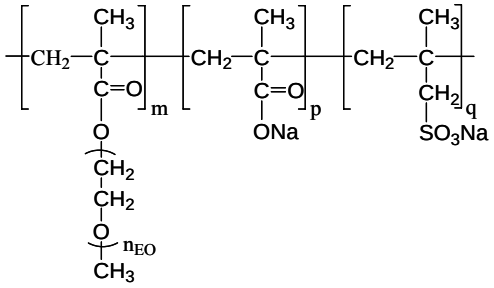

Figure 1. Chemical structure of ω-methoxy poly(ethylene glycol) methacrylate ester – co –methacrylic acid, polymerized in presence of methallyl sulfonic acid as chain transfer agent

Characterisation of the PCE polymers was performed by aqueous size exclusion chromatography (SEC) using a 2695 SEC separation module (Waters, Eschborn/Germany), equipped with a 2414 RI detector (Waters, Eschborn/Germany) and a Dawn EOS 3 angle light scattering detector (Wyatt Technologies, Clinton, IA/USA). Ultrahydrogel columns 500, 250, and 120 (Waters, Eschborn/Germany) with an operating range (PEO) of M_w = 100 to 1,000,000 g/mol were used. Eluent was NaOH at pH 12 with 0.1 mol/L $NaNO_3$. Anionic charge amount of the PCEs was determined in water and cement pore solution (PS). PS for charge detection was collected from a CAC slurry at w/c ratio of 0.52 by vacuum filtration via a diaphragm vacuum pump (Vaccubrand company, Wertheim/Germany) with filter paper (Schleicher & Schuell, Grade 589/3, 2d according to DIN 53 135) at a suction capacity of 1.7 m^3/hr. Charge titration was performed with 0.2 g/L PCE solution on a particle charge detector PCD 03 pH meter (Mütek, Herrsching/Germany) using Poly-DADMAC as the standard cationic counter polymer solution (0.001 mol/L). Based on the experiments above and following the calculation method from Ohta *et al.* (Ohta *et al.*, 2000), the properties of the PCE samples are shown in Table 2. The three PCE molecules differ with respect to their anionic charge amounts, which narrowed in cement pore solution due to the formation of complexes with Ca^{2+} present (Plank *et al.*, 2009).

Table 2. Properties of the methacrylate ester based PCE samples 45PC1.5, 45PC3 and 45PC6, respectively

Property	45PC1.5	45PC3	45PC6
Molar mass M_n [g/mol]	60,500	50,120	43,680
Molar mass M_w [g/mol]	170,600	156,700	156,400
Polydispersity index (PDI)	2.8	3.2	3.6
MAA : MPEG-MAA molar ratio	1.5 : 1	3 : 1	6 : 1
Trunk chain length [nm]	16	25	30
Specific anionic charge amount $_{water}$ [µeq/g]	289	756	1,526
Specific anionic charge amount $_{w/c=0.52}$ [µeq/g]	111	125	148

3. Experimental Procedures

'Mini Slump' test -- Dispersing effectiveness of the PCE samples was derived from the dosage necessary to achieve a paste flow of 26 ± 0.5 cm using a VICAT cone (height 40 mm, top diameter 70 mm, bottom diameter 80 mm). The test was performed as follows: At first, the w/c ratio required for a

paste spread of 18 ± 0.5 cm was established. Subsequently, the dosages of SPs required to reach spreads of 26 ± 0.5 cm were determined. PCE samples were dissolved in the mixing water for the paste prior to measurement. 300 g of CAC was added to the mixing water, agitated manually for 1 minute and left to stand for another minute. The paste was then stirred for another 2 minutes before transferring into the VICAT cone on a glass plate. The paste was filled to the brim of the cone and levelled before it was vertically lifted from the surface of the glass plate. The resulting spread of the paste was measured twice; the second measurement being perpendicular to the first. The final spread value was taken as the average of the two measured ones.

Synthesis and characterisation of the organo-mineral phases -- PCE solution was prepared at a concentration of 2.5 wt. % in 45 g water in a round-bottom flask equipped with a magnetic stirrer. 3 g of CAC were then added, which marks the start of the reaction. The system was stirred at room temperature for 2 hours and then centrifuged (8,500 rpm, 20 minutes) to separate the solid and liquid (colloidal) phases. To the solid phase, quenching was performed with acetone and subsequent centrifugation for another 15 minutes. The resulting solids were dried in oven at 40 °C for 24 hours. The liquid phase was pre-dried by rotary evaporation and post-dried by freezing drying. Thereafter, washing was done thrice with alkaline solution at pH 11.6 (w/NaOH) to remove excess polymer present. All dried products were analysed by XRD possessing a low angle scintillator, with a scanning range of 0.6 to 40 °2θ; step size of 0.10 sec/step; spin revolution time of 4 sec; aperture slit of 0.1 °. TEM images were captured with a JEOL JEM-2100 instrument (JEOL Company, Tokyo/Japan).

4. Results and discussions

Flowability of calcium aluminate cement paste containing PCE -- The w/c ratios required for a CAC paste spread of 18 ± 0.5 cm was verified to be 0.52 using the 'mini slump' test. Three different PCEs; 45PC1.5, 45PC3 and 45PC6, with increasing amount of anionic charge were tested. All PCE samples dispersed the cement effectively at dosages which were an order of magnitude lower than that required for OPC (Figure 2) (Yoshioka *et al.*, 2003). This implies that PCEs are extremely effective in the initial dispersion of CAC, signifying better workability in CAC than in OPC.

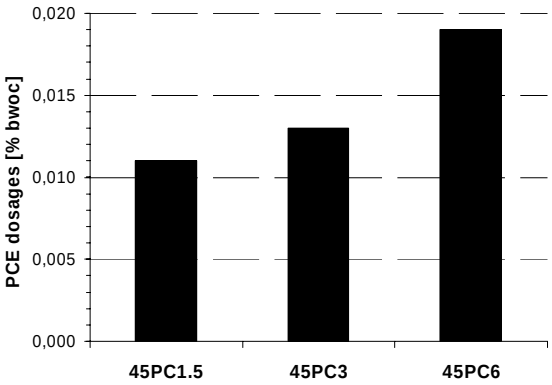

Figure 2. PCE dosages required to achieve a CAC paste spread of 26 ± 0.5 cm at a w/c ratio of 0.52

The trend presented in Figure 2 shows that for effective dispersion of CAC, higher dosage (0.019 % bwoc) of more anionic 45PC6 was required as compared to the less anionic copolymers 45PC3 (0.013 %bwoc) and 45PC1.5 (0.011 % bwoc) respectively. This finding is opposite to that observed in OPC where more anionic polymers generally disperse the cement more effectively (Uchikawa *et al.*, 1997). The observation in OPC can be accounted for by the greater electrostatic repulsion introduced by a more anionic polymer, thus increasing the dispersing power. This difference in dispersing ability of the copolymers in CAC as compared to OPC highlights a different mechanism in the sorption behaviour of polycarboxylate based superplasticizers.

Intercalation of PCE into calcium aluminate cement hydrates -- To probe into the mechanistic behaviour of these copolymers, further analysis on their absorption behaviour in CAC was performed via XRD analysis. As a control, the CAC sample was hydrated and analysed first in the absence of PCE. Next, syntheses were done under high PCE concentrations (2.5 wt. %) to ensure distinct and observable results.

For all samples, it was evident that hydrates possessing layered structures are formed in solution within the first 2 hours of hydration (Figure 3). The diffraction pattern for pure Ca–Al–OH–LDH shows a typical layered structure with a basal spacing (d-value) of 1.06 nm, corresponding to an aluminate hydrate which in cement chemistry is denoted as C_2AH_8 (JCPDS entry 54-564). For pure hydrated CAC, only a minute amount of C_2AH_8 and gibbsite were detected after 2 h of hydration. This product combination, i.e. the presence of both C_2AH_8 and AH_3, is to be expected due to the stoichiometric ratio of CaO: Al_2O_3 in the CAC sample (Table 1). When PCEs were present, no gibbsite was detected. Furthermore, C_2AH_8 was replaced by other layered structures with increasing d-spacing as a function of the charge amount of the polymers. In the presence of 45PC1.5, a broad and weak signal at about 7.5 °2θ was detected. This reflection is characteristic of C_2AH_x hydroxy aluminate hydrates with less water than isomorphous C_2AH_8. The remaining strong reflections were characteristic of the polyethylene oxide present in the PCEs. The absence of reflections at low 2θ angles signified that no detectable Ca-Al-45PC1.5-LDH was formed. When 45PC3 and 45CP6 were used, signals for layered structure representing *d*-spacings of 6.81 nm and 6.41 nm respectively were detected. This implies that intercalation of the PCEs had occurred, possibly in a compressed or coiled state. The results obtained here is in agreement with previous work where PCEs made from molar ratios MA acid: ester of 6: 1 with side chains up to 45 EOUs intercalate into Ca–Al–LDH formed during rehydration of C_3A (Plank *et al.*, 2010). On the other hand, PCEs possessing side chains longer than 45 EOUs resisted intercalation into C_3A hydrates due to the bulkiness of the polymers.

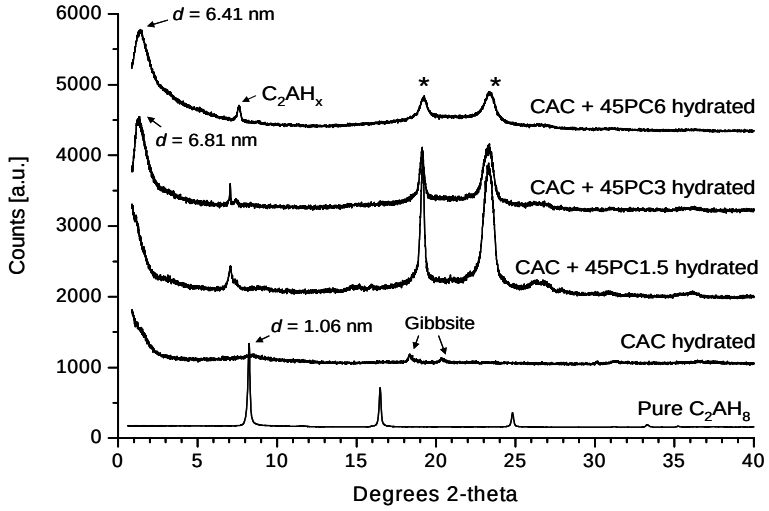

* reflective signals of the PCE polymers caused by the polyethylene oxide groups present in the side chains

Figure 3. X-ray diffraction patterns (bottom to top): C_2AH_8, the main hydrate during hydration of CAC at rt (relative intensity was reduced by a factor of 16 here); hydrated CAC sample; CAC hydrated in the presence of 45PC1.5; and Ca–Al–45PC3-LDH and Ca–Al–45PC6-LDH intercalates respectively

Here, the tendency for intercalation was shown to be charge dependent, where more anionic polymers can intercalate and stabilise the LDH structure better than their less anionic counterparts. This result confirms the importance of electrostatic host-guest interactions in the formation of the organo-mineral phases. Additionally, intercalation accounts for the higher dosages of more anionic polymers which were required to maintain a similar flow spread as compared to when less anionic PCEs (e.g. 45PC1.5) were applied (Figure 2).

As shown before, the trend in amount of copolymers required for effective dispersion is unlike that in OPC. In OPC, ettringite and monosulphate are rapidly formed during early hydration when sufficient concentrations of dissolved sulphate ions are present. The stability of these AF_t and AF_m phases make intercalation unfavourable, thus leaving PCEs for the dispersion effect which involves surface adsorption (Plank *et al.*, 2006). On the other hand, in a CAC system, no sulphate which can perturb intercalation is present, and rapid formation of the layered aluminate phase, C_2AH_8 during early hydration promotes consumption of these PCEs. The more anionic the polymer is, the higher the consumption rate. As a result, a higher amount of 45PC6 to account for consumption via intercalation was required to achieve the same flow spread as when 45PC1.5 was employed which is hardly consumed via absorption.

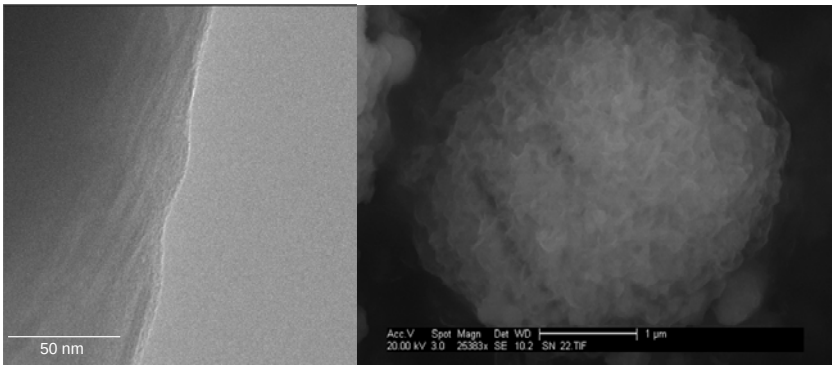

Figure 4. TEM (left) and SEM (right) images of nano composites obtained from CAC hydrated with PCE sample 45PC6 showing well layered structure, which occurs as intergrown nanofoils under SEM imaging

Further investigations via elemental analysis (Ca, Al, C, H) and TEM also confirmed the formation of novel organo-mineral phases during CAC hydration. From elemental analysis, the organic part (wt. %) in the Ca-Al-PC-LDHs was calculated as follows: 45PC6–LDH 54.4 %; 45PC3–LDH 38.9 %; 45PC1.5–LDH 17.8 %. The polymer contents found in samples obtained using 45PC3 and 45PC6 were much higher than the usual percentage for mere surface adsorption, thus confirming the formation of organo-mineral phases. On the other hand, the low organic content for the sample prepared with 45PC1.5 which contrasts the other two confirms the charge dependency for intercalation. Figure 4 shows TEM and SEM images of the Ca-Al-45PC6-LDH sample. There, layered nano composites were seen via TEM and a high carbon content was detected via EDX analysis, while intergrown nanofoils of Ca-Al-45Pc6-LDH can be observed from SEM imaging. The appearance of layers decreases with decreasing anionic charge amount of the PCE. No layered structure was found when 45PC1.5 was present during CAC hydration.

Still, the question remains whether the intercalation process observed here under idealised conditions can also happen in actual cement applications. To investigate, additional experiments were conducted under realistic application conditions (concentration of 45PC6 = 0.019 % bwoc, w/c ratio = 0.52). There, on XRD analysis, no distinctive reflections characteristic of organo-mineral phases was detected. Instead, only C_2AH_8 was found. The absence of the organo-mineral phases is probably owed to the nano crystallinity and low amount of Ca-Al-PCE-LDH formed under this condition. However, beside C_2AH_8, layered structures typical for organo-mineral phases possessing a *d*-spacing of ~ 6 nm (matching that obtained from TEM and XRD analysis under idealised conditions) were found in the dried solid under TEM imaging. Also, SEM imaging of dried solids showed nanofoils of intercalates exhibiting carbon contents of ~ 30 wt. % as determined by EDX technique. This signifies that formation of organo-mineral phases has indeed occurred. These results will be presented in detail in a subsequent paper.

5. Conclusion

Here, we showed that in solution at room temperature, PCEs can interact with calcium aluminate cement particles via both adsorption and absorption. When suspended in solution, CAC adopts a highly positive surface charge. This instigates adsorption of anionic PCE-based superplasticizers via electrostatic attraction. Concurrently, the formation of layered double hydroxides such as C_2AH_8 favours chemical absorption (intercalation) of highly anionic PCEs. The formation of organo-minerals in the presence of highly charged PCEs results in higher dosages required to achieve optimum fluidity of CAC pastes. Therefore, in CAC, it is important to focus not only on surface adsorption, but also on the route of intercalation of PCEs into hydrates.

These experiments suggest that when fluidizing such a calcium aluminate cement, the main criterion for the selection of the superplasticizer is the avoidance of intercalation, which is an effect arising from the balance between its charge density and side chain length.

6. Acknowledgement

Serina Ng gratefully acknowledges the scholarship provided by the Jürgen Manchot Stiftung, Düsseldorf/Germany.

7. References

- A. Ohta, T. Sugiyama, T. Uomoto, 2000. Study of dispersing effects of polycarboxylate-based dispersant on fine particles, in Sixth CANMET/ACI International Conference on Superplasticizers and Other Chemical Admixtures in Concrete, V.M. Malhotra Ed., Nice, France, ACI Publication SP-195, 283 – 297
- C. Bradbury, P. M. Callaway, D. D. Double, 1976. The Conversion of High Alumina Cement/Concrete, Mater. Sci. Eng., 23, 43–53
- H. Uchikawa, S. Hanehara, D. Sawaki, 1997. The Role of Steric Repulsive Force in the Dispersion of Cement Particles in Fresh Paste Prepared with Organic Admixture, Cem. Concr. Res. 27, 37–50
- J. Plank, Z. Dai, P. R. Andres, 2006. Preparation and Characterization of New Ca-Al-Polycarboxylate Layered Double Hydroxides, Mater. Lett. 60, 3614–7
- J. Plank, H. Keller, P. R. Andres, and Z. M. Dai, 2006. Novel Organo-Mineral Phases Obtained by Intercalation of Maleic Anhydride-Allyl Ether Copolymers Into Layered Calcium Aluminum Hydrates, Inorg. Chim. Acta, 359(15], 4901–8
- J. Plank, Z. M. Dai, H. Keller, F. Hössle, W. Seidl, 2010. Fundamental mechanisms for polycarboxylate intercalation into C_3A hydrate phases and the role of sulfate present in cement, Cem. Concr. Res 40, 45–57
- J. Plank, K. Pöllmann, N. Zouaoui, P.R. Andres, C. Schaefer, 2009. Synthesis and performance of methacrylic ester based polycarboxylate superplasticizers possessing hydroxy terminated poly(ethylene glycol) side chains, Cem. Concr. Res. 39, 1–5
- J. Plank, B. Sachsenhauser, 2009. Experimental determination of the effective anionic charge density of polycarboxylate superplasticizers in cement pore solution, Cem. Concr. Res. 39(1), 1-5
- J. Plank, B. Sachsenhauser, 2006. Impact of Molecular Structure on Zeta Potential and Adsorbed Conformation of a-Allyl-o-Methoxypolyethylene Glycol–Maleic Anhydride Superplasticizer, J. Adv. Concr. Technol. 4, 233–9
- K. Yoshioka, E. Tazawa, K. Kawai, T. Enohata, 2002. Adsorption Characteristics of Superplasticizers on Cement Component Minerals, Cem. Concr. Res. 32, 1507–13
- L. Raki, J. J. Beaudoin, L. Mitchell, 2004. Layered double hydroxide-like materials: nanocomposites for use in concrete, Cem. Concr. Res., 34, 1717-1724
- R. Rixom, N. Mailvaganam, Chemical Admixtures for Concrete, 3rd edition, E & FN Spon, London, UK (1999) 314–29
- S. Stöber, H. Pöllmann, 1999. Synthesis of a lamellar calcium aluminate hydrate (AFm phase) containing benzenesulfonic acid ions, Cem. Concr. Res. 29, 1841–1845
- V. Fernon, A. Vichot, N. Le Goanvic, P. Colombet, F. Corazza, U. Costa, 1997. Interaction Between Portland Cement Hydrates and Polynapthalene Sulfonates, Am Concr Inst, SP-173, 225–248
- V. S. Ramachandran, V. M. Malhorta, Superplasticizers, in Concrete Admixtures Handbook, Editor: V. S. Ramachandran, Noyes Publications, Park Ridge, NJ (1995) 410–517
- Y. Ohama, 1998. Polymer-based admixtures, Cem. Concr. Compos. 20, 189–212.

Paper 5

Occurrence of Intercalation of PCE Superplasticizers in Calcium Aluminate Cement under Actual Application Conditions, as evidenced by SAXS Analysis

S. Ng, E. Metwalli*, P. Müller-Buschbaum*, J. Plank

*Chair for Functional Materials, Department of Physics, Technische Universität München, James-Franck-Str. 1, 85747 Garching (Germany)

Cement and Concrete Research

(Submitted on 7th September 2012)

Occurrence of Intercalation of PCE Superplasticizers in Calcium Aluminate Cement under Actual Application Conditions, as evidenced by SAXS Analysis

Serina Ng[1], Ezzeldin Metwalli[2], Peter Müller-Buschbaum[2], Johann Plank[1*]

[1]Chair for Construction Chemicals, Department of Chemistry, Technische Universität München, Lichtenbergstr. 4, 85747 Garching (Germany)

[2]Chair for Functional Materials, Department of Physics, Technische Universität München, James-Franck-Str. 1, 85747 Garching (Germany)

*: Corresponding author
Tel.: +49 (0)89 289 13151
Fax.: +49 (0)89 289 13152
E-mail address: sekretariat@bauchemie.ch.tum.de (J. Plank).

Abstract

Intercalation of polycarboxylate (PCE) superplasticizers in calcium aluminate cement (CAC) during early hydration under both idealized and actual application conditions was confirmed by SAXS analysis. The CaAl-PCE-LDHs were characterized by XRD, TEM, SEM and elemental analysis, and exhibited interlayer distances (*d*-values) ranging from 5 – 24 nm, owed to the polydispersity of the PCE samples. Intercalating ability of the PCEs was dependent on their grafting density and anionicity, but was independent of their molecular weights. When highly anionic PCEs were utilized, significant amounts of nanocrystalline, colloidal intercalates were recovered, while few intercalates were detected when less anionic PCEs possessing high graft density were employed. Thus, contrary to OPC, less anionic PCEs disperse CAC better as little amount is wasted via intercalation, whereas higher dosages are required for more anionic PCEs, owed to abundant formation of organo-mineral phases. Finally, recommendations for reliable analysis of PCE intercalates in cement are given.

Key words: Small-Angle X-Ray Scattering (B), X-Ray Diffraction (B), Calcium Aluminate Cement (D), Polymer (D), Organo-Mineral Phases

1. Introduction

Organic admixtures possessing negative charges are widely used in modern concrete technology for improving workability, compressive strength and durability [1]. Among the superplasticizers commonly used in concrete are polycondensates (e.g. β-naphthalene sulfonate formaldehyde or melamine formaldehyde sulfite condensate) and polycarboxylates (PCEs; e.g. methacrylic acid – *ω*-methoxy poly(ethylene glycol) methacrylate ester

copolymers) [2, 3]. They strongly interact with cement through an adsorptive mechanism and develop dispersion either by electrostatic repulsion and/or a steric effect between cement particles [4, 5]. Performance of these superplasticizers in ordinary Portland cement (OPC) has been thoroughly investigated and their advantages are widely accepted. There, PCEs are highly effective dispersants and their dispersing power is proportional to their anionicity [6]. In applications utilizing calcium aluminate cement (CAC), however, surprisingly the performance of PCEs molecules which perform exceptionally well in OPC has been shown to be inferior [7]. Only few studies on the interaction of CAC with PCEs have been published [8].

During the hydration of CAC at room temperature, metastable C_2AH_8 and AH_3 are formed. The first hydrate converts to katoite (C_3AH_6) with time (**Scheme 1**) [9]. Formation of C_2AH_8 is thermodynamically favored by increasing temperature of hydration [10]. Similar to C_4AH_{13} and C_4AH_{19} which are formed during the hydration of the OPC clinker phase, C_3A, it possesses a layered structure. These hydrates which are also denoted as AF_m phases belong to the general group of layered double hydroxides, and more specifically, to the family of hydrocalumites. They are made up of cationic $[Ca_2Al(OH)_6]^+$ layers which are stabilized via electrostatic attraction of negatively charged anions such as e.g. OH^- present in the interlayer region (**Fig. 1**).

$$2\ CA + 11\ H \longrightarrow 2\ C_2AH_8 + AH_3$$
$$3\ C_2AH_8 \longrightarrow 2\ C_3AH_6 + AH_3 + 6\ H$$

Scheme 1. Hydration of calcium monoaluminate (the main clinker phase present in CAC) at room temperature

Fig. 1. Schematic illustration of the layer structure present in C_2AH_8, a hydrocalumite mineral

Due to the cationic charge of the main layer present in hydrocalumites, chemisorption of anionic molecules from solution is possible. Fernon *et al.* were the first to demonstrate experimentally that an anionic superplasticizer (here: BNS) can intercalate into calcium aluminate hydrates to form layered organo-mineral phases (OMP) of the general composition $[Ca_2Al(OH)_6](A)_x \cdot (OH)_y \cdot nH_2O$ [11]. Later, formation of such intercalates has been analytically proven in model systems such as hydrating C_3A [12–14]. Following this, we have shown that hydrating C_3A in the presence of PCEs can lead to the formation of organo-mineral phases of Ca-Al-PCE-LDH type [15, 16]. This sequestration of PCE into the AF_m crystallites depletes the dispersant from the pore solution and can reduce its effectiveness. Very recently, another research group has proposed a model describing the steric arrangement of intercalated PCE [17].

In a previous investigation, we have found that under the idealized condition of high PCE dosages (40 % by weight of cement, bwoc) and high water-to-cement ratio (w/c = 15), PCEs may be consumed by CAC in the same manner as by C_3A in OPC [18]. In CAC, it was observed that PCE superplasticizers behave entirely different than with OPC. The most striking observation was that the PCE dosages required to disperse CAC is an order of magnitude lower than for OPC. The second observation was a remarkable difference in the affinity of the PCEs for the two cements, depending on their anionic charge amounts. For effective dispersion of CAC, less anionic PCEs were found to be most effective while highly

anionic copolymers required substantially higher dosages. This behaviour is opposite to that in OPC (**Fig. 2**). The difference in performance of PCEs in CAC as compared to that in OPC was accounted for by chemisorption (plausibly intercalation) of the more anionic PCEs into the calcium aluminate hydrates. However, using XRD analysis, occurrence of chemisorption could only be shown under those idealized conditions, while under actual application conditions (PCE dosage < 0.1 % bwoc, w/c ~ 0.5), no organo-mineral phases could be detected. Also, due to the limitations of conventional powder X-ray diffraction analysis at very small angles, potential nano-sized intercalates possessing large *d*-spacings are not always reliably detectable. Therefore, small-angle X-ray scattering (SAXS) appears to be more suitable to clarify the intercalating behaviour of PCE in CAC pastes.

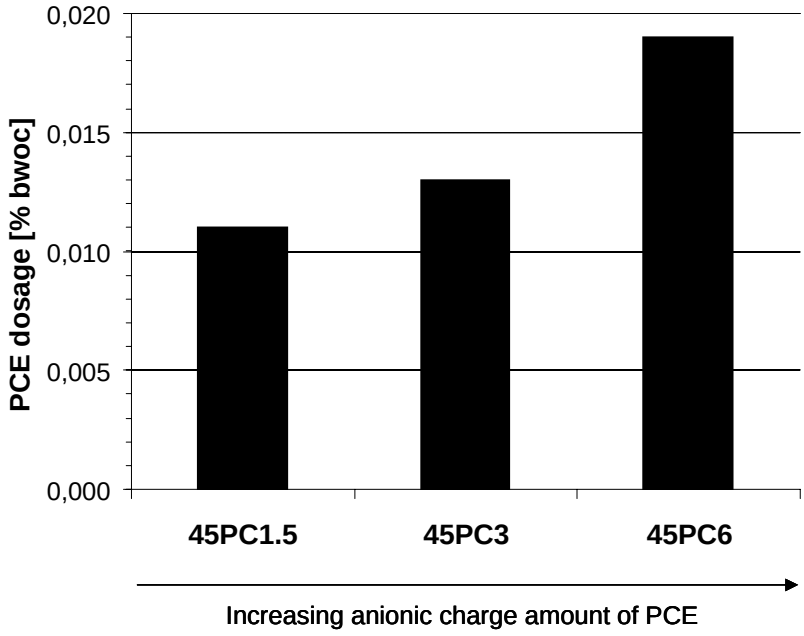

Fig. 2. PCE dosages required to achieve a CAC paste spread of 26 ± 0.5 cm at a w/c ratio of 0.52 [from 18]

The aim of the current investigation was to confirm the intercalating ability of selected PCEs molecules in CAC by SAXS analysis, first under idealized conditions, and followed by

realistic application conditions. For this investigation, a commercial white CAC was selected and hydrated for 2 h in the presence of those PCEs. Initial studies under idealized condition (PCE dosage 40 % bwoc, w/c = 15) will involve seven different PCEs with varying grafting densities and anionic charge amounts. Potential formation of PCE intercalates was probed via SAXS analysis. Thereafter, the PCE polymer possessing the highest intercalating ability was selected for further investigations using real application conditions (PCE dosage = 0.05 % bwoc, w/c = 0.52). All hydration products were characterised using XRD, SAXS, elemental analysis, TEM and SEM imaging. Based on our experience, a comment on the analytical detection methods suitable to identify PCE intercalates in cement and their shortfalls will be given. Finally, the relation between the formation of organo-mineral phases and the dispersing ability of PCEs in CAC will be discussed.

2. Materials and Experimental Procedures

2.1. Calcium aluminate cement (CAC)

A white CAC containing ~ 70 % Al_2O_3 (Ternal White® from Kerneos®, Neuilly Sur Seine Cedex/France) was used in this study. Its phase composition as obtained by quantitative XRD analysis (Bruker D8 advance instrument, software Topas 4.0) and oxide composition (X-ray fluorescence (XRF, SRS 303 Siemens, Karlsruhe/Germany) are presented in **Table 1**. The average particle size (d_{50} value, determined by laser granulometry using a CILAS 1064 instrument, Cilas, Marseille/France) was 7.76 µm. Its *Blaine* fineness was found at 3,800 cm²/g (Toni Technik, Berlin/Germany) and its density was 2.89 g/cm^2, measured by ultrapycnometry (Helium pycnometer, Quantachrome, Odelzhausen/Germany).

Table 1. Phase and oxide composition of the commercial white CAC sample

Phase [wt. %]	CA 65.8		CA_2 33.4		$C_{12}A_7$ 0.8	
Oxide [wt. %]	CaO 27.1	Al_2O_3 71.6	Na_2O 0.3	SiO_2 0.2	MgO 0.4	FeO 0.1

2.2. Polycarboxylate (PCE) samples

Seven PCE superplasticizers were synthesized according to a literature description by aqueous free radical copolymerization of methacrylic acid (MA) and methoxy terminated poly(ethylene oxide) methacrylate (MPEG-MA) ester at molar ratios of 1.5, 3 and 6 respectively [19]. Methallyl sulfonic acid (MAS) was used as chain transfer agent. From the PCE composed as 45PC6, four different versions exhibiting increasing molecular weights (M_w ranging from 19,700 to 184,000 Da) were synthesized, utilizing different amounts of the chain transfer agent (amounts of MAS: 45PC6a 0.4 g; 45PC6b 1.0 g; 45PC6c 1.5 g; and 45PC6d 3.0 g). The seven copolymers have side chains made up of 45 ethylene oxide units (EOUs). They are named as 45PCx, whereby 45 refers to the number of EOUs in the side chain, and x refers to the molar ratio of MAA:MPEG-MA. These copolymer compositions were selected because they represent the type of PCEs commonly used in precast (45PC6) and in ready-mix concrete (45PC1.5). The chemical formula of the PCEs is presented in **Fig. 3**. All seven superplasticizers were neutralized with aqueous NaOH and dialyzed against a membrane with a M_w cutoff of 8k Da (Spectra® Laboratories, Kehl, Rhein/Germany) before subsequent usage.

For polymer characterization, size exclusion chromatography (Waters Alliance 2695 from Waters, Eschborn/Germany) equipped with RI detector 2414 (Waters, Eschborn/Germany) and a 3 angle dynamic light scattering detector (mini Dawn from Wyatt Technologies, Santa Barbara, CA/USA) was used. Prior to application on the columns, the polymer solutions were

filtered through a 0.2 µm filter. The polymers were separated on an Ultrahydrogel™ precolumn and three Ultrahydrogel™ (120, 250 and 500) columns (Waters, Eschborn/Germany) using 0.1 M aqueous $NaNO_3$ solution (adjusted to pH 12.0 with NaOH) as an eluant at a flow rate of 1.0 mL/min. From this separation, the molar masses (M_w and M_n), the polydispersity index (PDI) and the hydrodynamic radius ($R_{h(z)}$) of the polymers were determined. The value of dn/dc used to calculate M_w and M_n for all polymers was 0.135 mL/g (value for polyethylene oxide) [20].

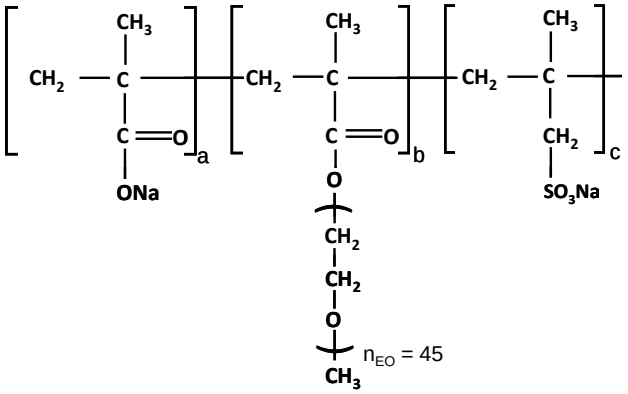

PCE sample 45PC1.5 : a:b:c = 1.5 : 1 : 0.02
PCE sample 45PC3 : a:b:c = 3 : 1 : 0.02
PCE sample 45PC6 : a:b:c = 6 : 1 : 0.02

Fig. 3. Chemical structure of the MPEG–type PCE samples employed in the study

Specific anionic charge amounts of the PCEs were determined in cement pore solution collected from pastes prepared at a w/c ratio of 0.52 to exemplify real CAC conditions, where high concentrations of both calcium and aluminate ions are present. The filtrates were gained by vacuum filtration using a diaphragm vacuum pump (Vaccubrand company, Wertheim/Germany) and filter paper (Schleicher & Schuell, Grade: 589/3, classification 2d according to DIN 53 135) at a suction capacity of 1.7 m^3/hr. Specific anionic charge amounts of the polymers were analyzed by a particle charge detector (PCD 03 pH from Mütek Analytic Company, Herrsching/Germany). Solutions containing 0.02 wt. % of anionic polymer dissolved in both DI water and cement pore solution (w/c = 0.52) were prepared and titrated against a 0.001N solution of cationic polydiallyl dimethyl ammonium chloride

(polyDADMAC) until charge neutralization was attained. The amount of negative charge per gram of polymer was calculated from the consumption of the cationic polyelectrolyte.

2.3. Synthesis of OMP under idealized conditions

Synthesis of organo-mineral phases (OMP) under ideal conditions was carried out following the method reported previously [18] to ensure high crystallinity of the CaAl-PCE-LDHs formed. In a 250 mL 1 necked round-bottom flask equipped with a magnetic stirrer, 45 mL of a 2.5 wt. % PCE solution were placed to which 3 g of CAC were added, marking the start of the reaction. Hydration was allowed to proceed for 2 hours at room temperature before centrifugation at 8,500 rpm for 20 minutes was performed to separate the solid and liquid (colloidal) phases. With the solid phase, acetone quenching followed by further centrifugation at 8,500 rpm for 15 minutes was conducted. The resulting solid was dried in an oven at 40 °C for 24 hours. The liquid phase (supernatant) was pre-dried by rotary evaporation and post-dried by freeze drying. As will be shown later, this supernatant contains most of the PCE intercalates as nano-sized, colloidal particles. It has a slightly turbid appearance and exhibits the Tyndall effect which is characteristic for ultrafine colloidal suspensions. XRD and SAXS analyses of the samples were performed immediately after synthesis. For elemental analysis, further washing was done thrice with alkaline solution at pH 11.6 (w/NaOH) to remove excess polymer present. Under these idealized conditions, the PCE dosage was 40 % bwoc.

2.4. OMP formation under real application conditions

For synthesis under real application conditions, 0.05 % bwoc of the PCE polymer 45PC6a were added to cement and pastes prepared following the general protocol established as so–called ‘mini slump’ test (according to DIN EN 1015) at a w/c ratio of 0.52. Here, the slurry

was stirred for 1 minute, allowed to stand for another 1 min, followed by manual stirring for a further 2 minutes. The cement slurry was then centrifuged at 8,500 rpm for 20 minutes to separate the supernatant which contains colloidal OMPs from the solid precipitate. The solid phase was quenched with acetone, centrifuged at 8,500 rpm for 15 minutes and dried in oven at 40°C overnight. The liquid phase (supernatant) was pre-dried by rotary evaporation, post-dried by freeze drying, and analysed as per obtained.

2.5. Structural investigation of OMP

All dried products were first analysed using a conventional powder XRD instrument (Bruker D8 advance, Bruker, Karlsruhe/ Germany) possessing a scintillator with a scanning range of 0.6 to 40 °2θ; step size of 0.15 sec/step; spin revolution time of 4 sec; aperture slit of 0.1°. For long scan analysis, the scan parameters were 0.6 to 40 °2θ; step size of 15 sec/step; spin revolution time of 4 sec; aperture slit of 0.1 °. Chemical analysis was conducted following the CHNS method on an Elementar vario EL apparatus (Elementar Analysensysteme GmbH, Hanau/Germany). TEM and SEM (with EDX) images were captured with a JEOL JEM-2100 instrument (JEOL Company, Tachikawa/Japan) and a XL30 ESEM FEG instrument (FEI Company, Eindhoven/NL) respectively.

Small-angle X-ray diffraction measurements (SAXS) were performed on a Ganesha 300XL SAXS-WAXS system (SAXSLAB ApS, Copenhagen/Denmark) equipped with a GENIX 3D microfocus X-ray source and optic, a three-slit collimation system, a fully evacuated sample chamber and beam path, and a movable 2D Pilatus 300K detector. The X-ray source was operated at 50 kV/0.6 mA with Cu anode (K_α, γ = 0.1542 nm). Angular calibration in the small-angle region was obtained using silver behenate as reference. Sample-to-detector distance was 1056 mm.

For SAXS measurements, the sample powders were filled into thin-walled capillary glass tubes (diameter 2 mm). The tubes were flame-sealed and placed vertically in a metal holder. Samples were investigated in the glass capillary at room temperature (25 °C) for 5 h. All SAXS data were presented as logarithmic scattering intensity vs. the magnitude of the scattering vector. The reflection peaks were fitted to a Lorentzian function. The *d*-spacing of the samples was determined by the Bragg equation, $d = 2л/q$, where q is the scattering vector.

3. Results and discussion

3.1. Molecular properties of PCE samples

The molecular characteristics and anionic charge amounts of the polymers are shown in **Table 2**. 45PC1.5, 45PC3 and 45PC6 vary according to their grafting densities. In the series of 45PC6 a–d, the polymers differ according to their molecular weights (M_w) which range from 19,700 – 184,000 Da. In DI water, the anionic charge amounts of the seven PCE polymers increase by the order as follows: 45PC1.5 < 45PC3 < 45PC6; all 45PC6 a–d polymers possess similar anionic charge amounts. Opposite to this, in cement pore solution all seven PCE polymers exhibit very low and almost comparable anionic charge densities (111 – 156 μeq/g), independent of their molar compositions. This suggests that in the highly calcium loaded pore solution, the carboxylate functionalities contained in PCE are mostly chelated by Ca^{2+} ions.

Table 2. Molecular properties and anionic charge amounts of the PCEs measured in DI water and cement pore solution

Property	45PC1.5	45PC3	45PC6	45PC6.a	45PC6b	45PC6c	45PC6d
Molar mass M_n [g/mol]	60,500	50,120	43,680	79,900	16,800	15,100	9,800
Molar mass M_w [g/mol]	170,600	156,700	156,400	184,400	45,700	35,100	19,700
Polydispersity index (PDI)	2.8	3.2	3.6	2.3	2.7	2.3	2.0
MAA : MPEG-MAA molar ratio	1.5 : 1	3 : 1	6 : 1	6 : 1	6 : 1	6 : 1	6 : 1
Hydrodynamic radius [nm]	9.5	9.5	9.9	10.1	4.3	4.1	3.3
Specific anionic charge	290[a]	760[a]	1530[a]	1850[a]	1790[a]	1930[a]	1700[a]
amount [µeq/g]	111[b]	125[b]	148[b]	154[b]	153[b]	156[b]	151[b]

[a]Measured in DI water
[b]Measured in cement pore solution obtained at a w/c ratio of 0.52

3.2. Intercalation under idealized condition

Previously, we have shown that intercalation of PCE into CAC hydrates may have occurred as revealed by both XRD and elemental analyses [18]. There, the experiments were performed under a huge excess of PCE polymer (PCE dosage 40 % bwoc) and at a high w/c ratio of 15 to ensure unambiguous analytical detectability of the OMPs formed. Under those conditions, the supernatant obtained after centrifugation of the CAC/PCE paste contained colloidal, nano-sized particles which were identified by powder XRD analysis as C_2AH_x and – for PCE polymers 45PC3 and 45PC6 – potentially as PCE intercalates, CaAl-PCE-LDHs (**Fig. 4**). However, the absence of the harmonic series of (00*l*) reflections which is characteristic for such layered compound [21] gave doubts as to whether the single reflection observed at low 2θ angles indeed can be attributed to a layered PCE intercalate, or whether it indicated a mere encapsulation of the PCE polymer by the colloidal inorganic CaAl-OH-LDH platelets. In such

case, the reflection (*d*-value) would simply indicate the size of the pore occupied by PCE polymer.

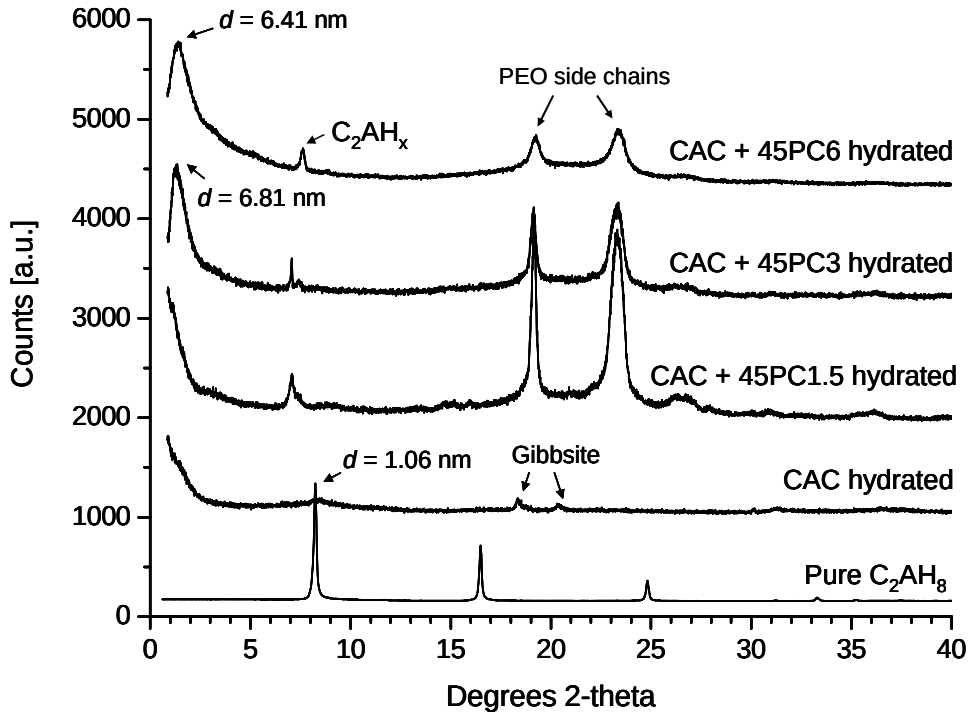

Fig. 4. X-ray diffraction patterns of (bottom to top): C_2AH_8, the main hydrate during hydration of CAC at RT (relative intensity reduced by a factor of 16); hydrated CAC sample; CAC hydrated in the presence of 45PC1.5; 45PC3 and 45PC6 [18]

Owed to these considerations, further confirmation of the successful intercalation was sought by utilizing small angle X-ray scattering (SAXS). In particular, it was attempted to exclude that the reflections observed by XRD were artefacts. SAXS has a high sensitivity at very low 2θ values, thus it is an ideal method in analysing intercalate samples possessing high *d*-spacings (or low 2θ values). For this analysis, PCE polymer 45PC6 was selected due to its highest intercalating ability (see **Fig. 4**).

The results from the SAXS analysis of the CAC sample hydrated in presence of 45PC6 are displayed in **Fig. 5**. The weak and broad peak shown in the SAXS profile indicates the

presence of an interlayer periodic distance. Because of the high *d*-spacing spanning from ~ 24 to 5 nm, with an average value of ~ 8.6 nm, this signal can only be attributed to an organo-mineral phase formed from PCE and CAC. Note that the *d*-values observed for CaAl-LDHs incorporating typical inorganic anions occurring in cement, such as e.g. OH^-, Cl^-, NO_3^-, SO_4^{2-} or CO_3^{2-} all lie below 1.2 nm [9]. The result obtained from SAXS analysis clearly suggests that SAXS is much preferable over conventional powder XRD, because it provides more detailed information on the intercalates formed.

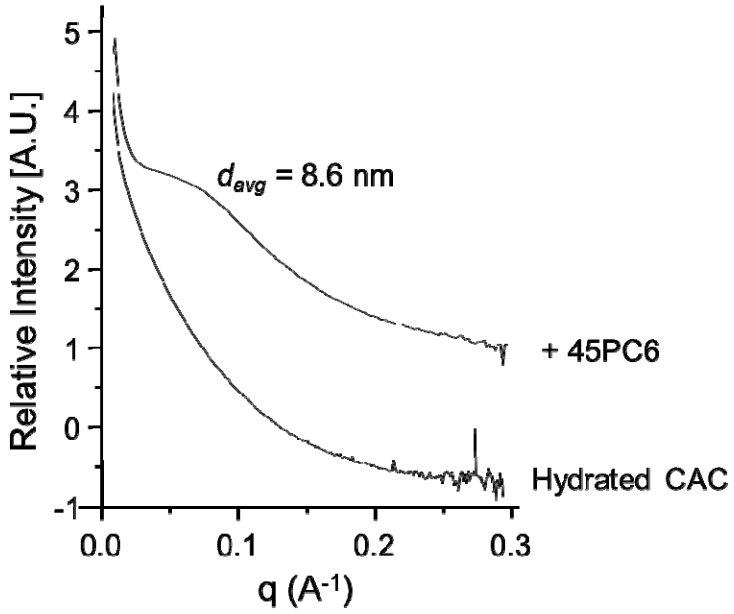

Fig. 5. SAXS profiles of CAC sample hydrated with and without 40 % bwoc of PCE polymer 45PC6 at a w/c ratio of 15, reacted for 2 h at room temperature.

The broad range of *d*-values can be attributed to the broad distribution of the intercalation distances within the sample, possibly due to the flexible chain which allows different modes of steric arrangement of the copolymer in the interlayer, and because of the high polydispersity index of 3.6 for 45PC6 polymer. As a result, a low and irregular stacking order of the layered double hydroxides can be expected. Alternatively, the broadness and low intensity of the reflections may also indicate a different form of chemisorption of PCEs by

hydrating cement. Choy *et al.* had previously shown that for DNA, layered double hydroxides can stack onto these helical structures and merely encapsulate them, with one broad reflection visible in their XRD spectrum which represents the sizes of the pores occupied by DNA, and not the interlayer distance [22]. The size of these nanocapsules was found to be dependent on the actual size of the available DNA strands. Likewise, here the inorganic C_2AH_8 platelets may stack onto or enclose PCE polymer 45PC6 which, coupled with the high PDI, can result in a wide variation of the range of *d*-spacings as observed. The average *d*-spacing obtained will then be dependent on the average size of the individual copolymer. Generally, the steric size (hydrodynamic radius in solution) of a PCE molecule is dependent on its overall chemical composition and its molecular weight (**Table 2**). Therefore, to affirm that the chemisorption of PCEs had indeed occurred via intercalation and not encapsulation, further experiments involving four different, specifically synthesized PCE polymers (45PC6 a–d) with molecular weights ranging from 19,700 to 184,000 Da (M_w) and thus different hydrodynamic radii (steric sizes) were performed. The rationale behind this experiment was that if here the PCEs were only encapsulated, then the pore size as indicated by the *d*-value would increase with the molecular weight of the PCE polymers. While in the case of intercalation, the *d*-values would remain constant and independent of M_w of the copolymers.

The PCE polymers labelled as 45PC6a, 45PC6b, 45PC6c and 45PC6d possess descending molecular weights (M_w = 184,400; 45,700; 35,100 and 19,700 g/mol respectively; see **Table 2**). All four polymers exhibit relatively low PDIs (2.0 to 2.3). In the experiment, CAC was hydrated in the presence of these copolymers using the same conditions of high PCE dosages of 40 % bwoc and at a w/c ratio of 15. **Fig. 6** displays the SAXS data for the samples containing these four copolymers.

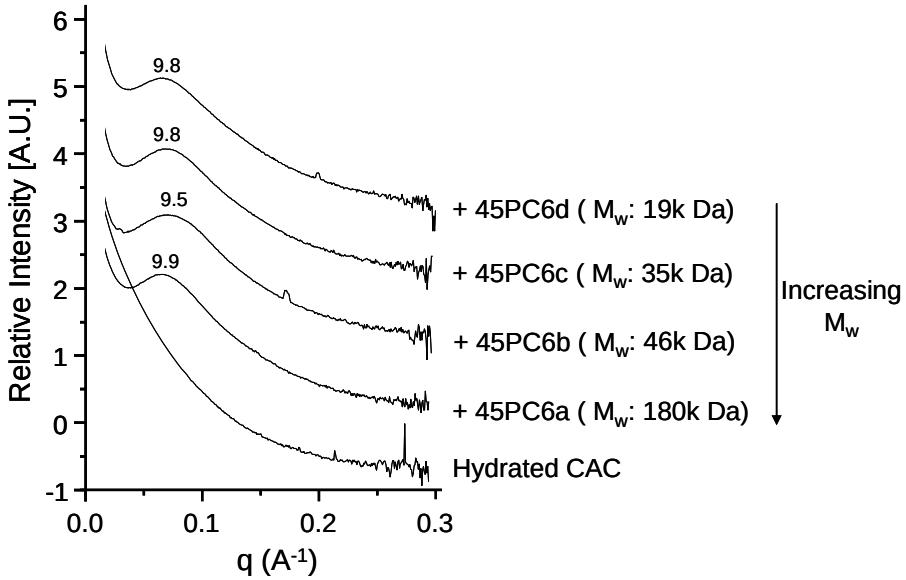

Fig. 6. SAXS profiles of CAC sample hydrated in the presence and absence of PCE polymers 45PC6 a–d possessing different molecular weights, reacted for 2 h at room temperature (w/c ratio of 15, PCE dosages: 40 % bwoc)

All samples showed even more defined reflections than the sample containing previous 45PC6 polymer. This effect was attributed to the lower PDIs of the 45PC6 a–d polymers, compared to 45PC6 (see **Table 2**) Also, all samples exhibited almost the same average layer distances (*d*-values of 9.5 – 9.9 nm). The consistency of the *d*-spacings and the narrow reflections of these polymers which were independent of the steric sizes or the molecular weights confirmed that indeed chemisorption of the PCEs had occurred. Therefore, consumption of such PCEs by calcium aluminate cement was clearly confirmed to be intercalation rather than encapsulation.

3.3. Intercalation under actual application conditions

With the knowledge from idealized conditions, the occurrence of intercalation under conditions of actual use of PCE polymers in CAC was next investigated. The aim was to

confirm whether such organo-mineral phases of CaAl–PCE–LDH type actually form in practical CAC systems holding PCE at dosages which are typically applied. These experiments were started by testing the PCE dosage required for a CAC paste with high fluidity. A 'mini slump' test was utilized to measure the spread value of the CAC paste (w/c ratio 0.52). PCE polymer 45PC6a was selected as the choice PCE due to its high molecular weight (similar to that of 45PC6), but lower and thus better PDI (2.3). To achieve the desired cement paste spread of 26 ± 0.5 cm which represents a highly fluid CAC paste, a dosage of 0.05 % bwoc of 45PC6a was determined.

At first, it was observed that the amount of colloidal nano-sized particles contained in the supernatant was significantly less compared to the idealized conditions. In fact, after drying of ~ 100 mL of the clear supernatant, only ~ 2.4 g of a white residue was obtained (cement = 300 g, PCE dosage = 0.05 % bwoc), as compared to ~ 14.9 g in the idealized test (cement = 10 g, PCE dosage = 40 % bwoc). This already hinted that here, formation of PCE intercalates – if any – was much reduced.

The results from the SAXS analysis of the colloids contained in the supernatant are shown in **Fig. 7**. From the 2D image of the CAC sample hydrated with added 45PC6a (**Fig. 7**, left), a diffuse ring of electron density extending up to ~ 0.8 $Å^{-1}$ is depicted. This corresponds to the shoulder shown in the SAXS profile which is an integration of the 2D image shown. This shoulder represents the (00*l*) lattice order of the layered structure present in the sample. The broad reflection signal indicates that a broad range of layer distances is present in the nano-sized organo-mineral phases, as has been observed before for PCE polymers intercalated under idealized conditions. On the average, the intercalates display an average *d*-spacing of 10.5 nm. Due to the short reaction time of 4 min, these organo-minerals phases possess very low crystallinity, also possibly due to the low stacking order of the intercalates which might

be owed to different orientations of the copolymers between the inorganic $[Ca_2Al(OH)_6]^+$ layers. The presence of a second, but highly diffuse ring of electron density in the 2D image confirms this turbostratic disorderness of the intercalates and also explains the absence of a (00*2*) lattice order in the SAXS profile. Thus, the formation of intercalates under real application conditions was clearly confirmed by SAXS analysis.

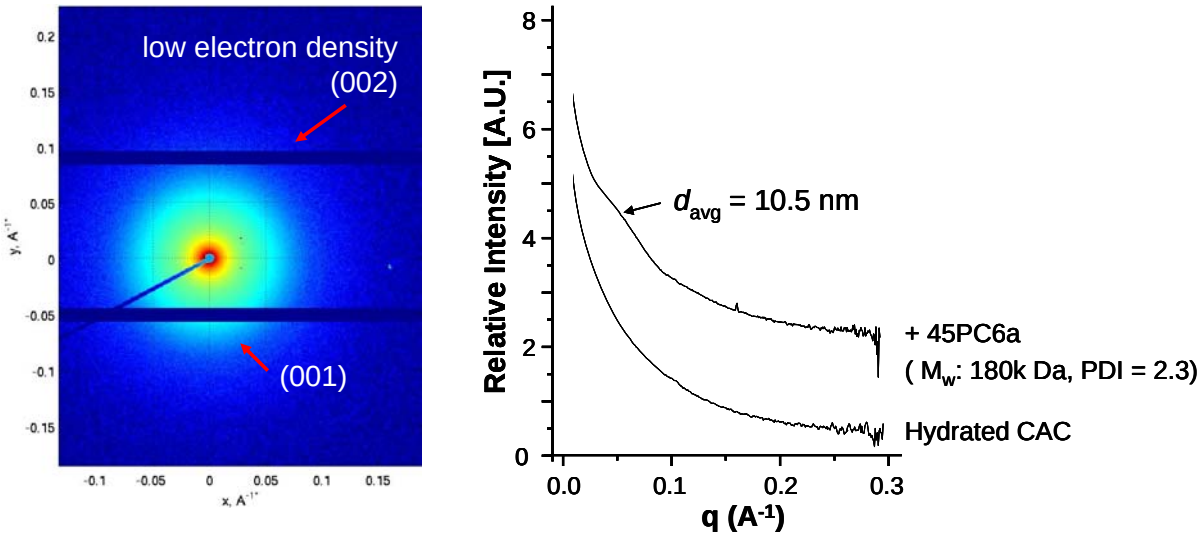

Fig. 7. SAXS (left) 2D image and (right) profiles of the CAC sample hydrated in the presence of 0.05 % bwoc of polymer 45PC6 at a w/c ratio of 0.52, reacted for 4 min at room temperature. SAXS profile of hydrated CAC sample is added as a reference.

For quantification of the amount of PCE intercalated, carbon analysis was conducted. Here, a mere 3.6 wt. % of organic material was detected for the hydration products of CAC formed in presence of 45PC6a. The low organic content can be attributed to the high amount of inorganic C_2AH_8 and C_3AH_6 present in the sample, and the low initial dosage of PCE added (0.05 % bwoc). However, this organic amount accounts for ~ 65 % of total amount of PCE added. These results signify that a high portion of the PCE added was consumed by the formation of organo-mineral phases.

For visual confirmation, analyses were carried out utilizing TEM and SEM imaging. In hydrated CAC samples (no PCE polymer present), only layered structures with a *d*-spacing of ~ 1 nm were detected, representing the inorganic layered structures of C_2AH_8. In contrast, a low amount of organo-mineral phases, similar to that observed for intercalates formed under idealized conditions, were detected when the samples from CAC hydration in presence of 45PC6 were analyzed (**Fig. 8**). Additionally, under SEM imaging, nanofoils possessing a high carbon content of ~ 30 % (as evidenced by EDX analysis) were found. Thus, the presence of intercalates was confirmed by the detection of these layered organic-inorganic hybrid structures.

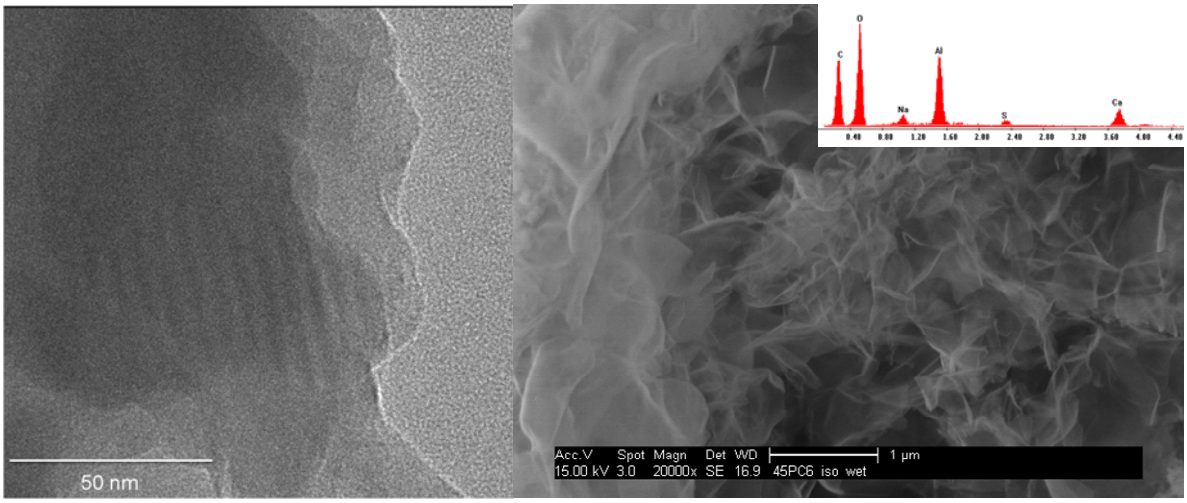

Fig. 8. TEM (left) and SEM (right) images of organo-mineral phases obtained from CAC in the presence of PCE polymer 45PC6 (w/c ratio of 0.52), showing layered structure (left) and morphology of intergrown nanofoils (right); EDX analysis (top right) shows high carbon content.

3.4. Comment on analysis of PCE intercalates

Based on our experience, proper identification of PCE intercalates in aqueous cement, C_3A or CA suspensions presents a major challenge.

At first, it is to be considered that PCE-LDHs typically are formed as very fine colloidal, nano-sized particles which concentrate in the supernatant of the centrifugate from the reaction. The typical appearance of PCE intercalates under SEM imaging is that of flower-like arranged nanofoils, with lengths of up to several μm and thicknesses of only ~ 50 nm (see **Fig. 8**). This specific morphology already implies that it will be difficult to obtain unambiguous XRD spectra. Therefore, non-occurrence of an XRD signal characteristic for PCE-LDHs does not necessarily exclude their presence.

In powder XRD analysis, we found it highly advantageous to monitor the diagram at very long scan durations. As an example, the XRD pattern of CAC hydrated in the presence of PCE polymer 45PC6a, recorded with short and long scan times are presented in **Fig. 9**.

There, the resolution of the diffractogram was greatly improved by increasing the scan time from 0.15 to 15 sec/step. While at short scan time, no indication of a PCE intercalate was obtained, a distinct reflection representing a layered organo-mineral phase with a *d*-spacing of ~ 10.2 nm was detected when applying a long scan (**Fig. 9**). This value is in line with the *d*-spacing observed from SAXS analysis before (10.5 nm, **Fig. 7**). Here, by altering only one scanning parameter, the increase in resolution made it possible to detect the formation of the organo-mineral phase, thus confirming the importance of selecting the most optimal parameters for XRD analysis. Also, the differences in the XRD spectra between idealized and real application conditions (**Fig. 4** and **9**) indicate that the intercalates formed here were

highly XRD amorphous, or very nano-sized foils. Therefore, a prolonged scan time is highly recommendable for detecting such intercalates.

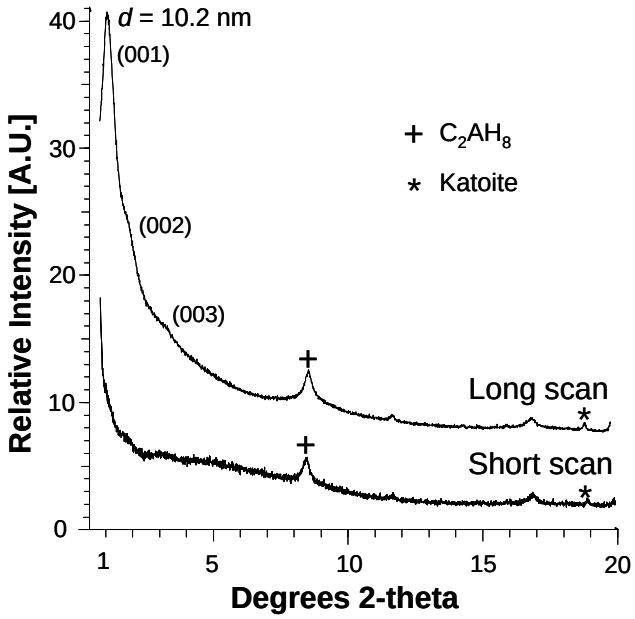

Fig. 9. XRD diffractograms of CAC sample hydrated in presence of 0.05 % bwoc of 45PC6a at a w/c ratio of 0.52, reacted for 4 min under two scanning conditions (short scan: scan time 0.15 sec/ step; long scan: scan time 15 sec/ step; Intensity of long scan reduced by a factor of 100)

Another obstacle in XRD analysis of PCE intercalates is the inhomogeneity of the polymers, especially in industrial products which most often constitute of blends of different copolymers. Here, with 45PC6a, a copolymer with particularly low PDI, OMPs of relatively little stacking disorders were formed, and therefore more clear signals were attained. Industrially made PCE polymers often possess PDIs of 3 – 6. The resulting intercalates will exhibit such a broad range of *d*-values that instead of a sharp signal, a very broad and unspecific hump will occur, if any can be found at all.

The results suggest that under carefully selected instrument conditions, XRD analysis can possibly detect the nano-sized PCE intercalates. A more reliable and accurate method, however, is SAXS analysis.

3.5. Intercalation and dispersing effectiveness of PCEs in CAC

As was shown in the 'mini slump' test, the trend in the amount of PCE copolymers required for effective dispersion was unlike that in OPC. In OPC, ettringite and monosulphate are rapidly formed during early hydration when sufficient concentrations of dissolved sulfate ions are present. The stability of these AF_t and AF_m phases make intercalation of PCE highly unfavourable, thus leaving PCEs for the dispersion effect which involves surface adsorption. Opposite to that, in a CAC system, no sulfate which can perturb intercalation is present, and rapid formation of the layered aluminate phase C_2AH_8 during early hydration promotes consumption of these PCEs. The more anionic the polymer is, the higher the consumption rate. As a result, a higher dosage of the more anionic 45PC6 to account for consumption via intercalation was required in achieving the same flow spread as when the less anionic 45PC1.5 was employed, which is hardly consumed via this chemisorption. Thus, the tendency of PCEs to intercalate in CAC explains the opposite behaviour of PCEs in CAC versus OPC whereby in CAC, the less anionic PCEs are the more powerful dispersants.

4. Conclusion

Here, we show that in actual calcium aluminate cement systems, PCEs can indeed intercalate into the hydrates of this cement during its hydration. In CAC, formation of such organo-mineral phases from CAC and PCE is not perturbed by sulfate anions, as is occurring in OPC.

The intercalation phenomenon leads to higher dosages of strongly anionic PCEs which are more prone to chemisorption to achieve optimum fluidity of CAC pastes. Therefore, in CAC, the less anionic PCEs possessing high grafting density are more effective superplasticizers.

These experiments suggest that when fluidizing such a calcium aluminate cement, the main criterion for the selection of the superplasticizer is the avoidance of intercalation, which is an effect arising from the balance between its charge density and side chain length.

Another conclusion from this study is that conventional XRD analysis cannot always clearly detect PCE–containing organo-mineral phases, because of their nanocrystallinity and their stacking disorder as a result of broad molecular weight distribution in the copolymers. SAXS appears to be the method of choice to reliably identify PCE intercalates, and to determine the range of interlayer distances present in the different OMPs. Applying this method to an OPC based system incorporating PCEs to detect potential intercalates there represents a challenge for future research.

Lastly, this study demonstrates that chemisorption (intercalation) of superplasticizers such as PCE indeed occurs in practical application systems, and that this phenomenon can have a significant impact on the performance of these superplasticizers.

Acknowledgement

Serina Ng gratefully expresses her gratitude to Jürgen Manchot Stiftung, Düsseldorf/Germany for the generous scholarship provided. Also, the authors would like to thank Dr. Marianne Hanzlik for taking the TEM images.

References

[1] R. Rixom, N. Mailvaganam, Chemical Admixtures for Concrete, 3rd edition, E & FN Spon, London, UK (1999) 314–329.

[2] V. S. Ramachandran, V. M. Malhotra, Superplasticizers, In: Concrete Admixtures Handbook, Editor: V. S. Ramachandran, Noyes Publications, Park Ridge, NJ (1995) 410–517.

[3] M. Kinoshita, T. Suzuki, K. Soeda, T. Nawa, Properties of Methacrylic Water-Soluble Polymer as a Superplasticizer for Ultra High-Strength Concrete, Malhotra V. M. Ed. 5th CANMET/ ACI International Conference on Superplasticizers and Other Chemical Admixtures in Concrete, ACI, Rome/Italy, SP–173 (1997) 143–162.

[4] H. Uchikawa, S. Hanehara, D. Sawaki, The Role of Steric Repulsive Force in the Dispersion of Cement Particles in Fresh Paste Prepared with Organic Admixture, Cem. Concr. Res. 27 (1997) 37–50.

[5] K. Yoshioka, E. Tazawa, K. Kawai, T. Enohata, Adsorption Characteristics of Superplasticizers on Cement Component Minerals, Cem. Concr. Res. 32 (2002) 1507–1513.

[6] A. Ohta, T. Sugiyama, Y. Tanaka, Fluidizing Mechanism and Application of Polycarboxylate-based Superplasticizers, Malhotra V. M. Ed. 5th CANMET/ ACI International Conference on Superplasticizers and Other Chemical Admixtures in Concrete, ACI, Rome/Italy, SP–173 (1997) 359–378.

[7] M. M. Alonso, T. Váquez, F. Puertas, M. Palacios, Compatibility between PCE Admixtures and Calcium Aluminate Cement, Proceedings of the 13th ICCC International Congress on the Chemistry of Cement, Abstract book, Madrid, Spain (2011) 382; full paper: ISBN: CD 978-84-7292-400-0 (7 pages).

[8] F. Massazza, U. Costa, A. Barrila, Interaction between Superplasticizers and Calcium Aluminate Hydrates, J. Am. Ceram. Soc. 65 (2006) 203–207.

[9] H. F. W. Taylor, Cement Chemistry, 3rd Ed., Thomas Telford Publishing, London, UK (1997).

[10] C. Bradbury, P. M. Callaway, D. D. Double, The Conversion of High Alumina Cement/Concrete, Mater. Sci. Eng. 23 (1976) 43–53.

[11] V. Fernon, A. Vichot, N. Le Goanvic, P. Colombet, F. Corazza, U. Costa, Interaction between Portland Cement Hydrates and Polynaphthalene Sulfonates, Malhotra V. M. Ed. 5th CANMET/ ACI International Conference on Superplasticizers and Other Chemical Admixtures in Concrete, ACI, Rome/Italy, SP–173 (1997) 225–248.

[12] L. Raki, J. J. Beaudoin, L. Mitchell, Layered Double Hydroxide-like Materials: Nanocomposites for Use in Concrete, Cem. Concr. Res. 34 (2004) 1717–1724.

[13] S. Stöber, H. Pöllmann, Synthesis of a Lamellar Calcium Aluminate Hydrate (AF_m Phase) containing Benzenesulfonic Acid Ions, Cem. Concr. Res. 29 (1999) 1841–1845.

[14] J. Plank, Z. Dai, P. R. Andres, Preparation and Characterization of New Ca-Al-Polycarboxylate Layered Double Hydroxides, Mater. Lett. 60 (2006) 3614–3617.

[15] J. Plank, H. Keller, P. R. Andres, Z. M. Dai, Novel Organo-Mineral Phases Obtained by Intercalation of Maleic Anhydride-Allyl Ether Copolymers Into Layered Calcium Aluminum Hydrates, Inorg. Chim. Acta, 359 (2006) 4901–4908.

[16] J. Plank, Z. M. Dai, H. Keller, F. Hössle, W. Seidl, Fundamental Mechanisms for Polycarboxylate Intercalation into C_3A Hydrate Phases and the Role of Sulfate present in Cement, Cem. Concr. Res. 40 (2010) 45–57.

[17] C. Giradeau, J.-B. d'Espinose de Lacaillerie, Z. Souguir, A. Nonat, R. J. Flatt, Surface and Intercalation Chemistry of Polycarboxylate Copolymers in Cementitious Systems, J. Am. Ceram. Soc. 92 (2009) 2471–2488.

[18] S. Ng, J. Plank, Formation of Organo-mineral Phases Incorporating PCE Superplasticizers During Early Hydration of Calcium Aluminate Cement, Proceedings of the 13th ICCC International Congress on the Chemistry of Cement, Abstract book, Madrid, Spain (2011) 251; full paper: ISBN: CD 978-84-7292-400-0 (7 pages).

[19] J. Plank, K. Pöllmann, N. Zouaoui, P.R. Andres, C. Schaefer, Synthesis and Performance of Methacrylic Ester based Polycarboxylate Superplasticizers possessing Hydroxy Terminated Poly(ethylene glycol) Side Chains, Cem. Concr. Res. 39 (2009) 1–5.

[20] S. Kawaguchi, K. Aikaike, Z.-M. Zhang, K. Matsumoto, K., Ito, Water Soluble Bottlebrushes, Polym J. 30 (1998) 1004–1007.

[21] N. Zou, J. Plank, Intercalation of Sulfanilic Acid-Phenol-Formaldehyde Polycondensate into Hydrocalumite Type Layered Double Hydroxide, Z. Anorg. Allg. Chem. (2012) In Print.

[22] D. H. Park, J. E. Kim, J. M. Oh, Y. G. Shul, J. H. Choy, DNA Encapsulation Into 2D Crystalline Lattice or X-Ray Nanoshell, 16th International Symposium on Intercalation Compounds, Seč-Ústupky, Czech Republic, P059 (2011) 125.

Full List of Publications

1. M. Lesti, S. Ng, J. Plank, Ca^{2+} Ion–Mediated Interaction between Microsilica and Polycarboxylate Comb Polymers in Model Cement Pore Solution, J. Am. Ceram. Soc., 93 (2010) 3493–3498.

2. S. Ng, J. Plank, Interaction Mechanisms between Na montmorillonite clay and MPEG-based Polycarboxylate Superplasticizers, Cem. Concr. Res. 42 (2012) 847–854.

3. J. Plank, S. Ng, S. Foraita, Intercalation of Microbial Biopolymers into Layered Double hydroxides, Z. Naturforschung., 67 (2012) 479–487.

4. S. Ng, J. Plank, Formation of Organo-Mineral Phases incorporating PCE Superplasticizers during Early Hydration of Calcium Aluminate Cement, Proceedings of the 13th ICCC International Congress on the Chemistry of Cement, Abstract book p. 251, Madrid/Spain (2011). ISBN: CD 978-84-7292-400-0. Reviewed.

5. S. Ng, J. Plank, Study on the Interaction of Na-montmorillonite Clay with Polycarboxylates, V. M. Malhotra (Ed.) 10th CANMET/ACI Conference on Superplasticizers and other Chemical Admixtures in Concrete, SP–288, ACI, Prague (2012) 407–420.

6. J. Plank, C. Liu, S. Ng, Interaction between Clays and PCE Superplasticizers in Cementitious Systems, V. M. Malhotra (Ed.) 9th CANMET/ACI Conference on Superplasticizers and other Chemical Admixtures in Concrete (Supplementary paper), ACI, Seville (2009) 279–298.

7. S. Ng, J. Plank, Interaction of a Sodium Bentonite Clay with a Polycarboxylate Based Superplasticizer in Cementitious Systems, GDCh-Monographie 42 (2010) 349–356.

8. S. Ng, J. Plank, Intercalation of PCE Superplasticizers into Calcium Aluminate Cement during Early Hydration, V. M. Malhotra (Ed.) 10th CANMET/ACI Conference on Superplasticizers and other Chemical Admixtures in Concrete (Supplementary paper), ACI, Prague (2012) 377–386.

9. S. Ng, J. Plank, Effect of Side Chain length of Methacrylate Ester Based PCE Superplasticizers on their Interactions with Na-Montmorillonite Clay, 18th Ibausil (2012).

10. S. Ng, 'Organo Mineral Phases incorporating Polycarboxylate Comb Polymers formed during the Early Hydration of Calcium Aluminate Cement', 16th International Symposium on Intercalation compounds, Seč-Ústupky/Czech Republic, 24th May 2011. Abstract.

11. S. Ng, 'CAC Hydrates and their Interaction with Superplasticizers', Fred Glasser Cement Science Symposium, Aberdeen/Scotland, 18th June 2009. Abstract.

12. S. Ng, J. Plank, Effect of Graft Chain length of Methacrylate Ester Based PCE Superplasticizers on their Interactions with Na-Montmorillonite Clay, *Submitted to Applied Clay Science.*

13. S. Ng, J. Plank, PCE Intercalation into Calcium Aluminate Cement under Real Application Condition using SAXS analysis. *Submitted to Cement and Concrete research.*